2012-12-20

Myxoma Virus Treatment for Brain Tumour Initiating Cells: Interrogating and Enhancing Myxoma-Mediated Cell Death

McKenzie, Brienne Alexandra

UNIVERSITY OF CALGARY

Myxoma Virus Treatment for Brain Tumour Initiating Cells: Interrogating and Enhancing Myxoma-Mediated Cell Death

by

Brienne Alexandra McKenzie

A THESIS

SUBMITTED TO THE FACULTY OF GRADUATE STUDIES

IN PARTIAL FULFILMENT OF THE REQUIREMENTS FOR THE

DEGREE OF MASTER OF SCIENCE

DEPARTMENT OF MEDICAL SCIENCE

FACULTY OF MEDICINE

CALGARY, ALBERTA

DECEMBER 2012

Abstract

Brain tumour initiating cells (BTICs) are stem-like cells hypothesized to mediate recurrence in high-grade gliomas. Preclinical success has been demonstrated in treating patient-derived BTICs with oncolytic virotherapy, using replication-competent viruses to target and kill malignant cells. Myxoma virus (MyxV) is an oncolytic candidate, which is highly effective in conventional glioma models, but only modestly effective in BTICs. The objective of this study was to improve MyxV efficacy in BTICs *in vitro*, combining chemotherapeutics and virotherapy. Using a pharmacoviral screen, eleven compounds that enhance MyxV-mediated cell death were identified. A lead compound, axitinib, was validated in multiple BTIC models. It was demonstrated that a virally encoded protein, M011L, prevents MyxV-induced apoptosis in BTICs, and M011L disruption was shown to greatly improve MyxV-mediated cell death through apoptosis induction. These studies have elucidated multiple strategies for improving MyxV efficacy in a preclinical glioma model, with implications for the future clinical development of MyxV.

Preface

Brienne McKenzie performed the majority of the experiments, analyses, and interpretations of the experiments, under the guidance of her supervisors, **Dr. Peter Forsyth** and **Dr. Ebba Kurz**. **Dr. Xueqing Lun** propagated and purified the viruses used in this thesis, all of which were provided by the laboratory of **Dr. Grant McFadden**. The laboratory of **Dr. Samuel Weiss** derived the five BTIC lines from patient samples. **Zhili Kang** provided valuable technical assistance for several of the immunoblots in Chapter III.

Funding for this project was provided by the Kids Cancer Care Foundation and the Canadian Cancer Society Research Institute, in the form of grants to Peter Forsyth. Funding was also provided through several graduate scholarships, including the Canadian Institutes of Health Research's Frederick Banting and Charles Best Graduate Scholarship - Masters Award, Queen Elizabeth II Graduate Award, Alexa Church Graduate Scholarship in Medical Sciences, and Alberta Graduate Student Scholarship.

Acknowledgements

I would like to extend my utmost thanks to my supervisor, Dr. Peter Forsyth, for your wisdom, guidance, and support in all my studies, and for bringing our research to life by sharing your clinical insights with your students. It has truly been a privilege to work under your guidance. To my co-supervisor, Dr. Ebba Kurz, thank you so much for your unwavering support, keen scientific insights, and steadfast encouragement. Your guidance and mentorship have been inspirational to me. To my committee members, Dr. Aru Narendran and Dr. Samuel Lawn, thank you for your thoughtful insights and unfailing support throughout this project. Your suggestions and experience have been instrumental in the completion of my studies. Thank you as well to Dr. Jennifer Chan for taking the Forsyth lab students under your wing with such good humour. A special thank you to the remaining members of the Forsyth lab: Lori, your support, kindness, and sense of humour have kept me going through the toughest times. Franz, you have been instrumental in shaping my growth and development as a scientist. Thank you for keeping my faith in science. To the former members of the Forsyth lab, Xueqing, Beichen, Juan Carlos, Henry, David, and Hongyuan, thank you for all your support and for making my experience such a memorable one. To Mark, thank you for your unwavering support, quiet encouragement, and faith in my ability every step of the way. Most importantly, to my parents and my sister Sierra, thank you for your boundless support, love, and encouragement along this journey.

To Grandad

A great thinker and teacher

with love

Table of Contents

ABSTRACT II
PREFACE III
ACKNOWLEDGEMENTS IV
DEDICATION V
TABLE OF CONTENTS VI
LIST OF TABLES IX
LIST OF FIGURES AND ILLUSTRATIONS X

CHAPTER ONE: INTRODUCTION 1
1.1 Glioblastoma Multiforme 1
1.1.1 Overview 1
1.1.2 Current Therapeutic Approaches and Limitations 1
1.1.3 Small Molecule Inhibitors in Cancer Therapy 2
1.1.4 Small Molecule Inhibitors in GBM Therapy 3
1.1.5 Tumour Heterogeneity in GBMs 4
1.2 Brain Tumour Stem Cells 5
1.2.1 Overview 5
1.2.2 Brain Tumour Initiating Cells in vitro and in vivo 6
1.3 Oncolytic Virotherapy 8
1.3.1 Development of OV therapy 9
1.3.2 Oncolytic Virotherapy: The Modern Era 11
1.3.3 Oncolytic virotherapy for gliomas 13
1.4 Myxoma Virus: A Next Generation Oncolytic Virus 15
1.4.1 The Myxoma Virus Genome 18
1.4.2 MyxV-mediated Evasion of Apoptosis and Cellular Antiviral Immunity 20
1.4.3 MyxV in Preclinial GBM Models 21
1.5 Combination Therapy with Oncolytic Viruses 22
1.5.1 Drugs with Systemic Mechanism of Action 23
1.5.2 Drugs with Local Mechanism of Action 24
1.6 Overview of Apoptotic Cell Death 27
1.6.1 Intrinsic and Extrinsic Pathways 28
1.6.2 Caspases: The Executioners of Apoptosis 30
1.6.3 Bcl-2 Family Members 32
1.6.4 Cancer Therapies and Apoptosis 33
1.6.5 Viruses and Apoptosis 34
1.6.6 Interactions of Viruses with Apoptotic Cell Death Machinery 35
1.6.7 MyxV M011L: Bcl-2 Homologue 35
1.6.8 Alternatives to Apoptosis: Autophagic Cell Death 36
1.7 Objective and Specific Aims 39

CHAPTER TWO: MATERIALS & METHODS 40
2.1 BTIC Isolation and Culture 40
2.2 Glioma Cell Line Culture 41
2.3 Viral Titration and Gene Expression Assays 41
2.4 Viability Assays 43

2.5 Caspase Activation Assays *43*
2.6 Immunoblots *44*
2.7 ZVAD-induced Caspase Inhibition *46*
2.8 Small molecule inhibitor drug screen *46*

CHAPTER THREE: CHARACTERIZATION OF BTIC SUSCEPTIBILITY TO MYXV 50
3.1 Introduction & Rationale *50*
3.2 BTICs demonstrate variable susceptibility to MyxV-induced cell death *53*
3.3 MyxV infects all BTICs tested *57*
3.4 Viral gene expression increases over time *60*
3.5 Induction of apoptosis is not responsible for MyxV-induced cell death *63*
3.6 Myxoma virus protein M011L mediates anti-apoptotic signalling in the BTIC model *71*
3.7 Autophagy-related signalling in response to MyxV infection *76*
3.8 Summary and significance *76*

CHAPTER FOUR: IDENTIFICATION OF SYNERGISTIC COMPOUNDS 79
4.1 Introduction & Rationale *79*
4.2 First-pass screen reveals eight potential candidates for further characterization *82*
4.3 Rescreen of twenty-two cytotoxic drugs reveals three more hits *93*
4.4 Six candidate compounds were shown to be synergistic with virus at the lowest dose tested following Chou-Talalay analysis *100*
4.5 Summary and significance *100*

CHAPTER FIVE: SELECTION AND FURTHER CHARACTERIZATION OF THE LEAD COMPOUND AXITINIB 103
5.1 Introduction & Rationale *103*
5.2 Axitinib in combination with MyxV leads to substantial cell killing in multiple BTIC lines *108*
5.3 Axitinib in combination with MyxV leads to substantial cell killing in conventional glioma cell lines *108*
5.4 Axitinib treatment alone or in combination with MyxV does not induce apoptosis *112*
5.5 Axitinib modulates downstream signalling pathways *112*
5.6 Summary and significance *116*

CHAPTER SIX: DISCUSSION 119
6.1 Characterization of MyxV-induced Cell Killing *120*
6.2 Small Molecule Inhibitor Drug Screen *128*
6.2.1 The Drug Screen Approach: Benefits and Limitations 129
6.3 Chou-Talalay Analysis *132*
6.4 Improved viral infection as a mechanism of synergy *133*
6.5 Characterization of the Lead Compound: Axitinib *134*
6.6 Limitations of the Cancer Stem Cell Hypothesis and the BTIC model *140*
6.7 Implications of anti-apoptotic MyxV signalling on pharmacoviral therapy *143*
6.8 Future Directions *144*
6.9 Conclusions & Significance *145*

REFERENCES 147

APPENDIX A: CHEMIETEK SMALL MOLECULE INHIBITOR DRUG LIBRARY 159
A.1. Characteristics of small molecule inhibitor drug library 159

APPENDIX B: PHARMACOVIRAL SCREEN OF SMALL MOLECULE INHIBITORS 162
B.1. Screen of 73 Small Molecule Inhibitors (1μM) 162
B.2. Additional Screen of 22 Cytotoxic Drugs at 100nM 169
B.3. Additional Screen of Six Very Highly Cytotoxic Drugs at 10nM 171

APPENDIX C: DOSE RESPONSE OF CANDIDATE COMPOUNDS WITH MYXOMA VIRUS ... 173
C.1. Dose response characterization of candidate compounds 173

List of Tables

Table 3.1: Characteristics of BTIC Panel 51

Table 4.1: Identification of Candidate Compounds (1μM Screen) 89

Table 4.2: Cytotoxic Drugs Identified in First Pass Screen..... 96

Table 4.3: Identification of Candidate Compounds (100nM Screen)..... 99

Table 5.1: Drug Development Status of Candidate Compounds 104

Table 5.2: Performance Summary of Synergistic Candidate Compounds 106

List of Figures and Illustrations

Figure 1.1 Life cycle of MyxV in a permissive tumour cell line 16

Figure 1.2. Extrinsic versus intrinsic pathways of apoptosis activation..... 29

Figure 3.1: BTICs demonstrate variable susceptibility to MyxV-induced killing 55

Figure 3.2: MyxV infection at high MOI results in cell death 56

Figure 3.3: All BTIC lines are infected by MyxV, with varying degrees of late viral gene expression..... 59

Figure 3.4: Late viral gene expression increases over time in all BTICs tested..... 62

Figure 3.5 Validation of Caspase 3/7 Glo© assay..... 64

Figure 3.6 MyxV does not induce caspase-3/-7 activation in any BTIC line tested and significantly decreases caspase-3/-7 activation in two BTIC lines 67

Figure 3.7: Immunoblots of caspase-3/-7 cleavage and PARP cleavage indicate that apoptosis is not induced by 48hr MyxV infection..... 70

Figure 3.8: MyxV-M011L-KO significantly enhances MyxV-induced cell death in BT025 and BT073 through induction of apoptosis 74

Figure 3.9: Inhibition of caspase activity may partially rescue MyxV-M011L-KO phenotype..... 75

Figure 3.10: Immunoblot for induction of autophagy is inconclusive 77

Figure 4.1: Experimental design for 73-compound small molecule inhibitor drug screen 84

Figure 4.2: Summary data for first-pass screen of BT025 with all 73 drugs, alone and in combination with virus 85

Figure 4.3: Each of the eight candidate compounds demonstrated a significant combination effect in BT025 88

Figure 4.4: Confirmation of viral luminescence as an appropriate surrogate measure for viral infection 91

Figure 4.5: Viral luminescence, a quantitative measure of MyxV infection, does not increase in response to pre-treatment of BT025 with any of the eight candidate compounds..... 95

Figure 4.6: Three of twenty-two cytotoxic drugs show a significant combination effect that is not attributable to an increase in viral infection..... 98

Figure 4.7: Calculation of combination indices reveals that six of eleven candidate compounds are synergistic with MyxV by Chou-Talalay analysis 101

Figure 5.1: Axitinib administration with MyxV is an effective combination in multiple BTIC lines 111

Figure 5.2: Axitinib administration with MyxV is an effective combination in multiple human glioma cell lines..... 113

Figure 5.3: Axitinib administration with MyxV does not induce apoptosis 115

Figure 5.4: Axitinib treatment moderately reduces Akt phosphorylation 117

Figure 6.1: Overview of VEGF signalling and downstream effectors 136

List of Symbols, Abbreviations and Nomenclature

Symbol	Definition
Abl	V-abl Abelson Murine Leukemia Viral Oncogene Homolog 1
APAF1	Apoptotic Protease-Activating Factor 1
ATCC	American Type Culture Collection
ATG	Autophagy-Related Genes
ATM	Ataxia Telangiectasia Mutated
B-RAF	B-Raf Proto-oncogene Serine/Threonine-Protein Kinase
BAD	Bcl-2 Associated Death Promoter
BAK	Bcl-2 Homologous Antagonist/Killer
BAX	Bcl-2 Associated X Protein
BCL-2	B-Cell Lymphoma-2
BCR-Abl	Breakpoint Cluster Region Abelson
BGMK	Baby Green Monkey Kidney
BH	Bcl-2 Homology
BID	BH3-interacting Domain Death Agonist
BTIC	Brain Tumour Initiating Cells
BrdU	Bromodeoxyuridine
c-Met-R	Mesenchymal-Epithelial Transition Factor Receptor
CAD	Caspase-Activated DNase
Caspase	Cysteine-aspartic proteases
CI	Combination Index
cIAP	Cellular Inhibitor of Apoptosis Protein
CMV	Cytomegalovirus
COX-2	Cyclooxygenase-2
CRTH2-R	Chemoattractant-Homologous Receptor Expressed on Th2 Cells
DMEM	Dulbecco's Modified Eagle's Medium
DMSO	Dimethyl Sulfoxide
DNA-PKcs	DNA-dependent Protein Kinase Catalytic Subunit
DV	Dead (UV-inactivated) Myxoma Virus
ECL	Enhanced Chemiluminescence
EGF	Epidermal Growth Factor
EGFR	Epidermal Growth Factor Receptor
EGFR VIII	EGFR with deletion of exons 2-7
ErbB-R	Erythroblastic Leukemia Viral Oncogene B receptor
ERK	Extracellular Regulated Kinase
FADD	Fas-Associated Death Domain

FBS	Fetal Bovine Serum
FDA	Food and Drug Administration
FDA	United States of America Food and Drug Administration
FGF	Fibroblast Growth Factor
Fluc	Firefly Luciferase
GBM	Glioblastoma Multiforme
GFP	Green Fluorescent Protein
GM-CSF	Granulocyte Macrophage Colony Stimulating Factor
HDAC	Histone Deacetylase
HRP	Horseradish Peroxidase
HSP	Heat Shock Protein
HSV	Herpes Simplex Virus
ICAD	Inhibitor of Caspase-Activated DNase
IFN	Interferon
IGF-1R	Insulin-like Growth Factor 1 Receptor
IRF	Interferon Response Factor
ISG	Interferon-Stimulated Genes
JAK	Janus Kinase
kb	Kilobasepairs
kDa	Kilodaltons
LC3	Microtubule-Associated Protein 1 Light Chain 3
LTR	Leukotriene Receptor
M	Molar
MAPK	Mitogen-activated Protein Kinase
Mcl-1	Myeloid Cell Leukemia-1
MEK	MAPK/ERK Kinase
MGMT	O6-Methylguanine-DNA Methyltransferase
MHC	Major Histocompatibility Complex
μM	Micromolar
mM	Millimolar
MOI	Multiplicity of Infection
MTD	Maximum Tolerated Dose
mTOR	Mammalian Target of Rapamycin
Myd88	Myeloid Differentiation Primary Response Gene 88
MyxV	Myxoma Virus
MyxV-dsRED	Myxoma virus tagged with dsRED reporter
MyxV-Fluc	Myxoma virus tagged with firefly luciferase reporter
MyxV-M011L-KO	Myxoma virus with M011L knock-out

NDV	Newcastle Disease Virus
NF-κB	Nuclear Factor Kappa B
NK	Natural Killer
nM	Nanomolar
NPM-ALK	Nucleophosmin-Anaplastic Lymphoma Kinase
NSCLC	Non-Small Cell Lung Cancer
OV	Oncolytic Virus
PARP	Poly-ADP Ribose Polymerase
PBS	Phosphate Buffered Saline
PDE4	Phosphodiesterase 4
PDGFR	Platelet-Derived Growth Factor Receptor
PGD2-R	Prostaglandin D2 Receptor
PI-3K	Phosphoinositide 3-Kinase
PLK	Polo-Like Kinase
PRR	Pattern Recognition Receptor
PTEN	Phosphate and Tensin Homologue
PUMA	p53 Up-regulated Modulator of Apoptosis
Rb	Retinoblastoma
RFP	Red Fluorescent Protein
RIG	Retinoic Acid Inducible Gene
RXR	Retinoid X Receptor
SDS	Sodium Dodecyl Suphate
SDS-PAGE	Sodium Dodecyl Suphate Polyacrylamide Gel Electrophoresis
shRNA	Small Hairpin RNA
siRNA	Small Interfering RNA
Src	Rous sarcoma oncogene cellular homolog
TBST	Tris Buffered Saline with Tween-20
TLR	Toll-Like Receptor
TMZ	Temozolomide
TNF	Tumour Necrosis Factor
TNFR1	Tumour Necrosis Factor Receptor 1
TRAIL	TNF-related apoptosis-inducing ligand
Trif	TIR-domain-containing adapter-inducing interferon b
vIAP	Viral Inhibitor of Apoptosis Proteins
vMLIA	Viral Mitochondria-Localized Inhibitor of Apoptosis
VSV	Vesicular Stomatitis Virus
ZVAD-FMK	Carbobenzoxy-valyl-alanyl-[O-methyl]-fluoromethylketone

Chapter One: Introduction

1.1 Glioblastoma Multiforme

1.1.1 Overview

Malignant gliomas are highly invasive and lethal adult brain tumours[1-3]. These tumours are distinguished by their rampant proliferation, diffuse infiltration into the normal brain, and aggressive clinical course[1,4]. Approximately 15,000 individuals are diagnosed with gliomas yearly in North America, of whom 60-70% have Grade IV tumours known as glioblastoma multiforme (**GBM**)[3]. GBMs are highly necrotic, vascularized, and heterogeneous tumours, which may arise *de novo* (known as primary glioblastomas) or from low-grade astrocytomas (known as secondary glioblastomas)[1-5]. These two distinct disease etiologies give rise to genetically distinct yet morphologically indistinguishable tumours, both of which are characterized by a poor prognosis and resistance to conventional therapies[1-5].

1.1.2 Current Therapeutic Approaches and Limitations

Current standard of care for GBM combines surgical resection, radiotherapy, and concomitant chemotherapy (using the alkylating agent temozolomide, **TMZ**, Temodar®), yet patients almost invariably succumb to recurrent disease[1-4,6]. The mean survival for GBM patients receiving standard of care is just 14.6 months, a marginal increase over radiotherapy and surgery alone (12.1 months)[6]. Conventional therapeutic approaches are hampered by a multitude of clinical challenges. For instance, GBM cells invade and form tendrils into the surrounding brain parenchyma, which severely limits the efficacy of

surgical resection and localized radiotherapy; invasive GBM cells have been found centimetres away from the primary tumour and have been known to cross into the contra-lateral hemisphere, facilitating recurrence[1,7]. Furthermore, GBMs are often refractory to chemotherapy, through either intrinsic or acquired resistance mechanisms. TMZ resistance is associated with expression of the DNA repair protein O6-methylguanine methyltransferase (**MGMT**), and subgroup analysis of GBM patients by *MGMT* promoter status demonstrates that while patients with *MGMT* promoter methylation derive significant benefit from TMZ, those lacking *MGMT* promoter methylation (>50% of patients studied) derive little or no therapeutic benefit from this agent[8-10]. The failure of conventional therapies to overcome these challenges and improve GBM patient prognosis provides a compelling reason to explore the mechanisms driving recurrence, and to pursue novel therapeutic strategies to overcome such formidable clinical challenges.

1.1.3 Small Molecule Inhibitors in Cancer Therapy

One approach that has been explored across a broad range of cancers, including GBM, is the development of small molecule inhibitors that are rationally selected to target aberrant signalling pathways within the tumour. Deep sequencing of the cancer genome, combined with high-throughput "omics" approaches, has revealed a plethora of potential drug targets in various malignancies[11,12]. Imatinib (Gleevec®, a BCR-Abl inhibitor) in chronic myeloid leukemia (**CML**) was an iconic clinical success[12,13], leading to an 80% decrease in mortality[12,14] and infusing the field with optimism that targeted therapies would usher in an era of personalized medicine. With over one hundred targeted agents approved for

various cancers, and several hundred more in preclinical and clinical trials, it is evident that the initial optimism has been borne out in many cases[15]. Some high-profile therapies that have successfully exploited this approach include the BCR-Abl inhibitor imatinib for CML, the epidermal growth factor receptor (**EGFR**) inhibitors gefitinib (Iressa®) and erlotinib (Tarceva®) for EGFR-mutant non-small cell lung cancer (**NSCLC**)[16], and the BRAF inhibitor vemurabenib (Zelboraf®) for BRAF-driven melanoma[17].

1.1.4 Small Molecule Inhibitors in GBM Therapy

Like many cancers, GBMs demonstrate various classical genetic alterations in pathways that govern cellular proliferation and survival[4,18-20]. These genetic aberrations and their associated signalling pathways are rational targets for small molecule inhibitor therapies. The most common genetic aberrations in GBMs include the inactivation or deletion of tumour suppressors, such as p53 (30-60% of patients), phosphatase and tensin homologue (**PTEN**; 5-40% of patients), $p16^{INK4a}$ (40-60% of patients), and retinoblastoma (**Rb**; 30% of patients); as well as amplification of growth factor receptors, such as EGFR (40-60% of patients) and platelet-derived growth factor receptor (**PDGFR**; up to 65%)[18]. Inhibition of tumour suppressors and over-expression of growth factor receptors lead to the constitutive activation of pro-survival signalling pathways such as the phosphoinositide-3-kinase (**PI-3K**)/Akt/mammalian target of Rapamycin (**mTOR**) pathway and the mitogen-activated protein kinase (**MAPK**) pathway[4,18-22]. Inhibition of such targets has proven successful in preclinical studies, leading to clinical trials using a variety of small molecule inhibitors, including drugs that target EGFR (e.g. erlotinib/Tarceva® and gefitinib/Iressa®); PDGFR (e.g. imatinib/Gleevec®); Akt (e.g.

perifosine); and mTOR (e.g. everolimus, temsirolimus, and sirolimus/rapamycin)[4,21,22]. Although the clinical and prognostic relevance of these pathways to GBMs has been repeatedly validated in high-throughput genomics studies[19-24], such targeted strategies have yet to meet with overwhelming clinical successes[21,25]. In gliomas, as in other cancers, multiple mechanisms of resistance to small molecule inhibitors have been observed, including mutations in kinase targets, activation of parallel signalling pathways, adaptive feedback loops, and the persistence of endogenous subpopulations with enhanced drug resistance[15,21]. These resistance mechanisms emerge as a consequence of intense selection pressure within the profoundly heterogeneous environment of the individual tumour. Innovative combinatorial therapy that overcomes the limitations of each individual therapy will be required to create durable therapeutic responses in these highly heterogeneous tumours.

1.1.5 Tumour Heterogeneity in GBMs

Various sources of molecular heterogeneity exist both within and between GBMs, complicating treatment. Multiple studies have used high-throughput genomics techniques to analyze glioma mutational landscapes and gene expression profiles[19,20]. These analyses have revealed four major GBM subtypes with distinct gene expression profiles (mesenchymal, classical, proneural, neural)[23,24]. These molecular classifications serve to highlight the heterogeneity of GBMs and provide a framework within which to study the efficacy of targeted therapies.

In addition, there is a growing appreciation for the immense molecular heterogeneity within individual tumours. Receptor tyrosine kinases, which are the target of many small molecule inhibitors, have been repeatedly demonstrated to be non-uniform within individual tumours[26,27], providing a mechanism for resistance to targeted therapies and highlighting the need for novel combinatorial approaches.

Another recent observation that highlights the profound intratumoral heterogeneity is the presence of stem-like cells within the tumour bulk of GBMs. The presence of such cells forms the basis of what is known as the brain tumour stem cell hypothesis.

1.2 Brain Tumour Stem Cells

1.2.1 Overview

According to the brain tumour stem cell hypothesis, GBM tumorigenesis and recurrence is mediated in part by brain tumour initiating cells (**BTICs**), which express stem cell markers and possess canonical stem cell properties, such as self-renewal and multi-lineage differentiation[2,28-31]. These populations are hypothesized to be resistant to conventional therapies and to form treatment-resistant disease reservoirs that mediate recurrence[29,30]. Stem-like cells have been successfully identified in a multitude of malignancies, including cancers of the prostate, breast, lung, pancreas, and skin[32-39].

Populations of cells with stem-like properties have been isolated from patient GBM samples and enriched using a variety of methods, most commonly neural stem cell

culture conditions[31,40]or CD133+ expression[41,42]. A wide variety of enrichment markers have been suggested for putative BTIC populations, including CD15[43,44], a6 integrin[45], and A2B5[46], though there currently exists no standardized collection of markers to unequivocally identify BTIC populations [47]. In the absence of a standardized set of markers, functional criteria have become extremely important in identifying BTIC populations. Typical functional criteria include: (i) the ability to self-renew, (ii) the ability to differentiate, and (iii) the ability to initiate tumours that accurately recapitulate the patient tumour[30,47,48]. These functional criteria are particularly important given that the molecular signature of BTICs remains controversial, and even classical neural stem cell markers such as CD133 do not unequivocally distinguish tumour-initiating cell populations from more lineage-committed cells within the tumour bulk[28,49,50]. Nonetheless, at the clinical level, the detection of stem cell markers, such as CD133 and nestin, by immunohistochemistry has repeatedly been shown to be an independent prognostic marker in glioma[51-53]. The ability of patient-derived cells to form neurospheres has also been shown to be a robust and independent predictor of progression[54]. These clinical observations highlight the need for therapies that can target both the stem-like and the more differentiated compartments of the tumour.

1.2.2 Brain Tumour Initiating Cells in vitro *and* in vivo

In order to preserve putative BTIC populations, patient-derived surgical samples are cultured as neurospheres in serum-free, growth factor-supplemented neural stem cell conditions[47]. These neurospheres are clonal, heterogeneous aggregates comprised of stem-like tumour initiating cells and more rapidly dividing transient amplifying cells[47].

Chen *et al* used clonal analysis to demonstrate that patient-derived neurospheres do not consist of phenotypically uniform populations, but rather contain a hierarchy of cells at different stages of differentiation, with varying gene expression profiles and capacities for tumour initiation[28]. Once isolated and propagated as neurospheres *in vitro*, the tumour-initiating capabilities of putative BTICs are verified by *in vivo* serial tumour formation assays. Central to the brain tumour stem cell hypothesis is the notion that BTICs have enhanced tumorigenic capacity compared to the bulk of tumour cells. Singh *et al* demonstrated that prospectively isolated $CD133^+$ patient-derived cells were capable of forming tumours from as few as 100 cells, while 1×10^5 $CD133^-$ cells did not initiate tumours[55]. Kelly *et al* demonstrated that as few as 10 BTICs, grown under neurosphere conditions and implanted intracranially in immunocompromised mice, were capable of forming tumours[31]. Importantly, these highly tumorigenic cells formed aggressive, highly vascularised, infiltrative tumours that phenocopied the original patient tumours with high fidelity[31]. Although the clinical relevance of BTICs remains controversial, this capacity to form tumours that accurately recapitulate patient GBMs makes them an extremely valuable model for preclinical drug development. In a side-by-side comparison, Lee *et al* demonstrated that patient samples cultured in neural stem cell-promoting conditions formed tumours that more accurately recapitulated the genotype and phenotype of the parent tumour than conventional cell lines[56]. Consistent with their hypothesized role as disease reservoirs, patient-derived BTICs also demonstrate mechanisms for radio-resistance[57] and chemo-resistance[58], and show variable susceptibility to TMZ[59,60]. Importantly, patient-derived BTICs also harbour many of the hallmark GBM genetic mutations (p53, PTEN, EGFR, etc.), in various combinations, making them a powerful

tool for elucidating the links between mutational status and therapeutic efficacy of different treatments. For all of these reasons, BTICs represent an important and relevant model for investigating novel therapeutics for GBM.

1.3 Oncolytic Virotherapy

Within the last several decades, oncolytic viruses (**OVs)** have emerged as a promising experimental therapeutic for a multitude of cancers, including GBMs. OV therapy utilizes non-pathogenic, replication-competent wildtype or engineered viruses to selectively target and kill malignant cells, with minimal effect on healthy tissue[61]. OV therapy is functionally distinct from gene therapy, which uses highly attenuated, non-replicating viral vectors as vehicles for gene delivery[62]. Importantly, the distinct hallmark characteristics that promote tumour growth (evasion of apoptosis, immune evasion, etc.) generally promote successful viral replication and repress antiviral immunity, thus making tumour cells attractive hosts for viruses[63].

The classical paradigm of OV therapy envisions selective viral infection of tumour cells, efficient viral replication within the tumour, lytic killing of infected cells, and the subsequent release of viral progeny[62]. In theory, this leads to a self-amplification effect, in which a modest initial dose of virus is amplified through successive rounds of viral replication within the tumour, eliminating the need for repeated administration[62]. As will be discussed further below, this paradigm represents an idealized model that may not accurately reflect the complexity of host-tumour-virus interactions.

1.3.1 Development of OV therapy

The idea of OV therapy first emerged in the early twentieth century, following sporadic anecdotal evidence that naturally occurring viral infections could temporarily induce profound tumour regression[64]. In 1896, a 42-year-old woman's acute leukemia underwent a "spontaneous" regression after she contracted an influenza-like illness; although this was 37 years before the influenza virus was even identified, the association of the remission with an infectious disease did not go unnoticed[64,65]. Over half a century later, in 1953, a 4-year-old boy diagnosed with 'lymphatic leukemia' experienced a dramatic regression after contracting chickenpox[66]. Such individual case studies continued to accumulate, all pointing towards the same conclusion: certain infectious diseases, which would later be proven to be of a viral etiology, could induce drastic, if often temporary, regressions in advanced malignancies. Due to the technological limitations of the time, purified virus was not available, and thus the first human OV trial in 1949 relied upon the injection of unpurified human serum from Hepatitis B-positive patients[64]. Of the original 22 patients in the Hepatitis B trial, all of whom were suffering from late stage Hodgkin's disease, fourteen developed hepatitis; seven witnessed some form of clinical improvement; and four saw a reduction in tumour size[64]. One died from the treatment[64].

The OV clinical trials that followed in the decades to come were coloured by some inspiring clinical successes, some disappointing treatment failures, and in a few conspicuous cases, astonishingly unethical clinical practices. Importantly, since *ex vivo* culture of immortalized human cell lines was only first accomplished in 1948 and did not become mainstream until well after that, *in vivo* models were not initially available as a

platform to test the safety and efficacy of OVs[64]. Thus, oncologists relied upon clinical data to demonstrate safety and efficacy of these experimental therapeutics. One such trial, in 1952, successfully demonstrated selective intratumoural replication of Egypt 101 virus, an early strain of West Nile virus, in 14 out of the 37 patients injected[67]. A later trial used the mumps virus for a variety of end-stage cancers, and determined clinical efficacy in a 90% of the 90 patients enrolled[68]. The virus was administered in a fascinating variety of ways, including inhalation, rectal administration, topical application to the skin, and oral administration of a piece of bread soaked in virus supernatant[64]. Nonetheless, subsequent clinical trials with the mumps virus were disappointing, and its initial clinical success was never recapitulated[64].

Following the development of *in vivo* models for OV therapy, a wide variety of viruses, from adenoviruses to avian plague virus, were tested in murine models, with mixed results[64]. By 1952, 42 viruses had been tested *in vivo*, and eleven had shown some evidence of success[65]. Although some viruses successfully induced tumour regression, the vast majority of effective OVs had a strong neurotropism, which often resulted in death of the animals[64]. Some viruses, however, such as the avian Newcastle disease virus (**NDV**), which is still in use today, demonstrated significant efficacy with minimal side effects[69]. It soon became apparent, however, that tumours were much more easily cured in xenograft models than in humans[64]. In order to overcome the limitations of xenograft models, an oncologist named Chester Southam performed subcutaneous implantations of cultured human tumours (including HeLa cells) into the forearms of healthy human "volunteers" (often prisoners[65,70]) and cancer patients, before treating them with

experimental OVs[71]. Although the immunocompetent healthy volunteers typically rejected the tumours, the grafts were successful in 20 of the 22 cancer patients. Those grafts that did not respond to OV therapy had to be surgically removed, some multiple times. Understandably, such practices considerably tarnished the field of OV research in the eyes of the public[64,65]. It took several decades for the field to recover, reinvigorated by advances in recombinant DNA technology that enabled the attenuation of OVs into safe, more efficacious targeted therapies[65].

1.3.2 Oncolytic Virotherapy: The Modern Era

The first engineered OV to enter clinical trials was adenovirus d11520 (ONYX-015), an adenovirus that was engineered to replicate solely in p53-deficient tumour cells[72-74]. A related serotype of the virus (Ad5) was later approved by the Chinese Food and Drug Administration following demonstrations of improved outcome in the treatment of head and neck cancer[75]. Phase I-III trials are currently underway or completed for a variety of other viruses, many engineered to attenuate pathogencitiy or improve oncolysis. These include vaccinia virus, reovirus, herpes simplex virus (**HSV**), NDV, and measles virus, amongst others, all of which have been well tolerated with minimal toxicity[76,77]. The vast majority of these viruses naturally infect humans, which can pose challenges due to off-target infections. Thus, many of the human viruses in clinical trials, including the oncolytic HSV construct OncoVex^{GMCSF} (developed by UK-based BioVex) and the vaccinia construct JX-594 (developed by San Francisco-based Jennerex Biotherapeutics), carry mutations in virulence factors in order to improve cancer selectivity, as well as immunomodulatory proteins (such as GM-CSF) to improve anti-tumour immunity[77,78].

Interestingly, although the traditional OV paradigm of direct viral lysis of infected tumour cells is well-established in preclinical models, it has not yet been demonstrated in clinical trials that a productive, lytic viral infection is capable of destroying a tumour[79]. This leaves the possibility that other, non-lytic mechanisms of cell death (such as immune clearance or apoptosis) are contributing to the observed clinical responses.

For all of the OVs currently in clinical trials, tumour selectivity is of paramount importance. The mechanism of selectivity varies widely between virus types, and ranges from naturally occurring tumour tropism (such as reovirus) to engineered tropism (e.g. JX-594). Wildtype reovirus (developed as Reolysin® by Oncolytics Biotech) has a mechanism of selectivity based upon activated Ras in malignant cells[80]. In contrast, JX-594 contains a deletion in its thymidine kinase gene, which is unnecessary for replication in cancer cells but required for replication in normal tissues[78]. HSV constructs currently in development employ a similar strategy, whereby a critical viral gene (such as DNA polymerase or ribonucleotide reductase) that is critical for replication in normal cells but dispensable in most cancer, is mutated[81]. Such mechanisms ensure that the virus's unique tropism for cancer cells is maintained.

OV therapy offers several advantages over conventional therapeutics. As previously discussed, OVs have a narrow tropism for cancer cells[77], and this intrinsic selectivity helps to minimize or avoid the plethora of off-target effects that plague conventional chemotherapeutics. Secondly, traditional mechanisms of resistance to chemotherapeutics, such as the expression of membrane-associated drug transporters, are not expected to

impede the efficacy of OV therapy[65]. Thirdly, OVs may offer a multi-pronged approach to treating the tumour. In addition to the intrinsic anti-tumour effects caused by the direct infection and killing of the cell by the virus, OV infection may also elicit a potent anti-tumour immune response that serves to further enhance tumour killing[61]. Furthermore, OVs can be "armed" with additional therapeutically relevant genes that are expressed only within the tumour cell due to the intrinsic selectivity of the virus. Examples of such genes include immune modulators such as GM-CSF; pro-drug-activating enzymes such as carboxylesterase, which converts irinotecan into its active form, SN-38[82]; and pro-apoptotic signalling proteins such as TNF-related apoptosis-inducing ligand (TRAIL)[83]. These properties offer significant advantages over many conventional cancer therapeutics.

1.3.3 Oncolytic virotherapy for gliomas

Of the multitude of viruses currently under investigation as oncolytic agents, 15 have been tested in preclinical glioma models, and several of these have already progressed to clinical trials[62]. The HSV-1 construct (*dlstk*) bearing a mutation in thymidine kinase to attenuate neurotoxicity was the first OV to undergo preclinical testing for GBM[84]. Since then, a plethora of second- and third-generation HSV-1 variants have been developed and several of these have been taken to clinical trials for GBM patients. For instance, HSV-1(1761) was utilized in three clinical trials that collectively demonstrated evidence of intratumoural viral replication, antiviral antibody production, and a lack of dose-limiting toxicities[85-87]. Importantly, maximum tolerated dose (MTD) was never reached in any of the trials, and several patients showed long-term survival[85-87]. The conditionally

replicating adenovirus ONYX-015 has also been explored in the context of GBMs. In one phase I clinical trial, ONYX-015 was evaluated in 24 patients, and although no evidence of efficacy was noted, the MTD was never reached, highlighting the safety of intratumoral viral injections[88]. Wildtype reovirus, which demonstrates a natural tropism for humans but causes no known disease, has also been tested in a Phase I trial for GBM. Of the twelve patients treated, one long-term survivor emerged, and no dose-limiting toxicities were observed[89]. Lastly, following several promising case studies in recurrent GBM patients, a Phase I/II trial was undertaken for attenuated NDV, in which one complete response and several long-term survivors were observed[90].

Following over a decade of experience with OVs in GBM clinical trials, several themes have emerged. Firstly, OVs are extremely well-tolerated in GBM patients, with no known dose-limiting toxicities observed in any GBM trial to date[62]. This parallels observations in other cancers, wherein even the highest feasible OV doses produce minimal toxicity[79]. Given that the initial viruses were chosen based on optimal safety and not necessarily optimal oncolysis, these results are not necessarily surprising. Such trials have established a successful record of safety in the field, and thus laid the groundwork for more potent viruses to be introduced in future trials[62]. Secondly, although some viral replication has been observed in treated patients, the field has yet to witness overwhelming evidence that viral replication leads to improved clinical outcome. Clearly, the paradigm of a single infected cell giving rise to a wave of infection that ultimately kills the tumour has not been realized[91]. Immunologically-mediated inhibition of virus replication is a widely acknowledged limitation, highlighting the need for new strategies to circumvent this

issue[91]. Potential approaches include the use of multimodal therapies that inhibit the antiviral immune response and/or enhance viral efficacy, the strategic use of OVs as immunotherapies, and the development of new second- and third-generation OV's that are less immunogenic in human hosts. All of these strategies are currently the subject of much investigation in the OV field.

1.4 Myxoma Virus: A Next Generation Oncolytic Virus

MyxV, a double-stranded DNA rabbit poxvirus, is a potent oncolytic candidate with significant efficacy in various preclinical models of GBM[92-94]. The life cycle of this virus is described in *Figure 1.1*. MyxV has been shown to productively infect 70% of the human cancer cell lines tested from the National Cancer Institute's reference collection[63]. One of several oncolytic poxviruses under development, MyxV has a narrow tropism for transformed human cells, and has been shown in many cancers to infect transformed cells while leaving non-transformed cells unharmed[63]. As discussed in further detail below, several of the hallmarks of cancer, such as inhibition of apoptosis and immune evasion, make tumour cells an ideal environment for poxvirus replication[63,95]. While tumour cells often display defective anti-viral signalling, non-transformed cells, such as primary human macrophages and fibroblasts, mount a robust antiviral response to MyxV that involves viral detection by retinoic acid-inducible gene (**RIG-I**), activation of interferon response factors 3/7 (**IRF 3/7**), and the production of both Type I interferon (**IFN**) and tumour necrosis factor α (**TNFα**)[96,97]. In addition to a defective IFN response, cellular activation of Akt in transformed cells has been proposed to facilitate MyxV infection and

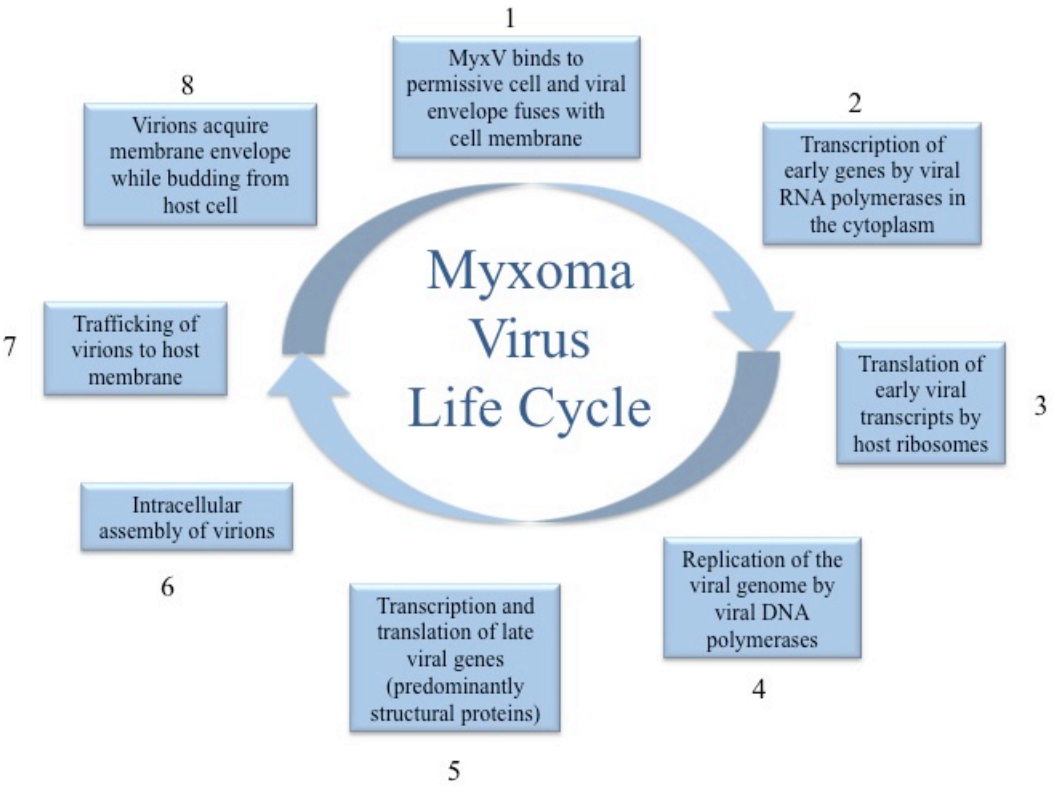

Figure 1.1 Life cycle of MyxV in a permissive tumour cell line

replication[98]. Since the tropism for malignant cells is based upon intracellular signalling rather than the expression of specific cell surface receptors, MyxV's tropism, like other poxviruses, is not limited to a single tumour type[63,95].

Several other therapeutically relevant characteristics make MyxV an attractive oncolytic candidate. Importantly, MyxV has an extremely narrow host tropism outside of human cancers. While the virus causes the lethal infection myxomatosis in the European rabbit (*Oryctolagus cuniculus*), it causes only benign infections in the North American bush rabbit (*Sylvilagus californicus*) and disease has never been observed in any other non-rabbit species[63]. No tropism for other vertebrates was observed when the virus was intentionally release in Australia in the early 1950's to control the over-population of feral European rabbits[99]. Such limited species specificity helps alleviate concerns about off-target infections clinically. Furthermore, MyxV has a large (161.8kb), double-stranded DNA genome, which has been fully sequenced[99]. This facilitates genetic manipulation and the potential insertion of experimentally relevant (e.g. green fluorescent protein (**GFP**)/red fluorescent protein (**RFP**)/luciferase) or therapeutically relevant (e.g. proapoptotic/immunomodulatory/immunostimulant) transgenes into the viral genome[63]. Given the recent successes of "armed" oncolytic virus in clinic[100-102], the ability to introduce transgenes into oncolytic virus candidates constitutes a major advantage. Lastly, like other poxviruses, MyxV DNA replication occurs exclusively in the cytoplasm[99], which obviates safety concerns about viral integration into the host genome[95].

1.4.1 The Myxoma Virus Genome

The genome of MyxV is large and complex, encoding over 150 genes, many of which serve to prevent cell death, attenuate antiviral immunity, and modulate host-virus interactions[99]. The centrally located genes within MyxV's linear genome consist mainly of essential structural proteins (~27) and housekeeping genes (~43) that are highly conserved within the poxvirus family. The more divergent host range and immunomodulatory genes, which appear to have evolved specifically to promote infection within MyxV's natural host, are found in the flanking regions. This latter group of genes includes decoy cytokine receptors (such as TNF decoy receptor M002L/R), complement neutralizing proteins (such as M144R), and anti-inflammatory serpins (such as M008.1L/R), amongst others. The unique nature of the immunomodulatory proteins encoded in these regions likely contributes to the strict host tropism of MyxV; although most known poxviruses encode various immunomodulatory proteins, their targets (which consist of host cytokines, chemokines, and other immune molecules) may not possess a high degree of homology between species[103]. Thus, MyxV's immunomodulatory proteins may be ineffectual against the immune response in other species, leading to swift clearance of infected cells.

In addition to the immunomodulatory proteins, the flanking regions of the MyxV genome also encode several classes of proteins that prevent death or cell cycle arrest by intrinsic cellular factors[99]. For example, M005R/L has been shown to prevent cell cycle arrest in response to viral infection. Poxviruses encode their own transcriptional/translational machinery, which means they do not need to promote cell division for the purpose of

hijacking cellular transcriptional/translational machinery; however, the promotion of cell division does ensure a constant turn-over of essential nucleotides and amino acids that can be sequestered for virion production. Furthermore, various anti-apoptotic proteins, such as M004R/L, M005R/L (MT-5), and M011L, ensure that the host cell remains in a viable state long enough to sustain the production of virions[99,104]. Such anti-apoptotic proteins are preserved across the poxvirus family, with varying degrees of homology[99]. The evolutionary conservation of such proteins highlights the importance of maintaining host cell viability throughout viral infection, and suggests that in the absence of such proteins, poxviruses would induce a swift apoptotic response that would be detrimental to the replication of the virus. In addition to encoding anti-apoptotic proteins, MyxV also encodes a homologue for epidermal growth factor (**EGF**) called M010L, which promotes survival signalling in the infected cell[99,104]. The array of genes designed to prevent host cell death illustrates the urgency with which MyxV must protect its host cell in order to ensure its own survival and replication.

It is clear, even from a cursory observation of the MyxV genome, that many of the proteins it encodes will have profound implications for the efficacy of oncolytic virotherapy. Thus, in investigating MyxV as an oncolytic candidate, one must keep in mind the natural tendencies of the virus to evade the immune system and prevent apoptosis, and strategically design both engineered viruses and combinatorial treatments to exploit these tendencies.

1.4.2 MyxV-mediated Evasion of Apoptosis and Cellular Antiviral Immunity

The plethora of anti-apoptotic proteins conserved across the poxvirus family strongly suggests that in the absence of virally encoded anti-apoptotic proteins, poxviruses induce an apoptotic response that is detrimental to viral replication[105]. *In vivo*, presentation of viral antigen by major histocompatibility complex I (**MHC-I**) can lead to detection of the infected cell by cytotoxic T-lymphocytes (**CTL**) and subsequent induction of apoptosis via the Fas death receptor or granzyme release[105]. Not surprisingly, MyxV and other poxviruses encode proteins (e.g. M153R) that inhibit MHC antigen presentation[99]. However, down-regulation of MHC targets cells for killing by natural killer (NK) cells, and thus MyxV has evolved additional proteins that mimic the ligands for NK cell inhibitory receptors in order to avoid NK-mediated destruction[106]. This complex interplay illustrates the elegance and efficiency of MyxV's multi-faceted anti-apoptotic strategies.

In addition to lymphocyte-mediated apoptosis, several cell-intrinsic pathways are induced in response to viral infection that lead to apoptosis. The production and subsequent autocrine signalling of IFN, the quintessential antiviral cytokine, in response to viral infection can induce a potent apoptotic response[105]. Thus, MyxV and other poxviruses encode secreted decoy IFN receptors (such as M007L/R), which sequester extra-cellular IFN and prevent the induction of apoptosis[104]. TNFα is another important antiviral cytokine, whose corresponding receptor TNF receptor 1 (**TNFR1**) is a well-characterized death receptor[107]. Thus, autocrine signalling by TNFα can potently induce apoptosis in an infected cell. To prevent this, MyxV has evolved soluble decoy TNFα receptor homologues (such as M002L/R) to scavenge and sequester extracellular TNFα[104]. These

two examples illustrate how MyxV's cytokine receptor homologues play a substantial anti-apoptotic role in MyxV infections.

Last but not least, MyxV and other poxviruses employ strategies to directly inhibit intra-cellular apoptotic signalling. M011L is Bcl-2 structural homologue that is localized to the outer mitochondrial membrane, where it inhibits mitochondrial membrane permeablization and the subsequent release of cytochrome *c*, which activates caspases[108]. M011L will be discussed in further detail in later sections.

In the field of OV therapy, it is necessary to question whether the anti-apoptotic effects of MyxV are therapeutically beneficial. Although strategies (viral or pharmacological) that improve viral replication may lead to a more sustained infection in the tumour, overcoming the virus's antiapoptotic signalling mechanisms may lead to more efficient cell death.

1.4.3 MyxV in Preclinial GBM Models

In vitro, MyxV has demonstrated significant oncolytic efficacy against established human glioma cell lines[92], established rat glioma cell lines[94], and patient-derived BTICs[109]. *In vivo*, MyxV effectively cures human MG xenografts in immunocompromised mice with a single orthotopic injection[92] and demonstrates significant efficacy against racine glioma orthografts in immunocompetent syngenic rat models, when used in combination with the immunosuppressant mTOR inhibitor, rapamycin[94]. When used alone or in combination with rapamycin in BTIC xenografts, MyxV significantly prolongs survival but cures are

not obtained, despite a productive viral replication in BTIC tumours[109]. The mechanism driving the reduced susceptibility of BTICs to MyxV has not yet been identified. We are currently investigating mechanisms conferring MyxV resistance and exploring alternative chemotherapeutics as candidates for combination therapy.

1.5 Combination Therapy with Oncolytic Viruses

As with any novel anticancer therapy, OV therapy is most likely to be used clinically in combination with more established therapeutic approaches. As such, significant preclinical testing has been dedicated to determining which drugs and viruses synergize *in vitro* and *in vivo* to provide the most efficacious therapy. The mechanisms of drug-virus interactions tend to fall within four broad categories: (i) drugs act locally upon tumour cells or the tumour microenvironment in order to improve viral replication and/or cell killing, (ii) drugs act systemically upon the immune system to improve viral delivery and reduce immune-mediated viral clearance, (iii) drugs improve virus-induced anti-tumour immunity, and (iv) drugs are administered in combination with rationally-designed viruses that contain drug-activating properties/molecules. Combination treatments that enhance anti-tumour immunity represent a fascinating and complex field that will not be discussed in detail here. Likewise, virus-drug pairs that have been rationally-designed as a self-activating system will not be discussed. However, the first two mechanisms of drug-virus interaction will be discussed in further detail below.

1.5.1 Drugs with Systemic Mechanism of Action

Immune clearance of systemically administered viruses is a major limitation to OV therapy[79]. Thus, several classes of drugs that modulate the innate and adaptive antiviral responses have been shown to improve the efficacy of systemic OV therapy. Since these drugs do not specifically act upon the tumour cells, their combinatory effects with OVs are only observable using *in vivo* systems.

One well-studied example is cyclophosphamide, a DNA cross-linking agent that inhibits DNA replication and induces cell death. Cyclophosphamide has been shown to impair the function of a wide variety of innate and adaptive immune cells, resulting in transient immunosuppression[110]. These immunosuppressive effects contribute to the observed synergy of cyclophosphamide with a wide variety of oncolytic viruses, including reovirus[111,112], HSV[113], adenovirus[114], measles virus[115], VSV[115], and vaccinia virus[116]. Such studies have revealed a multitude of different mechanisms by which cyclophosphamide can inhibit antiviral immunity, including inhibition of complement[117], reduction in levels of virus-neutralizing antibodies[112,115,117], reduction in the intra-tumoral recruitment of phagocytes[113], and reduction in the levels of antiviral cytokines such as IFNα/β and IFNγ[113]. The transient nature of cyclophosphamide-induced immunosuppression makes it an excellent candidate for pre-conditioning the immune system prior to OV therapy. Clinical trials using cyclophosphamide in addition to OV therapy are currently underway[118].

Cyclooxygenase-2 (COX-2) inhibitors have also been shown to synergize with OVs through modulation of the systemic immune system. COX-2 inhibitors have been demonstrated to target B lymphocytes and thus decrease the production of neutralizing antibodies following systemic administration of OVs[119].

The mTOR inhibitor rapamycin has also been shown to demonstrate both local and systemic mechanisms of action. Systemically, rapamycin has been shown to inhibit the proliferation of T and B lymphocytes, reducing levels of neutralizing antibodies against the virus[116]. The local mechanisms of action for rapamycin will be discussed further below.

1.5.2 Drugs with Local Mechanism of Action

A vast array of chemotherapeutics and small molecule inhibitors have been identified that synergize with OVs in a local fashion. Some chemotherapeutics serve to enhance viral replication by suppressing cellular antiviral immune responses; others synergistically induce apoptosis, while still others modulate intracellular signalling to optimize conditions for productive viral infection. Yet others may synergize with OVs by targeting different populations within highly heterogeneous tumours, though this has not been definitively shown. Several examples of drug classes that have been shown to synergize with OVs are discussed below.

Histone deacetylase (**HDAC**) inhibitors, such as valproic acid, vorinostat, and trichostatin A, are transcriptional modulators, which both up- and down-regulate a plethora of genes

(~10% of the human transcriptome), ultimately resulting in cell cycle arrest and apoptosis[120]. These compounds have garnered much attention due to their ability to modulate the cellular antiviral response, thus circumventing the problem of swift viral clearance through the induction of IFN-stimulated genes[120]. HDAC inhibitors have been shown to synergize with a variety of OVs, including VSV[121] and HSV[122,123]. Although the mechanisms of synergy may vary amongst viruses and amongst tissues, down-regulation of IFN-stimulated genes has been suggested as a common mechanism mediating this synergistic interaction[123]. The inhibition of these innate antiviral responses ultimately leads to enhanced viral replication and oncolysis[121,123]. Other mechanisms of synergy include HDAC-induced activation of NF-κB, a transcription factor that is necessary for the successful replication of certain viruses, such as HSV-1, which commandeers NF-κB to promote early viral gene expression[122,124].

Topoisomerase II poisons are another known class of agents that synergize with OVs. Etoposide has been shown to synergize with HSV-1 in a glioma stem cell model through the synergistic induction of apoptosis[125]. Doxorubicin has also been repeatedly shown to synergize with various OVs, including adenovirus[126], coxsackievirus[127], and VSV[128]. Interestingly, VSV was shown to synergize with doxorubicin through the virally-mediated degradation of the anti-apoptotic protein myeloid cell leukemia-1 (**Mcl-1**), resulting in the synergistic induction of apoptosis upon combination treatment[128].

Mitotic inhibitors have also been repeatedly shown to synergize with a variety of OVs. Paclitaxel, a well-characterized tubulin-stabilizing agent, has been repeatedly shown to

synergistically induce apoptosis in mitotically arrested cells when combined with HSV[129,130]. A similar mechanism is observed when taxanes are used in combination with adenovirus[131] and reovirus[131].

Small molecule inhibitors that target the PI-3K/Akt/mTOR pathway have demonstrated synergy with OVs in a variety of distinct ways. For instance, the mTOR inhibitor rapamycin, as discussed above, has been shown to improve viral replication and oncolysis through several mechanisms, including (i) modulation of antiviral responses by inhibiting Type I IFN production[94] (ii) reduction of macrophage infiltration into tumours[94] (iii) activation of Akt to improve susceptibility to MyxV[93,132] and (iv) activation of autophagy[133,134]. Inhibition of PI-3K itself has been shown to synergistically induce apoptosis in combination with HSV-1[135]. Additionally, inhibition of upstream growth factor receptors such as EGFR by erlotinib has been shown to augment cell death in combination with OV therapy, but the interaction was considered additive and no mechanism of synergy was suggested[136].

As the standard-of-care chemotherapeutic in glioma, TMZ has been repeatedly examined for possible synergistic interactions with OVs. In one recent study, HSV-1 was shown to sensitize glioma-initiating cells to TMZ treatment by sequestering DNA damage sensing proteins (such as ataxia telangiectasia mutated, **ATM**) in the HSV replication compartment[137]. In another study, TMZ was shown to enhance adenovirus-mediated killing through the synergistic induction of autophagy[133].

It is noteworthy that many of the combinatorial approaches explored thus far focus upon conventional, standard-of-care chemotherapeutics. This is undoubtedly motivated by the practice of combining standard-of-care therapeutics with experimental therapeutics in early clinical trials, and thus there is a need to characterize such drug-virus interactions prior to the inception of clinical studies. However, the focus on synergy with conventional therapeutics has meant that newer targeted small molecule inhibitors have not been explored as thoroughly.

1.6 Overview of Apoptotic Cell Death

It is clear from the sections above that the induction of programmed cell death is one of the most common mechanisms for synergy between drug and virus. Apoptosis is a form of programmed cell death whereby cellular structures are systematically dismantled and the debris taken up by surrounding phagocytes[138-140]. Some of the key morphological events in apoptosis include fragmentation of the nucleus, hydrolysis of nuclear DNA into short (~200bp) fragments, breakdown of the Golgi apparatus, endoplasmic reticulum, and mitochondrial networks, and blebbing of the plasma membrane[138-140]. Over four hundred cellular proteins are proteolytically cleaved during apoptosis, a process orchestrated by the caspase family of proteases[141]. Importantly, apoptosis is a non-inflammatory form of cell death; unlike necrotic cells, apoptotic cells sequester their cytoplasmic contents into small apoptotic vesicles that can be taken up by phagocytes, instead of releasing the contents of the cytoplasm directly into the extracellular environment[138]. In contrast, necrosis involves the detection of the 'hidden self' (heat shock proteins, single-stranded

RNA, genomic DNA, etc.) in the extracellular space, which elicits a massive inflammatory response that can result in significant bystander damage to surrounding tissues[138]. Thus one of the major functions of apoptosis is to eliminate unnecessary cells discreetly, without the release of proinflammatory danger signals into the extracellular milieu.

1.6.1 Intrinsic and Extrinsic Pathways

A wide variety of stimuli have been shown to activate apoptosis, and these are broadly categorized into intrinsic and extrinsic activation pathways. These pathways are outlined in *Figure 1.2*. In the extrinsic activation pathway, extracellular death ligands such as **TNFα** or Fas ligand bind to their cognate death receptors, TNFR1 and Fas, on the cell membrane. This triggers the recruitment of adapter proteins (such as Fas-associated death domain protein, **FADD**), which then orchestrate the recruitment and activation of initiator caspases, such as caspase-8[138-140]. In the intrinsic pathway, various cellular stress signals, such as DNA damage or withdrawal of growth factors, activate pro-apoptotic members of the B-cell lymphoma-2 (**Bcl-2**) family called BH3-only proteins, typically in a p53-dependent manner[138]. Sufficient activation of these proteins counteracts the signal provided by the anti-apoptotic Bcl-2 family members, and initiates a series of mitochondrial events culminating in the permeabilization of the mitochondrial membrane and the release of the electron transport chain protein cytochrome *c* into the cytoplasm[138-140]. Interestingly, the extrinsic pathway can activate the same pro-apoptotic mitochondrial response as the intrinsic pathway, through caspase-8-mediated pathway crosstalk[139].

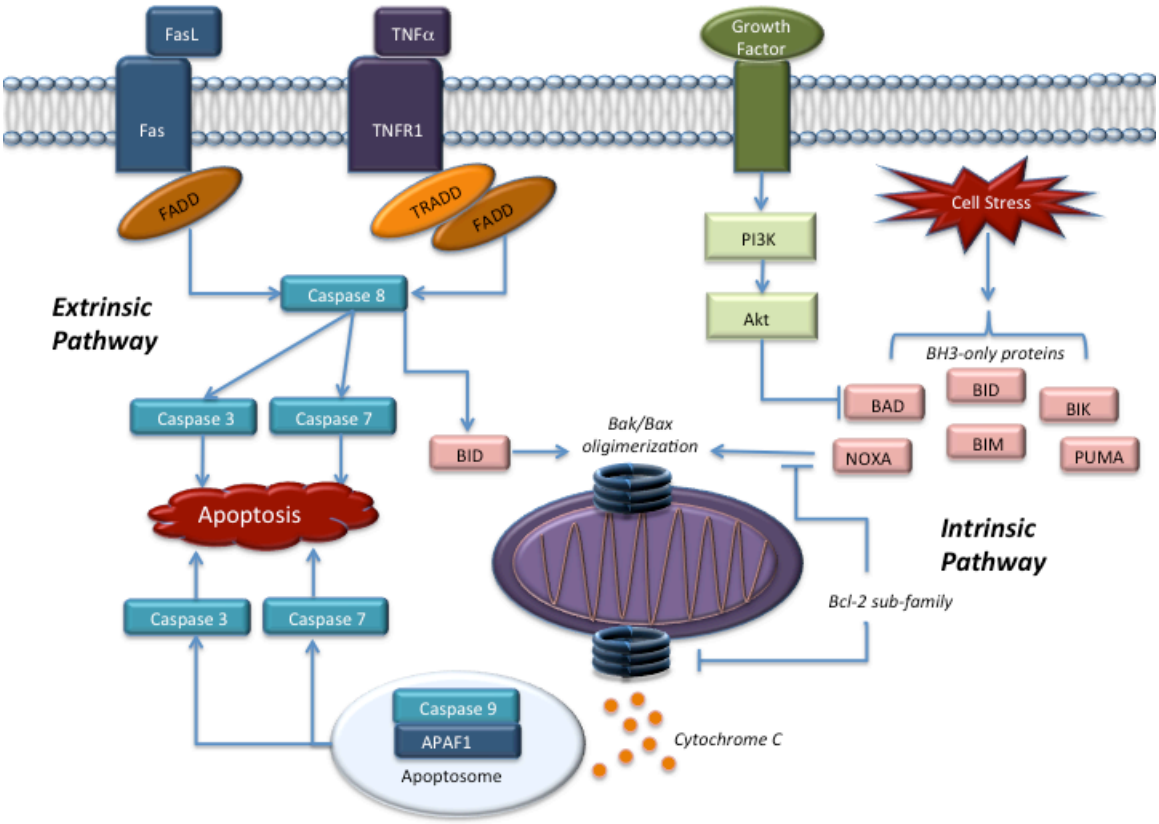

Figure 1.2. Extrinsic versus intrinsic pathways of apoptosis activation

1.6.2 Caspases: The Executioners of Apoptosis

The caspase family, otherwise known as the cysteine aspartic acid-specific protease family, is a highly conserved group of proteases that orchestrate both the initiation and execution of apoptosis. Fourteen mammalian caspases have been identified thus far, eleven of which are known to function in humans[139]. Of these eleven, seven are known to function in apoptosis, while the other caspase family members are modulators of inflammation[139]. The apoptotic caspases can be grouped into the initiator caspases (caspase-2,-8,-9 and -10), which auto-activate, and the effector caspases (caspase-3,-6, and -7), which are activated by the initiator caspases[138]. Effector caspases are responsible for the majority of substrate cleavage events throughout apoptosis.

Importantly, all known caspases are zymogens; in order for a given caspase to become activated, it must be cleaved from its catalytically inactive form. This cleavage reaction yields a large (~20kDa) and small (~10kDa) subunit, which subsequently associate to form a heterodimer; this activation process enables the catalytic site of the caspase to assume its active conformation[138,139]. Caspases typically exist as heterotetramers, composed of two heterodimers that are either constitutively dimerized (for the effector caspases) or dimerize upon apoptotic stimuli (for the initiator caspases). The dimerization of initiator caspases upon apoptotic stimulation allows for auto-cleavage and subsequent activation of the caspase cascade[138].

As mentioned previously, the effector caspases (-3, -6, and -7) are responsible for the vast majority of the morphological changes associated with apoptosis. For instance, these caspases cleave nuclear lamins, as well as various nuclear envelope proteins, resulting in the fragmentation of the nucleus[138,140]. Caspases also regulate the cleavage of DNA itself, though they possess no intrinsic endonuclease activity; instead, the caspases proteolytically cleave a repressor known as protein inhibitor of caspase-activated DNase (**ICAD**). This cleavage event releases caspase-activated DNase (**CAD**), an endonuclease typically repressed by ICAD, which then translocates to the nucleus and cleaves DNA directly[138]. Effector caspases also proteolytically cleave essential proteins involved in DNA metabolism, replication, and repair, such as poly-ADP ribose polymerase (**PARP**), the catalytic subunit of the DNA-dependent protein kinase (**DNA-PKcs**) and DNA topoisomerase II[140]. Other targets of the effector caspases include proteins of the focal adhesion and cell-cell adhesion sites, which facilitates the detachment of the apoptotic cell from neighbouring cells; Golgi stacking proteins, which facilitates degradation of the Golgi network; protein kinases, such as protein kinase C and Akt1, which impairs signal transduction; and important components of the cytoskeleton such as actin, myosin, and tubulins[138,140]. This weakening of the cytoskeleton is believed to enable membrane blebbing[138].

Effector caspase are also essential for shutting down transcription and translational machinery. The targets of caspases include transcription factors (such as NF-κBp65); translation initiation factors (such as eIF2a, eIF3, and eIF4B); and ribosomal proteins (such as p70S6 kinase)[138]. The inhibition of transcription and translation early in

apoptosis is believed to relate to the function of apoptosis as a protective mechanism against viral infection; disabling this cellular machinery helps to prevent it from being hijacked by replicating viruses[138].

1.6.3 Bcl-2 Family Members

The delicate balance between intracellular pro- and anti-apoptotic signals is mediated by a diverse array of proteins, whose interactions fundamentally determine cell fate. Crucial to the process of apoptotic regulation is the Bcl-2 family, which consists of both pro- and anti-apoptotic proteins. Three sub-groups of this family have been identified, each containing a distinctive combination of Bcl-2 homology (**BH**) domains. All Bcl-2 family members contain between one and four of these BH domains. The anti-apoptotic family, which includes proteins such as Bcl-2 and Mcl-1, each contain four discrete BH domains (BH1-4), while the pro-apoptotic family, which includes proteins such as BAK and BAX, contain only BH1-BH3[138]. The third family, the BH3-only family, are highly variable in structure and generally promote the oligomerization and activation of pro-apoptotic proteins, often in a p53-dependent manner[138]. This group includes proteins such as BID, BAD, BIK, and PUMA. The interactions between these three major classes of Bcl-2 family proteins ultimately determine whether a cell will live or die. Under normal circumstances, the anti-apoptotic proteins prevent the BH3-only family members from promoting the oligomerization and activation of the pro-apoptotic family members. In the presence of an apoptotic signal, as illustrated in *Figure 1.2*, the BH3-only proteins are activated en masse; once this activation reaches the critical threshold, the BH3-only proteins induce oligomerization and activation of the pro-apoptotic family members,

leading to outer mitochondrial membrane permeabilization, and the resultant release of cytochrome *c*. Cytosolic cytochrome *c* induces the formation of the apoptosome, a cytosolic complex containing caspase-9 homodimers in combination with the apoptotic proease-activating factor-1 (**APAF1**). This complex facilitates the activation of the caspase cascade[138,139]. The exception to this pattern occurs upon activation of the extrinsic cell death pathway, when, under some circumstances, caspase-8 can cleave BH3-only proteins, such as BID, which activates them, inducing mitochondrial release of cytochrome *c* and subsequent apoptosome formation[138].

Importantly, the Bcl-2 family represents only one mechanism of apoptosis regulation. Other mechanisms, such as regulation of zymogen transcription and direct inhibition of caspases by cellular inhibitor of apoptosis proteins (**cIAPs**), add layers of complexity to the regulation of apoptosis.

1.6.4 Cancer Therapies and Apoptosis

Evasion of pro-apoptotic signalling is a hallmark of cancer, and malignant cells have developed an impressive and diverse array of strategies for avoiding apoptosis[142,143]. These include down-regulation of the tumour suppressor p53 (which occurs in over 50% of human cancers); up-regulation of anti-apoptotic Bcl-2 family proteins; down-regulation of pro-apoptotic Bcl-2 family proteins; as well as constitutive activation of growth and survival pathways such as the PI-3K-Akt axis[142,143]. Innumerable therapeutic strategies have been developed over the years with the intent of reversing this hallmark, ranging from highly pro-apoptotic DNA damaging agents such as topoisomerase poisons

to targeted therapies that inhibit growth factor-driven survival pathways, such as the EGFR inhibitor erlotinib. Small molecule inhibitors that directly inhibit anti-apoptotic Bcl-2 proteins are also under investigation. As discussed in Section 1.5, many combination therapies with viruses have been shown to induce apoptosis, highlighting the importance of pro-apoptotic signalling in pharmacoviral anticancer treatment strategies.

1.6.5 Viruses and Apoptosis

Viral infection has long been recognized as a trigger for apoptotic cell death[138]. The apoptotic response is intended to minimize the opportunity for viral replication and spread, thus limiting infection of adjacent tissues[144]. One important mechanism by which viral infection induces apoptotic signalling is through the induction of cytokines such as IFNα/β and TNFα, which signal in an autocrine manner to promote a swift antiviral response in infected cells. TNFα signalling is a known extrinsic activator of caspase-8-dependent apoptosis (signalling through TNFα's cognate transmembrane death receptor[138]), while IFNα/β signalling activates apoptosis through both intrinsic and extrinsic mechanisms[145]. For instance, IFNα/β signalling triggers the induction of several hundred interferon-stimulated genes (**ISGs**), which include >15 genes with known pro-apoptotic functions. These ISGs include Fas and TRAIL (activators of the extrinsic apoptotic pathway) as well as caspase-8 and caspase-4, among others[145]. Since the induction of apoptosis is generally considered a protective mechanism to prevent further replication and spread of viruses, it stands to reason that viruses have evolved a plethora

of anti-apoptotic mechanisms to combat these and other elements of the pro-apoptotic cellular antiviral response.

1.6.6 Interactions of Viruses with Apoptotic Cell Death Machinery

Viruses have evolved a vast array of mechanisms to modulate the apoptotic response to viral infection[144]. For instance, human cytomegalovirus (**CMV**) encodes a viral protein called viral mitochondria-localized inhibitor of apoptosis (**vMIA**), which inhibits mitochondrial apoptosis by binding to the pro-apoptotic protein Bax[146]. Some viruses, including baculoviruses, also encode viral inhibitor of apoptosis proteins (**vIAPS**), which bind directly to caspases-3 and -7 (among others) and inhibit their catalytic activity[144]. Some viruses, such as adenovirus, encode proteins that directly bind to p53, inhibiting the pro-apoptotic activity of this transcription factor, while other viruses such as HPV-16 encode proteins that help to target p53 for ubiquitin-mediated degradation[144,147]. Adenovirus was the first virus shown to encode a viral homologue for the cellular anti-apoptotic protein Bcl-2[144]. This adenovirus protein (E1B-19K) was shown to sequester cellular pro-apoptotic proteins such as Bak and Bax. Since this discovery, Bcl-2 homologues have been discovered in a variety of viruses, including herpesviruses and poxviruses, among others.

1.6.7 MyxV M011L: Bcl-2 Homologue

Amongst the most well-characterized of MyxV's anti-apoptotic proteins is the 160 amino acid viral Bcl-2 homologue M011L. M011L was first identified as a crucial virulence factor in MyxV-induced myxomatosis in rabbits, and the M011L knock-out (**MyxV-**

M011L-KO) virus was initially shown to be associated with impaired virus replication and attenuated disease[148]. Recent work has verified that M011L is a structural but not sequence homologue of Bcl-2[149].

Molecular characterization of M011L has shown that this protein is localized to the mitochondria[150], where it interacts with the membrane permeability pore and prevents the loss of membrane integrity that is associated with mitochondrial apoptosis[151]. M011L localization to the membrane pore prevents the release of cytochrome *c* from the mitochondria and thus attenuates pro-apoptotic signalling following exposure to staurosporine[151]. Subsequent studies demonstrated that M011L not only associates with the membrane pore, but also associates with (and inhibits) the pro-apoptotic proteins BAK and Bax, but not other Bcl-2 family members[108,152]. It was also shown that this association serves to block the induction of apoptosis in response to pro-apoptotic stimuli such as Fas-ligand binding, and that the anti-apoptotic functions are species independent, perhaps due to the high degree of homology observed in the mammalian Bcl-2 family[152]. Knocking out viral M011L appears to attenuate viral replication compared to wildtype virus in some cell lines[153]; however, the possibility of using the knock-out virus as a pro-apoptotic anti-cancer agent has not been explored.

1.6.8 Alternatives to Apoptosis: Autophagic Cell Death

Autophagy is a highly conserved catabolic process whereby cytoplasmic contents and organelles are encapsulated in vacuoles known as autophagosomes and delivered to the lysosome for degradation[154-156]. The result of this degradation process is an abundance of

molecular building blocks, such as amino acids, fatty acids, and nucleotides, which are shuttled back into the cytoplasm to be recycled in anabolic cellular processes[155]. The process is regulated by a family of autophagy-related genes (**ATGs**) that tightly regulate the five steps of the autophagosome's life cycle (initiation, elongation, closure, maturation, and degradation). The initiation stage of autophagy is largely but not exclusively regulated by mTOR, which acts as a nutrient sensor; when nutrients are abundant, mTOR binds to and represses the activity of the ULK1/2 complex (the mammalian homologue of ATG1)[155]. In conditions of nutrient deprivation, mTOR signalling is reduced and the ULK1/2 complex is activated, initiating autophagosome formation. The Vps34-p150-Beclin-1 complex provides an additional level of regulation at the initiation step[155]. The subsequent elongation and closure stages of autophagosome formation are regulated by a variety of proteins, including the ATG5-ATG12 complex and the microtubule-associated protein 1 light chain 3 (**LC3**)[155]. LC3 is present in the double membrane of autophagosomes and is widely used as a marker of autophagy. Other conventional markers of autophagy include the formation of autophagosomes detectable by electron microscopy and the processing of LC3 through cleavage and lipidation to form LC3-II, which is detected as a faster migrating band on immunoblots[155].

Autophagy is often considered a double-edged sword: on the one hand, it is a crucial survival mechanism, particularly under conditions of nutrient starvation, which allows essential nutrients to be recycled by the cell[156]. On the other hand, autophagy is often considered the second type of programmed cell death (apoptosis constitutes type I programmed cell death)[156]. Various chemotherapeutics have been suggested to kill

glioma cells through the induction of autophagy, including TMZ[157], ceramide[158], and arsenic trioxide[159].

Autophagy is a common cellular response to viral infection, as this process provides a mechanism for engulfing and degrading whole virus particles[144]. Additionally, autophagy provides a mechanism for intra-cellular pattern recognition receptors (**PRRs**) to detect viral infection. For instance, Toll-like receptors (**TLRs**) -3, -7/-8, and -9, which detect double-stranded DNA, single-stranded RNA, and CpG DNA respectively, are endosomal; autophagy provides a mechanism to deliver virus particles to the endosome where they may be detected by the cell's innate antiviral machinery[154]. Interestingly, activation of certain TLRs, including TLR-3 and -7, can induce autophagy directly; TLRs induce autophagy through their adapter proteins TRIF and Myd88, which, upon activation, may associate directly with Beclin-1, resulting in the formation of Vps34-Beclin-1 complexes and the subsequent induction of autophagy[154]. In order to avoid the induction of antiviral immunity, many viruses, such as herpesviruses, have evolved mechanisms to inhibit autophagic cell death[144]. One such strategy employed by herpesvirus family members is to inhibit Beclin-1, thus blocking the autophagic pathway[154]. Both hepatitis B and C are known inducers of autophagy, yet successfully inhibit autophagosome acidification in the late stages of autophagy[154].

Interestingly, inhibition of apoptosis and inhibition of autophagy are seldom employed by the same virus; inhibition of one form of cell death serves to positively reinforce cell death through the alternate mechanism. For example, influenza virus can inhibit

autophagy through viral matrix protein 2, yet this process facilitates apoptotic cell death in infected cells.[144] Conversely, bystander T cells whose apoptosis pathways are inhibited during HIV infection are pushed down an autophagic death pathway[144]. Given the dysregulated apoptotic pathways in malignant cells, and the host of anti-apoptotic mechanisms encoded by viruses, it is prudent to include autophagic cell death in the discussion of mechanisms by which viruses selectively kill cancer cells.

1.7 Objective and Specific Aims

Previous work in our lab has confirmed that BTICs are only moderately susceptible to MyxV *in vitro* and *in vivo*. The objective of this thesis is to investigate the mechanism of MyxV-mediated cell death in BTICs and to identify chemotherapeutic agents that synergize with MyxV using a small molecule inhibitor drug screen approach.

The following aims will be addressed:

(i) To verify the baseline susceptibility of a panel of BTICs to MyxV infection and killing, and to interrogate the mechanism of MyxV-mediated cell killing

(ii) To screen a library of 73 small molecule inhibitors against a candidate BTIC line *in vitro* to identify compounds that synergize with MyxV

(iii) To characterize one of the lead compounds in a panel of BTICs and to determine downstream target modulation

Chapter Two: Materials & Methods

2.1 BTIC Isolation and Culture

BTIC lines were initially derived from GBM patient specimens by personnel in the laboratory of Dr. Samuel Weiss, on behalf of the Neurologic and Pediatric Tumour and Related Tissue Bank, Foothills Hospital, Calgary, Alberta. Multiple BTIC lines were transferred to the Forsyth Lab with permission under a Material Transfer Agreement.

In contrast to conventional immortalized cell lines (e.g. U87), BTICs were cultured under highly specialized neural stem cell conditions initially developed at the University of Calgary[160]. Instead of growing as an adherent monolayer, BTICs were cultured as neurospheres at 37°C in a humidified 5% CO_2 incubator using serum-free neural stem cell media (Stem Cell Technologies, Vancouver, BC, Canada). Media was supplemented with recombinant human EGF (20ng/mL; Stem Cell Technologies) and FGF (20µg/µl; Stem Cell Technologies) as described previously[31]. Since traditional concepts of confluency do not apply to non-adherent BTICs, neurosphere size is used as a guide to inform frequency of passaging. To avoid cell death in the center of growing neurospheres, BTICs were passaged every 3-5 days. BTICs were dissociated using 1X Accumax Cell Detachment Solution (a cell aggregate dissociation medium containing collagenolytic and protease components, Stem Cell Technologies) as follows: cells were incubated with equal volumes of media and Accumax for five minutes at 37°C, then rinsed with phosphate buffered saline (PBS; 137mM NaCl; 2.68mM KCl; 8.1mM

Na_2HPO_4; 1.47mM KH_2PO_4; pH 7.5) and reseeded at ~1x10^5/mL in polystyrene tissue culture flasks.

2.2 Glioma Cell Line Culture

Immortalized human glioma cell lines (U87, U251, U118) were purchased from the American Type Culture Collection (ATCC; Manassas, VA, USA) and cultured in Dulbecco's Modified Eagle's Medium, nutrient mixture F-12 (DMEM-F12; GIBCO Life Technologies, Burlington, ON, Canada) with 10% fetal bovine serum (FBS; GIBCO Life Technologies) at 37°C in a humidified 5% CO_2 incubator. Cell were passaged at ~80% confluency through enzymatic dissociation using 0.05% 1X Trypsin-EDTA with phenol red (GIBCO) and replated in DMEM-F12.

2.3 Viral Titration and Gene Expression Assays

Virus was obtained from the McFadden laboratory (University of Florida, Gainesville, FL). MyxV-dsRed consists of wildtype MyxV with a discosoma red fluorescent protein (dsRED) cassette under the control of a late viral promoter. MyxV-FLuc contains both a green fluorescent protein (GFP) and an enhanced firefly luciferase (FLuc) reporter under the control of an early viral promoter[109]. MyxV-M011L-KO, which has been extensively characterized elsewhere[151,153] contains a LacZ reporter under the control of an early viral promoter. Virus was propagated by Dr. Xueqing Lun as described elsewhere[161] and stored in aliquots at -80˚C. Titration of viral stock was performed on baby green monkey kidney (BGMK) cells, using fluorescent foci-forming assays (MyxV-dsRED, MyxV-FLuc) and plaque-forming assays (MyxV-M011L-KO) respectively. Briefly, BGMKs

were seeded at 2.5 x 10^5 cells/mL in duplicate 6-well plates and grown until confluent. Cells were treated with diluted viral stock (10^{-3}- 10^{-8} virions) for 48hrs (foci-forming assay) or 96hrs (plaque-forming assay). Foci were counted using the rhodamine filter on a Zeiss inverted microscope (Axiovert 200M) at 40x magnification. Plaques were counted at 100x magnification on a Zeiss inverted microscope following staining of the cells with crystal violet (0.1%w/v in 20% ethanol) as described elsewhere[161]. Briefly, media was aspirated and 0.5mL crystal violet (kind gift from the laboratory of Dr. Paul Beaudry) added to each well of duplicate 6-well plates. Plates were incubated for 1hr at room temperature (gently swirling), then crystal violet was aspirated and plates inverted to dry wells. Unstained plaques were counted at 100x magnification. All virus work was performed in a dedicated biological safety cabinet, Thermo Fisher Scientific Model 1387.

Dead virus was prepared by irradiating MyxV-dsRED with ultraviolet light (UVC band) for 4-6hrs. Dead virus-treated cells were visually confirmed to have no evidence RFP expression using fluorescence microscopy 48hrs post-infection.

Late viral gene expression was measured over time by infecting BTICs with RFP-tagged MyxV-dsRED at the indicated multiplicity of infection (**MOI**) in black-sided 96-well plates and monitoring fluorescence (excitation = 544nm, emission = 590nm) using the GloMax Multi Detection System plate reader (Promega; Madison, WI, USA). RFP expression was verified visually using the Zeiss inverted microscope. Early viral gene expression was measured by infecting BTICs with firefly luciferase-tagged MyxV-FLuc at the indicated MOI in black-sided 96-well plates, with or without the indicated

concentrations of drugs. All treatments were performed in quadruplicate. Luminescence (total photon flux emission, measured in photons/sec) was measured (following a ten minute incubation with the luciferase substrate, 150μg/mL D-luciferin potassium salt in sterile water, Caliper Life Sciences, Waltham, MA, USA) in virus-only, drug-only, and combination-treated BTICS 24hrs post-infection using the GloMax Multi Detection System plate reader, with an integration of 0.5sec. Luminescence values were normalized to 1 MOI of virus. All treatments were performed in quadruplicate.

2.4 Viability Assays

BTIC susceptibility to virus alone was assessed by plating cells (10,000 cells/well) in 96-well clear-bottom tissue culture plates, and infecting with MyxV-dsRED at the indicated MOI. All treatments were performed with internal replicates of six. At the indicated time point, viability was measured using Alamar blue (Invitrogen, New York, USA) according to manufacturer's instructions. Absorbance was measured on a Spectra Max plate reader at 570nm. Background absorbance values at 600nm were subtracted from the absorbance values at 570nm. The resulting values were subsequently expressed as a percentage of the untreated control absorbance.

2.5 Caspase Activation Assays

Caspase-3/-7 activity was measured using the Caspase-3/-7 Glo© assay from Promega. BTICs were plated at 1 x 10^4 per well in black-walled 96-well plates and treated with UV-inactivated virus, MyxV-dsRED, or MyxV-M011L-KO at 10MOI unless otherwise indicated; with 1μM doxorubicin (ChemieTek, Indianapolis, IN, USA in water) as a

positive control for apoptosis, or with 1μM ionomycin (in dimethyl sulfoxide (**DMSO**) kindly provided by the laboratory of Dr. Jaideep Bains) as a control for necrotic cell death. The pan-caspase inhibitor ZVAD-FMK (carbobenzoxy-valyl-alanyl-aspartyl-[O-methyl]-fluoromethylketone) (Promega) was also included as a negative control for caspase activation (1hr pre-treatment with 1μM ZVAD). The Caspase-3/-7 Glo© assay was performed according to manufacturer's instructions, with internal replicates of four. Luminescence was measured using a GloMax Multi Detection System plate reader, using an integration of 0.5sec. Results were normalized to the untreated control.

2.6 Immunoblots

BTICs were seeded in a 6-well plate at $5x10^5$ cells/well and treated with MyxV (at the indicated MOI), dead virus (at equivalent MOI), doxorubicin (1μM unless otherwise stated), rapamycin (ChemieTek; 1μM unless otherwise stated), or axitinib (ChemieTek; 300nM unless otherwise stated). Cells harvested for target modulation were incubated for 24hrs. Cells harvested for cell death experiments were incubated for 48hrs.

After the appropriate incubation, BTIC cells were collected, rinsed with PBS, and lysed using Triton X-100-based lysis buffer (20mM Tris, 400mM NaCl, 1mM EDTA, 1% Triton-X-100), supplemented with Complete™ protease and phosphatase inhibitor cocktail tablets (Roche, Mississauga, ON, Canada) and sodium orthovanadate (1mM final concentration; New England Biolabs, Ipswich, MA, USA). Protein concentrations were measured using a colorimetric Bradford protein assay (BioRad, Hercules, CA, USA) and normalized to a bovine serum albumin standard curve. Protein samples were mixed with

5x reducing buffer [0.2M Tris HCl buffer (1.25M Tris, 0.4% sodium dodecyl sulphate (SDS), pH 6.8), 20% v/v glycerol, 10mM β-mercaptoethanol, 10% w/v SDS, 0.05% w/v bromophenol blue] and double-distilled water to a total volume of 20µl, boiled for five minutes at 95˚C, and loaded in 12% poly-acrylamide (37.5:1 acrylamide:bis-acrylamide ratio; BioRad) or 8% poly-acrylamide gels. Proteins were separated by sodium dodecyl sulphate polyacrylamide gel elecrophoresis (**SDS-PAGE**) using running buffer (25mM Tris, 192mM glycine, 3.47mM SDS in double-distilled water) and transferred in transfer buffer (25mM Tris, 193mM glycine in double-distilled water with 20% v/v methanol) to a nitrocellulose membrane (40V for 180 minutes at 4˚C). The membrane was blocked in 5-20% low-fat milk in Tris-buffered saline with 0.2% Tween-20 (**TBST**; 20mM Tris, 137mM NaCl, 0.2% w/v Tween-20) for 1hr at room temperature. Blots were subsequently probed using the following antibody combinations, diluted in 5% bovine serum albumin in TBST: Caspase-3(3G2) mouse monoclonal antibody (1/1000, Cell Signaling #9668), with horseradish peroxidase (**HRP**)-tagged goat anti-mouse secondary antibody (1/5000); Caspase-7 Antibody (1/1000; Cell Signaling #9492) with HRP-tagged goat-anti-rabbit secondary antibody (1/5000); LC3B antibody (1/200, Cell Signaling #2775) with HRP-tagged goat-anti-rabbit secondary antibody (1/5000); PARP Antibody (Cell Signaling #9542, 1/1000) with HRP-tagged goat-anti-rabbit secondary antibody (1/5000); PathScan Multiplex Western Cocktail I (1/1000, Cell Signaling #5301) with HRP-tagged goat-anti-rabbit secondary antibody (1/5000). Primary antibodies were incubated at 4˚C overnight, while secondary antibodies were incubated at room temperature for 2hrs. Prior to being developed, blots were washed three times for 15min in TBST at room temperature. Protein bands were detected using Western Lightning Plus

Enhanced Chemiluminescence (**ECL**; Fisher Scientific, Toronto, ON, Canada). Blots were probed with β-actin (1/1000, Cell Signaling #4970) with HRP-tagged goat-anti-rabbit secondary (1/5000) as a loading control.

2.7 ZVAD-induced Caspase Inhibition

The cell-permeable caspase inhibitor ZVAD-FMK (Promega) was used to block caspase activation. ZVAD was added 1hr prior to treatment at a concentration of 1μM unless otherwise indicated.

2.8 Small molecule inhibitor drug screen

The drug library, compiled by ChemieTek, was a generous gift from Dr. Aru Narendran. The library consists of 73 small molecule inhibitors in various stages of preclinical and clinical development (*Appendix I*). The initial high-throughput screen was performed as follows: BT025 cells were plated at 1 x 10^4 cells per well in a 96-well plate and treated with either drug alone (1μM), virus alone (1MOI) or a combination of drug and virus (1μM and 1 MOI), in internal replicates of six. Combination treatments involved pre-treatment of cells with drug for four hours prior to viral infection. At 48hrs post-infection, BTIC viability was assessed via Alamar blue. Results were graphed as the difference in cell viability between drug-only and combination-treated BTICs. Compounds were considered to be hits when the difference in cell viability between drug-only and combination-treated BTICs exceeded 20%.

For the 22 drugs that demonstrated high cytotoxicity in the initial screen (>70% cell death at 48hrs with drug alone), the same assay was repeated with drug doses of 100nM, three independent times. Drugs were considered hits when the combination killed significantly (p<0.05) more cells than either treatment alone. For the drugs that demonstrated high cytotoxicity at 100nM, a third screen was performed at 10nM using the same conditions.

Chou-Talalay analysis

Cells were plated at 1 x 10^4/well in 96-well plates and treated as follows in internal replicates of eight: (i) no treatment (ii) drug alone (1μM, 3μM, 10μM for high-dose hits; 100nM, 300nM, and 1000nM for low-dose hits) (iii) virus alone (1 MOI, 3 MOI, 10 MOI) and (iv) combination treatments including every combination of drug and virus concentration listed. For each of the combination treatments, cells were pre-treated with drug for 4hrs prior to infection with virus. Cells were incubated as described above for 48hrs and viability measured by Alamar blue.

Combination indices (**CI**) were calculated using the Chou-Talalay method[162], which stipulates that a CI>1 indicates antagonism, a CI =1 indicates an additive effect, and a CI<1 indicates synergy. CI values were calculated according to the following formula for drugs with a mutually exclusive mechanism[162]:

$$CI = \frac{(D)_1}{(D_x)_1} + \frac{(D)_2}{(D_x)_2}$$

where $(D_x)_1$ and $(D_x)_2$ represent the concentration of drugs 1 and 2 alone required to achieve 50% cell kill, while $(D)_1$ and $(D)_2$ represent the concentrations of each drug required to achieve 50% cell kill in combination. A sample calculation is provided below.

Drug A has an IC_{50} of 500nM when administered alone.

Drug B has an IC_{50} of 300nM when administered alone.

When Drug A is administered at a range of doses in combination with Drug B at 100nM, the IC_{50} of Drug A is shown to be 250nM.

The CI calculation would thus be performed as follows:

$(D_x)_A$ = 500nM, $(D_x)_B$ = 300nM, $(D)_A$ = 250nM and $(D)_B$=100nM.

CI = (250/500) + (100/300) = 0.833

The CI <1 indicates that this interaction is synergistic when Drug B is administered at 100nM.

In an alternative scenario, if the IC_{50} of Drug A is shown to be 200nM when administered at a range of doses in combination with Drug B at 200nM, the CI would be performed as follows:

$(D_x)_A$ = 500nM, $(D_x)_B$ = 300nM, $(D)_A$ = 200nM and $(D)_B$=200nM

CI = (200/500) + (200/300) = 1.067

The CI ≈ 1 indicates that the same two drugs are not synergistic at this dose but rather the combination effect is additive in nature.

In our investigation, the IC_{50} of MyxV was calculated at given doses of each drug (rather than IC_{50} values of drugs calculated at given concentration of virus), so that the IC_{50} values of MyxV could be directly compared across an array of combination treatments.

Statistical analysis

All statistical analysis was performed using Microsoft Excel. Student's T-tests are two-sided and considered significant at $p<0.05$.

Chapter Three: Characterization of BTIC Susceptibility to MyxV

3.1 Introduction & Rationale

As discussed in Chapter I, BTICs represent an important preclinical model in the development of novel therapeutics for GBM. Although conventional glioma cell lines are exquisitely sensitive to MyxV-mediated cell death *in vitro* and *in vivo*, achieving durable cures with a single intracranial injection of MyxV, patient-derived BTICs have been shown to be only moderately susceptible to MyxV-mediated cell death *in vitro* and *in vivo*[109]. Previously, our lab has demonstrated that MyxV-mediated cell death can be improved by co-treatment with the mTOR inhibitor rapamycin[109]. Although rapamycin enhances cell killing *in vitro* and prolongs survival *in vivo*, durable cures are still not obtained[109]. In this investigation, we sought to identify other pharmacological agents that improve MyxV-mediated BTIC cell death *in vitro.*

In order to identify compounds that sensitize BTICs to MyxV-induced cell death, it was first essential to verify the baseline susceptibility of the BTICs to MyxV infection and killing. For this characterization, we utilized a panel of genetically distinct BTICs bearing different combinations of clinically relevant GBM mutations, such as loss of PTEN, mutation or loss of p53, and mutation or over-expression of EGFR. The characteristics of these BTIC lines and their associated mutational profiles are shown in *Table 3.1.* These BTIC lines were initially derived and characterized by the laboratory of Dr. Samuel

Table 3.1: Characteristics of BTIC Panel

BTIC	EGFR Status	p53 Status	PTEN Status	TMZ Resistance	Growth Pattern	Gene Expression Data
BT012	Wt	Wt	(N49I)	Resistant	Spheres	Yes
BT025	Wt	(T125R)	(G129R)	Resistant	Spheres	Yes
BT048	(K294R) (G598V)	Wt	Deletion at residue 17 (frameshift, truncation)	Susceptible	Spheres	Yes
BT073	EGFR VIII	(V272L) (R273H)	Insertion at intron 4 causing frameshift	Resistant	Spheres	Yes
BT124	Wt	Stop at 182	In frame deletion 293-342	Unknown	Spheres	No

Weiss, and were used with permission in the Forsyth Lab under a Material Transfer Agreement. The susceptibility of three of these BTIC lines (BT012, BT025, and BT048) to MyxV has previously been characterized in our lab[109], while the more recently derived lines (BT073 and BT124) were previously uncharacterized in terms of MyxV susceptibility.

A variety of factors were considered when designing the panel of BTICs to be used in this investigation, including: (i) the inclusion of several BTICs whose response to MyxV has already been well-characterized (BT012, BT025, BT048), (ii) the inclusion of both relatively MyxV-resistant (BT048, BT025) and MyxV- susceptible (BT012) BTIC lines, (iii) the inclusion of multiple TMZ-resistant cell lines (BT012, BT025, BT073)[59], (iv) the exclusion of cells that do not grow as typical neurospheres in culture (e.g. BT042), (v) the inclusion of BTICs with varied mutational profiles, (vi) the inclusion of BTICs that grow relatively quickly in culture, and (vii) the inclusion of multiple BTICs for which gene expression profiling data were available (BT012, BT025, BT048, BT073). Based upon all these criteria, a panel of diverse BTICs was assembled for further study.

In addition to determining baseline susceptibility of BTICs to MyxV-mediated cell death, the mechanism of cell death in MyxV-infected BTICs was also investigated. Several mechanisms of OV-mediated cell death have been described in the literature, including lysis[163], apoptosis[164], and autophagy[165], but this remains an active area of investigation with complex implications for OV therapy. In this study, the mechanism of cell death was hypothesized to have important implications for combination therapy. For instance, a

virus that kills by apoptosis may synergize with other pro-apoptotic agents, while the same virus may antagonize agents that kill by autophagy. An understanding of the mechanism by which MyxV mediates BTIC cell death would help to inform the mechanism by which synergistic compounds identified in later chapters might improve MyxV-mediated cell death.

3.2 BTICs demonstrate variable susceptibility to MyxV-induced cell death

Viability of BTICs following infection was assessed via colorimetric assay (Alamar blue) at 24, 48, and 72hrs post-infection at 0-10 MOI (*Figure 3.1*). Susceptibility to MyxV-mediated cell death was variable, with BT012 demonstrating the greatest susceptibility to MyxV, BT124 demonstrating moderate susceptibility to MyxV, and BT025, BT048, and BT073 demonstrating the least susceptibility to MyxV-induced cell death. Complete cell death (0% viability) was only observed in one BTIC line (BT012) at 72 hrs post-infection at the highest MOI tested (10 MOI). By contrast, the majority of the BTIC lines (including BT025, BT048, and BT073) retained ~40-50% viability despite 72-hr treatment with 10 MOI of MyxV. This solidified previous observations that many BTICs are only moderately susceptible to MyxV *in vitro*[109], which may underlie the limited efficacy of MyxV as a monotherapy *in vivo*[109]. To verify that the observed decrease in viability was due to cytotoxic and not cytostatic effects, absolute values of the absorbances obtained in the Alamar blue assay were analyzed (*Figure 3.2*). Absolute values that decrease over time indicate a treatment-induced loss of cell viability, whereas absolute values that remain steady over time indicate a lack of cell replication. At 10 MOI, absorbance values demonstrated a downward trend over time. At 1 MOI, absolute

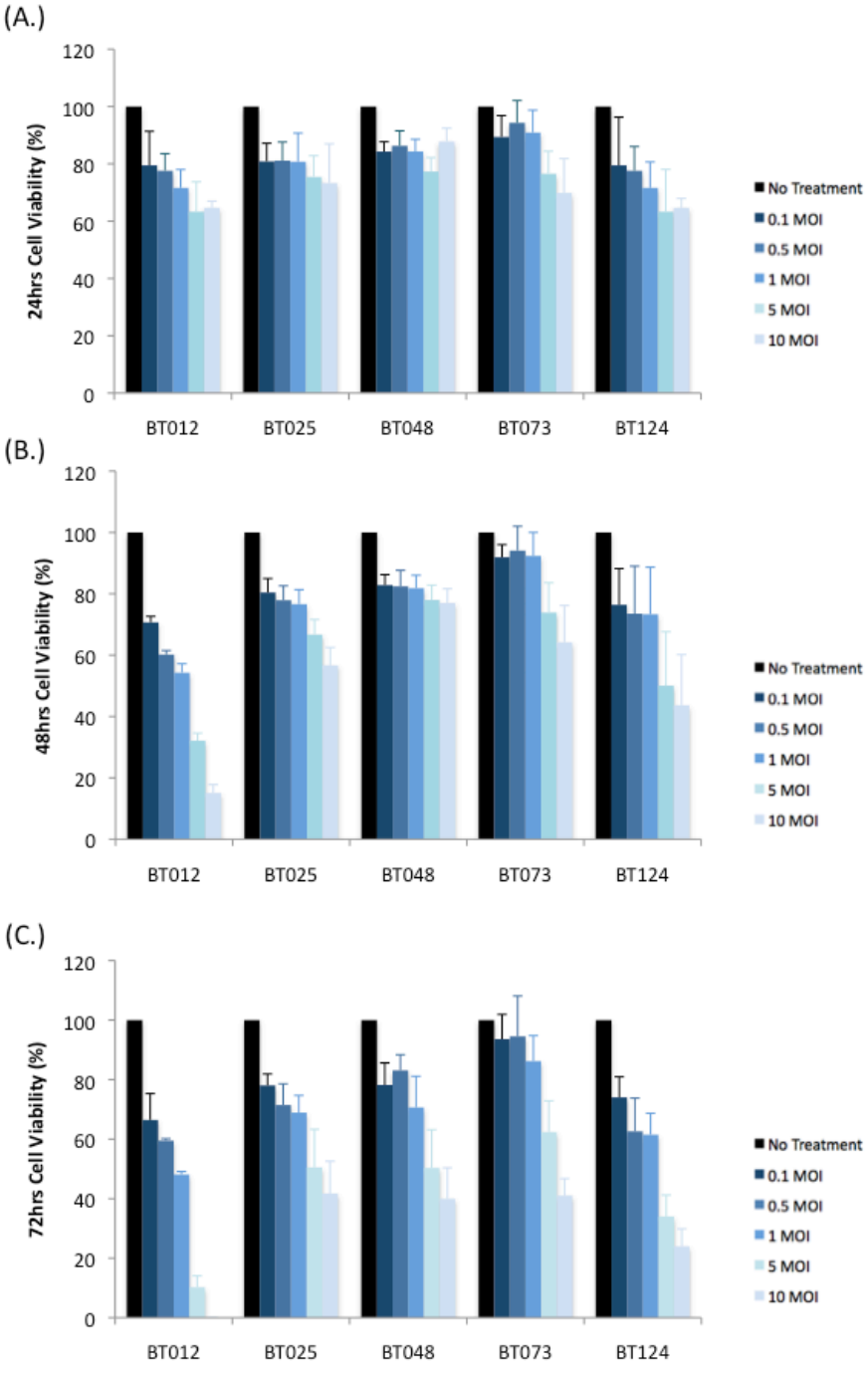
(A.)
24hrs Cell Viability (%)
120
100
80
60
40
20
0
BT012
BT025
BT048
BT073
BT124
No Treatment
0.1 MOI
0.5 MOI
1 MOI
5 MOI
10 MOI
(B.)
48hrs Cell Viability (%)
120
100
80
60
40
20
0
BT012
BT025
BT048
BT073
BT124
No Treatment
0.1 MOI
0.5 MOI
1 MOI
5 MOI
10 MOI
(C.)
72hrs Cell Viability (%)
120
100
80
60
40
20
0
BT012
BT025
BT048
BT073
BT124
No Treatment
0.1 MOI
0.5 MOI
1 MOI
5 MOI
10 MOI

Figure 3.1: BTICs demonstrate variable susceptibility to MyxV-induced killing

Five BTIC lines were each disrupted into a single cell suspension and seeded at $1x10^4$ cells/well in a 96-well plate in serum-free neural stem cell media (+EGF,+FGF). Twenty-four hours later, the cells were infected with the indicated MOI of MyxV-RFP (0.1-10MOI) or a no-treatment, media-only control (NT), and allowed to incubate for 24hrs (*panel A*), 48hrs (*panel B*) or 72hrs (*panel C*) post-infection. Cell viability was assessed colorimetrically using Alamar blue according to the manufacturer's instructions, with absorbance values normalized to the no-treatment control. Data are presented as mean +/- standard error and represent three independent experiments, each with six internal replicates.

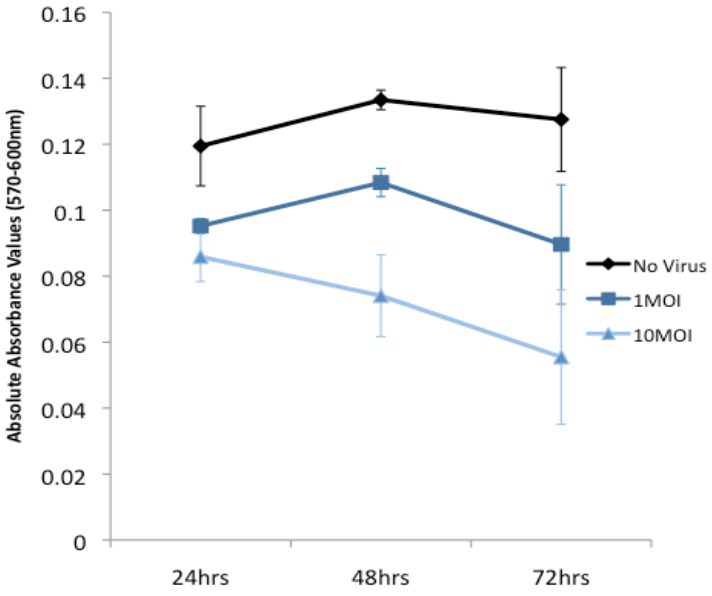

Figure 3.2: MyxV infection at high MOI results in cell death

BT025 neurospheres were disrupted into single cell suspension and seeded at $1x10^4$ cells/well in a 96-well plate in serum-free neural stem cell media (+EGF, +FGF). Twenty-four hours later, the cells were infected with the indicated MOI of MyxV-RFP (1 or 10 MOI) or a no-treatment, media-only control (NT), and allowed to incubate for the indicated time. Cell viability was assessed colorimetrically using Alamar blue according to manufacturer's instructions, and raw absorbance values were plotted. Data are presented as mean +/- standard error and represent three independent experiments, each with six internal replicates. The data show that absolute absorbance values of MyxV-treated BT025 tend to decrease over time at high MOI, and do not change at low MOI. This indicates that cell death occurs at high MOI, though not necessarily at low MOI.

absorbance did not change over time, indicating that virus-induced cell death may be offset by cell replication of uninfected cells at low MOIs.

3.3 MyxV infects all BTICs tested

The absence of dramatic BTIC killing following infection with MyxV may be attributed to a failure of the virus to either effectively infect or replicate in BTICs. To verify that MyxV establishes a productive viral infection, we utilized a MyxV construct tagged with RFP under the control of a late viral promoter (MyxV-dsRED). Although certain other MyxV constructs bear more sensitive reporters than MyxV-dsRED, such as MyxV-FLuc which has a luciferase reporter under the control of an early viral promoter, dsRED was preferred for several reasons: (i) the fluorescent reporter can be monitored over multiple time points without cumulative dilution of the sample, (ii) a reporter under the control of a late viral promoter indicates that viral genomic replication has occurred, whereas a reporter under the control of an early viral promoter merely indicates entrance of the virus into the cell, and (iii) viral infection and replication are not primary endpoints for the drug screen, and thus sensitivity is not of the utmost importance. As demonstrated in *Figure 3.3,* all BTIC lines expressed RFP at 48 hours post-infection with MyxV. For four of the five BTIC lines tested, the majority of spheres are infected at 48hrs following treatment with 10 MOI MyxV (75-100% of neurospheres by visual inspection at time of infection), while only a minority of BT048 spheres are infected (<50% by visual inspection at time of infection). This late viral gene expression provides a strong indication that both viral entry and genomic replication have occurred, demonstrating that the virus is not eliminated from the cell by innate antiviral responses early within its life

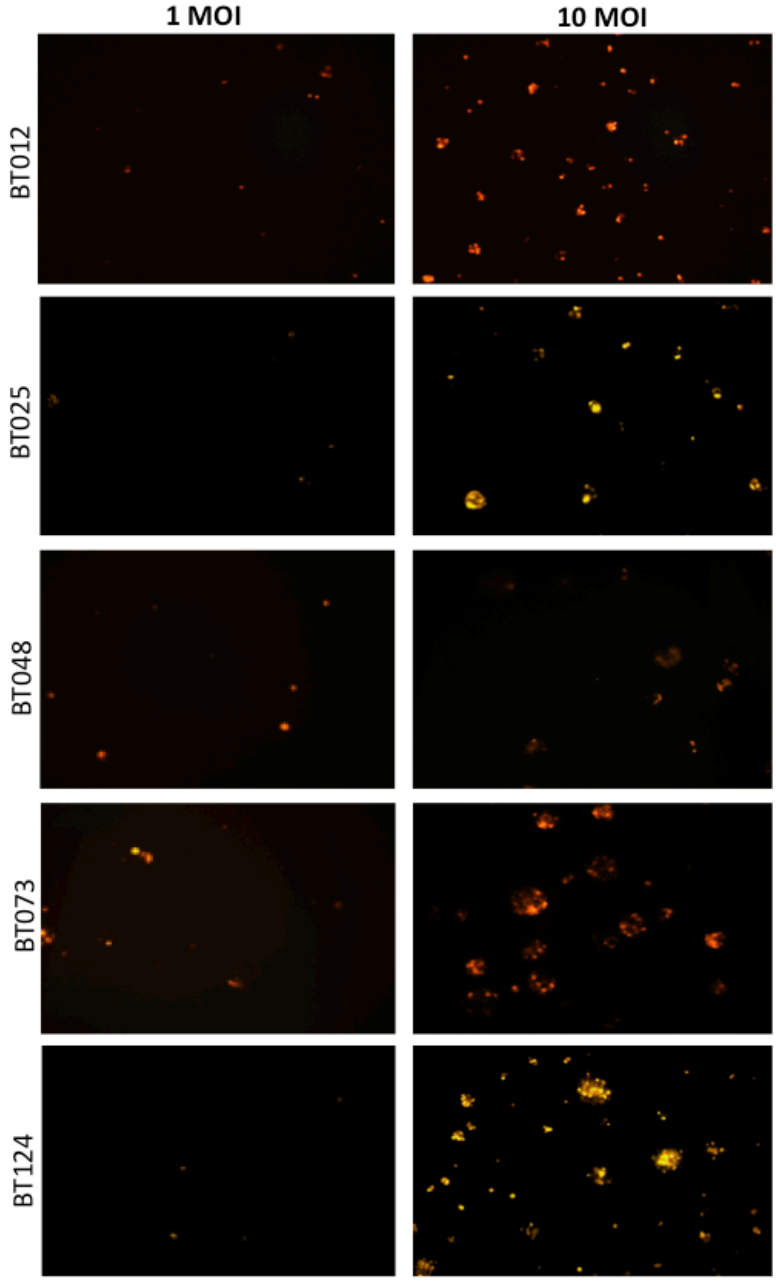
1 MOI
10 MOI
BT012
BT025
BT048
BT073
BT124

Figure 3.3: All BTIC lines are infected by MyxV, with varying degrees of late viral gene expression

Five BTIC lines were each disrupted into a single cell suspension and seeded at $1x10^4$ cells/well in a 96-well plate in serum-free neural stem cell media (+EGF, +FGF). Twenty-four hours later, the BTICs were infected with the indicated MOI of MyxV-RFP (1 or 10 MOI) and incubated for an additional 48hrs. Cells were imaged using a Zeiss Axiovert microscope at 100x magnification using a rhodamine filter (excitation 530-560nm, emission 590-650nm).

cycle. Interestingly, viral gene expression does not appear to be sufficient to predict MyxV susceptibility. Although limited viral gene expression in BT048 may partially explain its moderate resistance to MyxV, BT025 and BT073 displayed robust viral gene expression, yet were not substantially more susceptible to MyxV than BT048 (*Figure 3.1*). This strongly suggests that factors other than viral infection dictate susceptibility of BTICs to MyxV-mediated cell killing.

3.4 Viral gene expression increases over time

In order to assess whether viral gene expression increased over time, BTICs were infected with 0-10MOI of virus and RFP expression was quantified over time. As illustrated in *Figure 3.4*, viral gene expression in all cell lines increased over time. Only a modest increase in viral gene expression was observed in BT012, BT025, and BT048 over time. In BT012, the increase in viral gene expression was likely limited by MyxV-induced cell death, since the viability of these cells at 72hrs post-infection with 10MOI is near zero (*Figure 3.1*). In BT025 and BT048, the modest increase in viral gene expression is likely attributable to intrinsic cellular factors that limit viral replication and subsequent cell killing. Virally-induced IFN production and lack of endogenous Akt activation have both been shown to limit MyxV efficacy in certain cells[96,98,132], but previous work in our lab has demonstrated that neither of these factors dictate susceptibility to MyxV infection in BTIC lines[109]. Paradoxically, the most dramatic increase in viral gene expression occurred both in BT073, a moderately MyxV-resistant BTIC line, and in BT124, a comparatively MyxV-susceptible BTIC line. This illustrates

(a.)

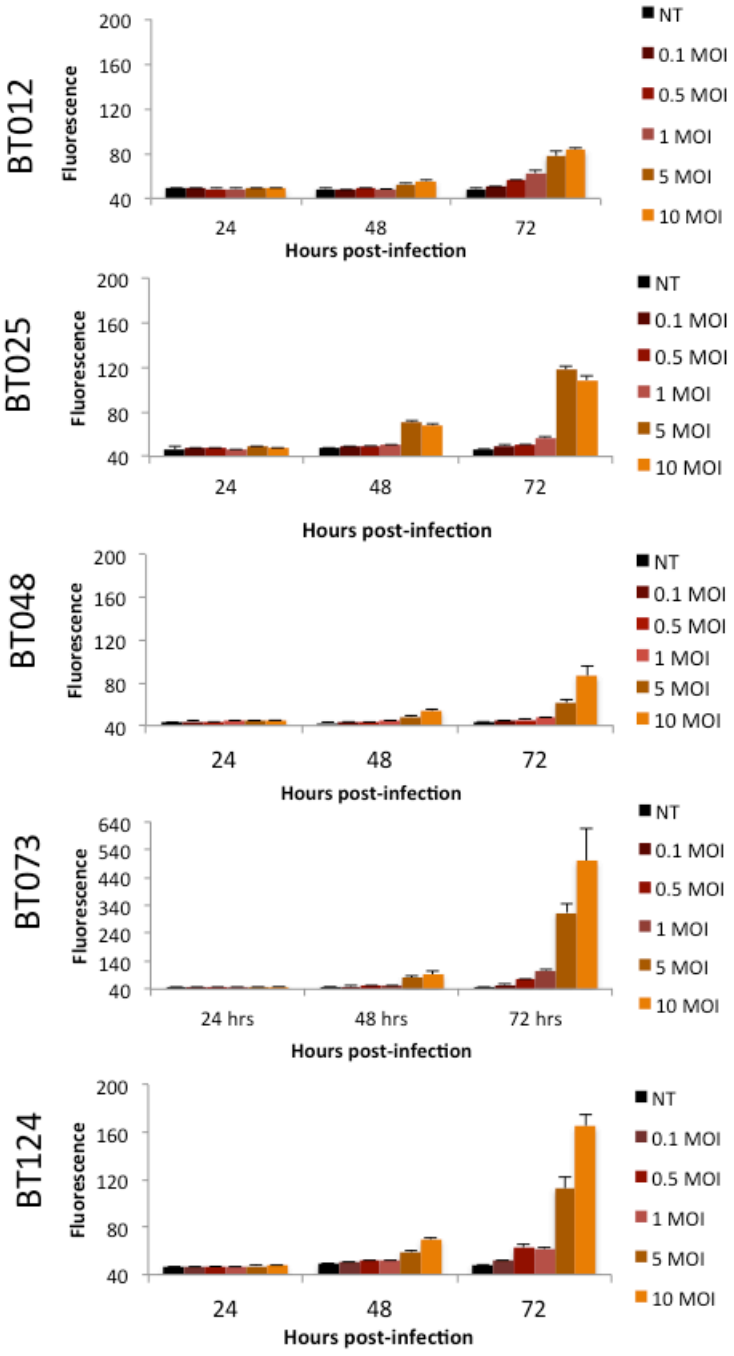
BT012
Fluorescence
200
160
120
80
40
24
48
72
Hours post-infection
NT
0.1 MOI
0.5 MOI
1 MOI
5 MOI
10 MOI
BT025
Fluorescence
200
160
120
80
40
24
48
72
Hours post-infection
NT
0.1 MOI
0.5 MOI
1 MOI
5 MOI
10 MOI
BT048
Fluorescence
200
160
120
80
40
24
48
72
Hours post-infection
NT
0.1 MOI
0.5 MOI
1 MOI
5 MOI
10 MOI
BT073
Fluorescence
640
540
440
340
240
140
40
24 hrs
48 hrs
72 hrs
Hours post-infection
NT
0.1 MOI
0.5 MOI
1 MOI
5 MOI
10 MOI
BT124
Fluorescence
200
160
120
80
40
24
48
72
Hours post-infection
NT
0.1 MOI
0.5 MOI
1 MOI
5 MOI
10 MOI

Figure 3.4: Late viral gene expression increases over time in all BTICs tested

A panel of five BTIC lines were each disrupted into a single cell suspension and seeded at $1x10^4$ cells/well in a clear-bottomed, black-sided 96-well plate in serum-free neural stem cell media (+EGF,+FGF). Twenty-four hours later, the BTICs were infected with the indicated MOI of MyxV-RFP (0.1-10 MOI) and incubated for the indicated time (48-96hrs). Red fluorescence (excitation 554nm, emission 595nm) was quantified using a SpectraMax plate reader. Data are plotted as mean +/- standard error and represent three independent experiments, each with six internal replicates.

that a high level of late viral gene expression (a surrogate marker for viral replication) is not predictive of cellular sensitivity to MyxV. In a lytic system, viral replication ultimately culminates in cell death through lysis; the absence of cell killing despite evidence of viral replication in certain BTIC lines suggests that the MyxV-BTIC system is not ultimately a lytic one. As such, we sought to explore whether MyxV-induced cell death in BTICs occurs through an alternative mechanism, such as programmed cell death in response to virus infection, instead of true "oncolysis".

3.5 Induction of apoptosis is not responsible for MyxV-induced cell death

To quantitatively examine apoptotic signalling in MyxV-infected BTICs, a luminescent caspase-3 and -7 activation assay was utilized. The assay was initially validated as shown in *Figure 3.5*, wherein it was demonstrated using BT025 that apoptotic signalling (as measured by caspase-3/-7 activation) tends to be induced after 48-hr treatment with doxorubicin (1μM), but not in response to treatment with the necrotic cell death inducer, ionomycin (1μM), or in response to UV-inactivated virus. It was also demonstrated that a 1 hr pre-treatment with 1μM of the pan-caspase inhibitor ZVAD was capable of significantly reducing both basal levels of caspase-3/-7 activation in controls, and abrogating caspase-3/-7 activation in doxorubicin-treated cells ($p<0.05$).

Following validation of the caspase-3/-7 activation assay, the ability of MyxV to induce caspase-3/-7 signalling was tested. Upon examination of the activation of the executioner caspases-3 and -7, it was apparent that caspase-3/-7 activation was not significantly induced in response to infection with high-dose (10 MOI) MyxV at 48hrs post-infection

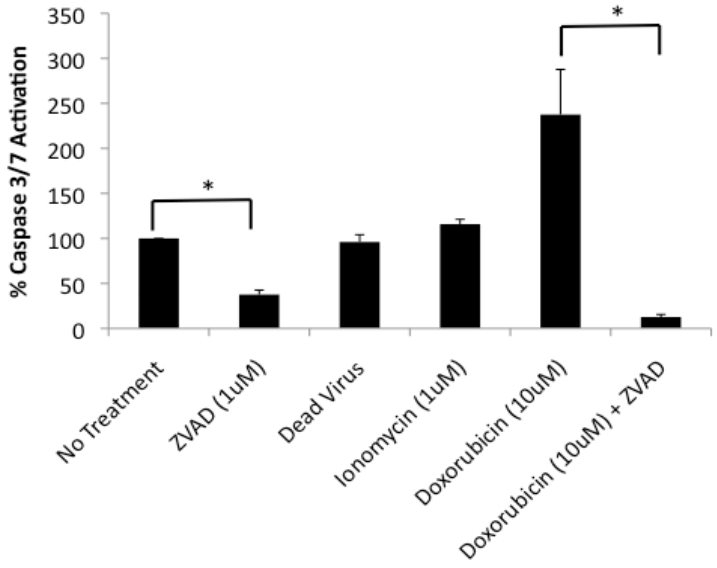

Figure 3.5 Validation of Caspase 3/7 Glo© assay

BT025 neurospheres were disrupted into single cell suspension and seeded at $1x10^4$ cells/well in a clear-bottomed, black-sided 96-well plate in serum-free neural stem cell media (+EGF, +FGF). Twenty-four hours later, the cells were treated with the indicated treatment: media control, pan-caspase inhibitor ZVAD (1μM), UV-inactivated MyxV (dead virus), ionomycin (1μM; negative control for non-apoptotic cell death), doxorubicin (positive control for apoptotic cell death), or ZVAD + doxorubicin (1hr pretreatment with 1μM ZVAD, 1μM doxorubicin). As predicted, caspase-3/-7 activation is not significantly induced in response to the negative controls, dead virus or ionomycin, at 48 hrs post-treatment in BT025. In contrast, the pan-caspase inhibitor ZVAD significantly ($p<0.05$; *) reduces caspase-3/-7 activity of untreated and doxorubicin-treated cells. Data are presented as mean +/- standard error and represent two independent experiments, each with four internal replicates.

(A.)

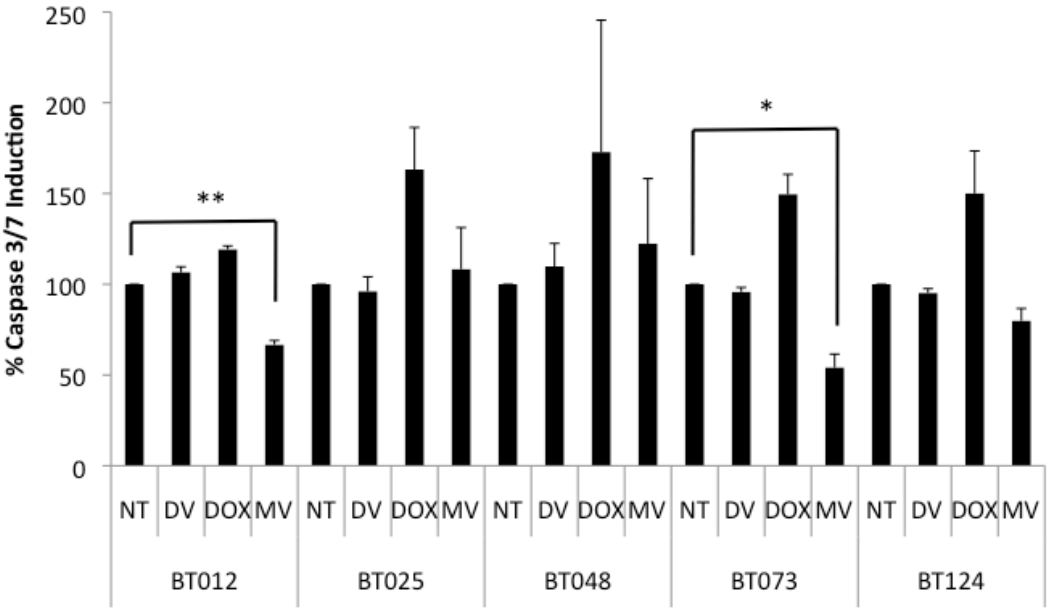
% Caspase 3/7 Induction
250
200
150
100
50
0
**
*
NT DV DOX MV NT DV DOX MV NT DV DOX MV NT DV DOX MV NT DV DOX MV
BT012
BT025
BT048
BT073
BT124

(B.)

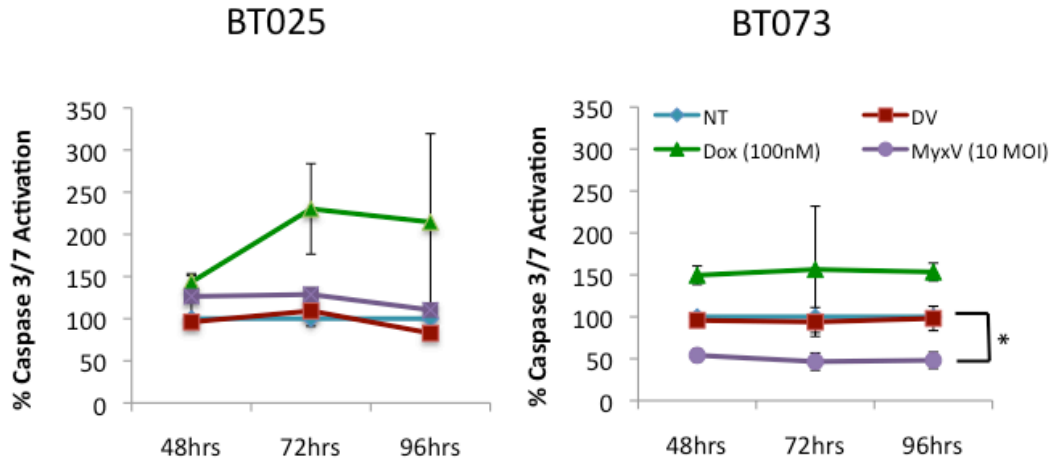
BT025
BT073
% Caspase 3/7 Activation
350
300
250
200
150
100
50
0
48hrs
72hrs
96hrs
NT
DV
Dox (100nM)
MyxV (10 MOI)
*

(C.)

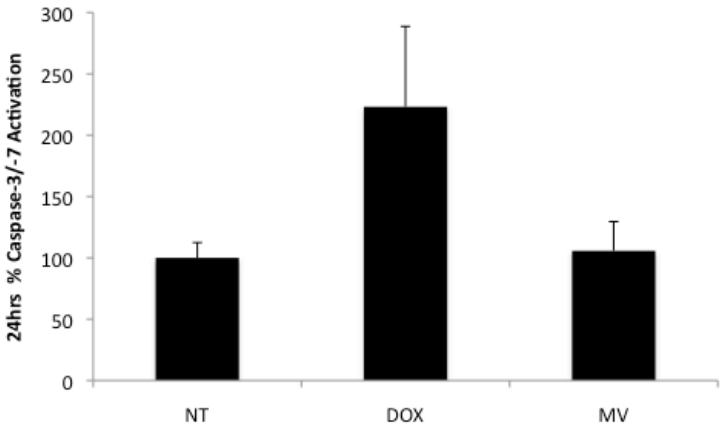

Figure 3.6 MyxV does not induce caspase-3/-7 activation in any BTIC line tested and significantly decreases caspase-3/-7 activation in two BTIC lines

(A) Five BTIC lines were each disrupted into single cell suspension and seeded at $1x10^4$ cells/well in a black-sided 96-well plate in serum-free neural stem cell media (+EGF, +FGF). Twenty-four hours later, the BTICs were treated with 10 MOI of MyxV-RFP (MV), 1μM doxorubicin (DOX), or UV-inactivated MyxV (DV) for 48hrs. Caspase-3/-7 activation was measured using the Caspase 3/7-Glo© assay and normalized to the untreated control (NT). Caspase-3/-7 activation was not significantly increased above the untreated control in any of the five cell lines tested ($p>0.05$). In contrast, caspase-3/-7 activation was significantly reduced below basal levels in BT012 and BT073 ($p<0.0001$; ** and $p<0.05$; *, respectively) following MyxV treatment. Data are presented as mean +/- standard error and represent 2-4 independent repeats, with 4 internal replicates per experiment. (B) To verify that MyxV was not induced at later time points, time courses were performed using the conditions described in (A) with incubations from 48-96hrs. MyxV did not significantly induce caspase-3/-7 activation in BT025 ($p>0.05$) at any time point tested. MyxV significantly reduced caspase-3/-7 activation in BT073 at 48-96hrs ($p<0.05$; *). Data are presented as mean +/- standard error and represent two independent experiments, each with four internal replicates. (C) To determine whether pro-apoptotic signalling was occurring prior to the 48hr time point, caspase-3/-7 activation was measured at 24 hrs post-infection in BT025. MyxV infection (5 MOI) does not significantly induce caspase-3/-7 activation ($p>0.05$). Doxorubicin (100nM) served as a positive control for apoptosis. Data are presented as mean +/- standard deviation of six internal replicates in a single experiment.

in all five BTIC lines (*Figure 3.6*). This time point was carefully selected based on several factors: (i) late viral gene expression is apparent at 48hrs, indicating that a viral infection has been well-established (*Figure 3.3*), and thus any pro-apoptotic antiviral responses will have been activated, and (ii) substantial loss of cell viability can be observed between 48hrs and 72hrs in most BTIC lines (*Figure 3.1*), indicating that pro-death mechanisms are active during this period. As shown in *Figure 3.6A*, caspase-3/-7 activation increases in response to treatment with the highly pro-apoptotic topoisomerase II poison doxorubicin, but not in response to treatment with live (10 MOI MyxV) or dead (UV-inactivated) virus in all BTIC lines tested. Interestingly, MyxV treatment significantly ($p<0.05$) lowers caspase-3/-7 activity below basal levels in two of the five cell lines tested (BT012 and BT073) at 48 hrs post-infection. In order to demonstrate that the 48-hr time point was not anomalous, a caspase-3/-7 time course was performed in BT025 and BT073 (*Figure 3.6B*), demonstrating that the observed trends were preserved up to 96 hrs post-infection. To eliminate the possibility that apoptotic signalling was happening earlier than 48hrs, the same assay was performed at 24 hrs post-infection, and no induction of caspase-3/-7 activity was observed at an early time point following viral infection (*Figure 3.6C*).

To verify caspase activation, PARP immunoblots (*Figure 3.7*) were performed using extracts from treated BT025 cells (which strongly induce caspase activation in response to doxorubicin and which do not activate caspases in response to MyxV) and BT012 cells (which only mildly induce caspase activation in response to doxorubicin and which lose

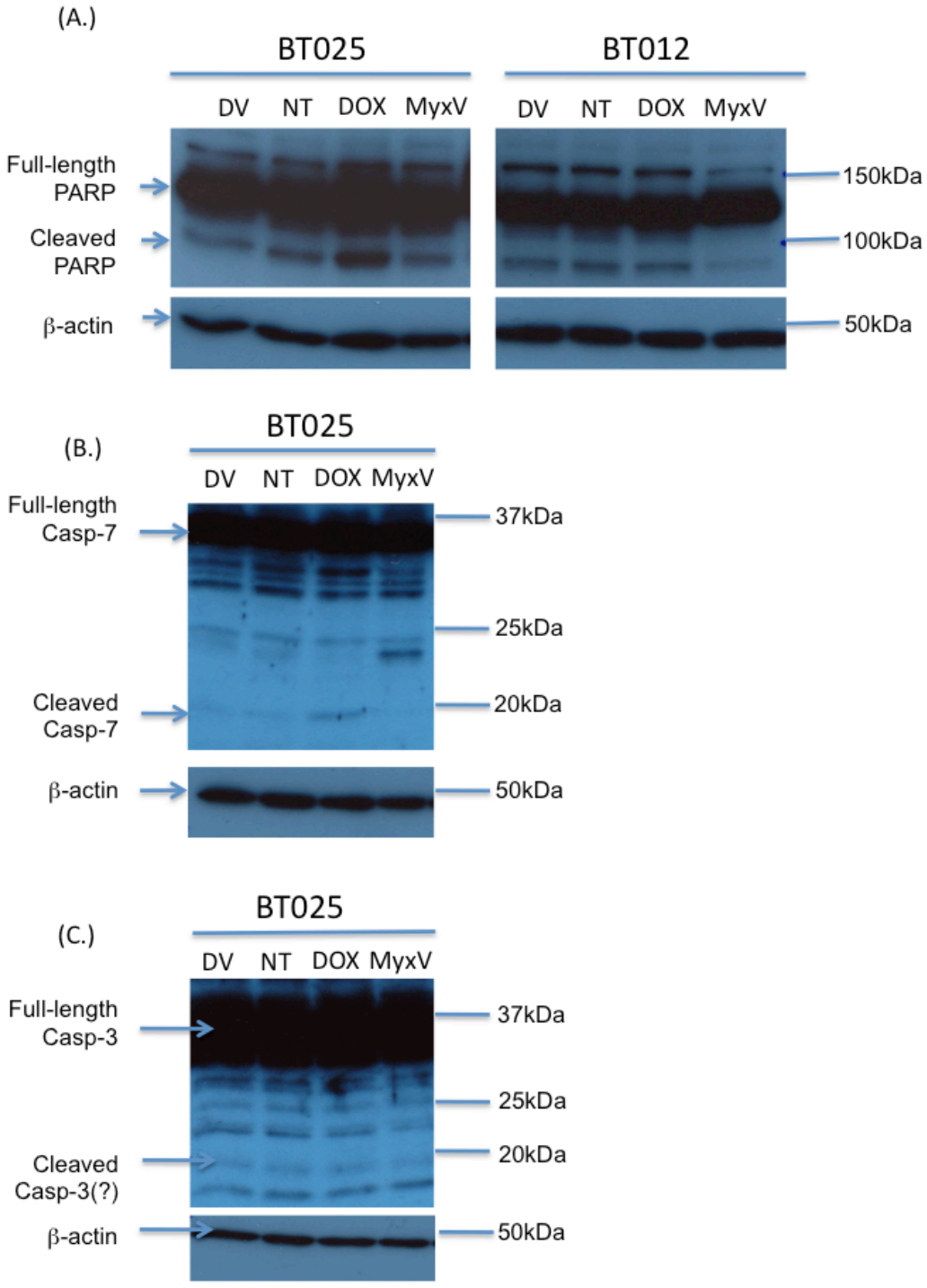
(A.)
BT025
BT012
DV NT DOX MyxV
DV NT DOX MyxV
Full-length PARP
Cleaved PARP
β-actin
150kDa
100kDa
50kDa
(B.)
BT025
DV NT DOX MyxV
Full-length Casp-7
Cleaved Casp-7
β-actin
37kDa
25kDa
20kDa
50kDa
(C.)
BT025
DV NT DOX MyxV
Full-length Casp-3
Cleaved Casp-3(?)
β-actin
37kDa
25kDa
20kDa
50kDa

Figure 3.7: Immunoblots of caspase-3/-7 cleavage and PARP cleavage indicate that apoptosis is not induced by 48hr MyxV infection

To validate the observation that MyxV does not induce caspase-3/-7 activation, BTICs were treated with MyxV (10MOI), UV-inactivated dead virus (DV), doxorubicin (1μM) as a positive control for apoptosis, or no treatment and incubated for 48hrs prior to preparation of whole cell extracts and immunblotting. (A) BT025 and BT012 extracts were immunoblotted for PARP, whereby cleavage of PARP from its full-length (116 kDa) to cleaved (89kDa) form is indicative of apoptosis. In BT025, doxorubicin treatment strongly induced PARP cleavage, but MyxV infection did not. In BT012, doxorubicin treatment did not appear to induce PARP cleavage, but infection with MyxV did appear to decrease levels of cleaved PARP below basal levels. The relative position of the molecular mass standards is indicated to the right of the blots. (B) BT025 extracts were immunoblotted for full-length (35kDa) and cleaved (20kDa) caspase-7. While doxorubicin treatment induced a distinct band at 20kDa corresponding to cleaved caspase-7 (indicative of apoptosis), infection with MyxV does not appear to induce caspase-7 cleavage. (C) BT025 extracts were immunoblotted for full-length (35kDa) and cleaved (17kDa) caspase-3. Neither doxorubicin treatment nor MyxV infection induced caspase-3 cleavage at this time point.

basal caspase activity in the presence of MyxV). As shown in *Figure 3.7A*, PARP cleavage corroborates precisely with the caspase-activation data. BT025 was shown to induce substantial PARP cleavage after 48hrs in response to doxorubicin, and showed no evidence of PARP cleavage in response to MyxV, beyond that which was observed in the untreated control. BT012 did not substantially induce PARP cleavage in response to doxorubicin, but did show almost complete abrogation of PARP cleavage in response to MyxV. This corroborates the suggestion that MyxV infection does not induce apoptosis, and in a subset of BTIC lines, may actively counteract pre-existing apoptotic signals.

We also verified the expression of full-length caspase-3 and-7 in these BTIC lines using immunoblots (*Figure 3.7B and C*). In this experiment, caspase-7 cleavage was clearly induced in response to doxorubicin, but not in response to MyxV infection. The presence or absence of caspase-3 cleavage could not be ascertained, since doxorubicin did not appear to induce caspase-3 cleavage at the time point examined. The absence of detectable doxorubicin-induced caspase-3 cleavage by immunoblot suggests that the doxorubicin-induced caspase-3/-7 activation observed at the 48hr timepoint in *Figure 3.6a* may be predominantly attributable to the activity of caspase-7.

3.6 Myxoma virus protein M011L mediates anti-apoptotic signalling in the BTIC model

Based upon the observation that MyxV infection decreases caspase-3/-7 activity below basal levels in BT012 and BT073, and does not induce caspase-3/-7 activation in any BTIC line following infection, we hypothesized that the viral protein M011L, a well-

characterized anti-apoptotic protein[108,149,152], was mediating anti-apoptotic signalling in the BTIC model. We further speculated that infection with the MyxV-M011L-KO virus should induce apoptosis, thus enhancing cell killing. As shown in *Figure 3.8A*, infection with MyxV-M011L-KO significantly improved BTIC killing compared to wild-type virus ($p<0.05$, *) at 3MOI and 10 MOI in both BTIC lines tested, and at 1 MOI in BT025 alone. To test whether this improvement in cell killing was attributable to the induction of apoptosis, caspase-3/-7 activation was measured at 48hrs post-infection in BT025. Although wild-type virus did not significantly induce caspase-3/-7 activation 10 MOI, MyxV-M011L-KO infection at both 1 MOI and 10 MOI significantly increased caspase-3/-7 activation ($p<0.05$) (*Figure 3.8B*). In all cases, induction of caspase signalling was abrogated, or basal levels reduced, in response to co-treatment with the pan-caspase inhibitor ZVAD ($p<0.01$) (*Figure 3.8B*).

To confirm the role of apoptosis in MyxV-M011L-KO cell killing, a rescue experiment was performed in which the ability of ZVAD to abrogate MyxV-M011L-KO cell killing was assessed (*Figure 3.9*). As a positive control, it was shown that doxorubicin-induced cell killing is partially abrogated by inhibiting caspase activity with ZVAD. Wild-type MyxV cell killing does not appear to be affected by caspase inhibition. However, MyxV-M011L-KO cell killing is partially abrogated by inhibition of caspase activity, indicating that caspase-dependent apoptosis is at least partially responsible for MyxV-M011L-KO-induced cell death.

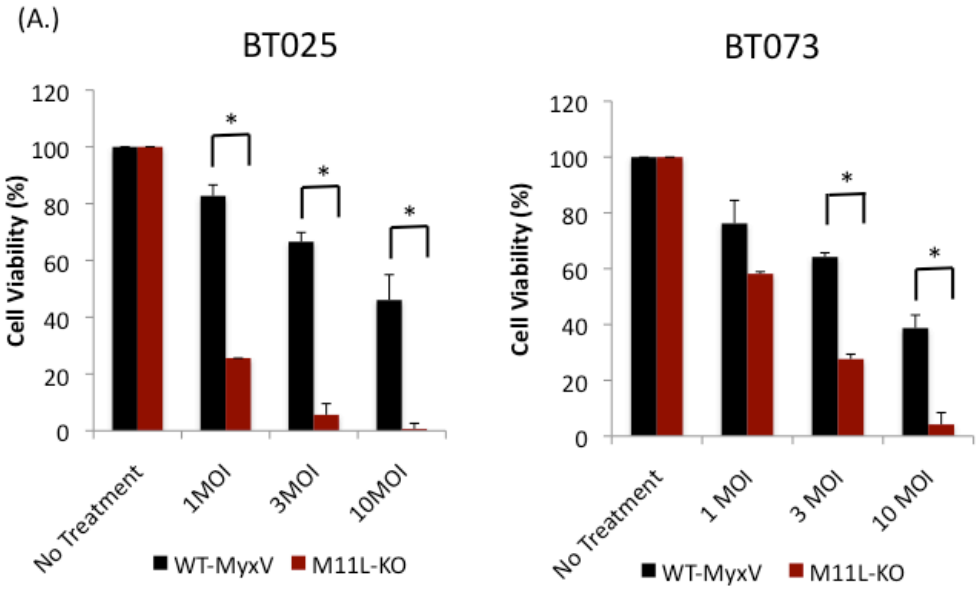
(A.)
BT025
BT073
Cell Viability (%)
120
100
80
60
40
20
0
*
No Treatment
1MOI
3MOI
10MOI
1 MOI
3 MOI
10 MOI
WT-MyxV
M11L-KO

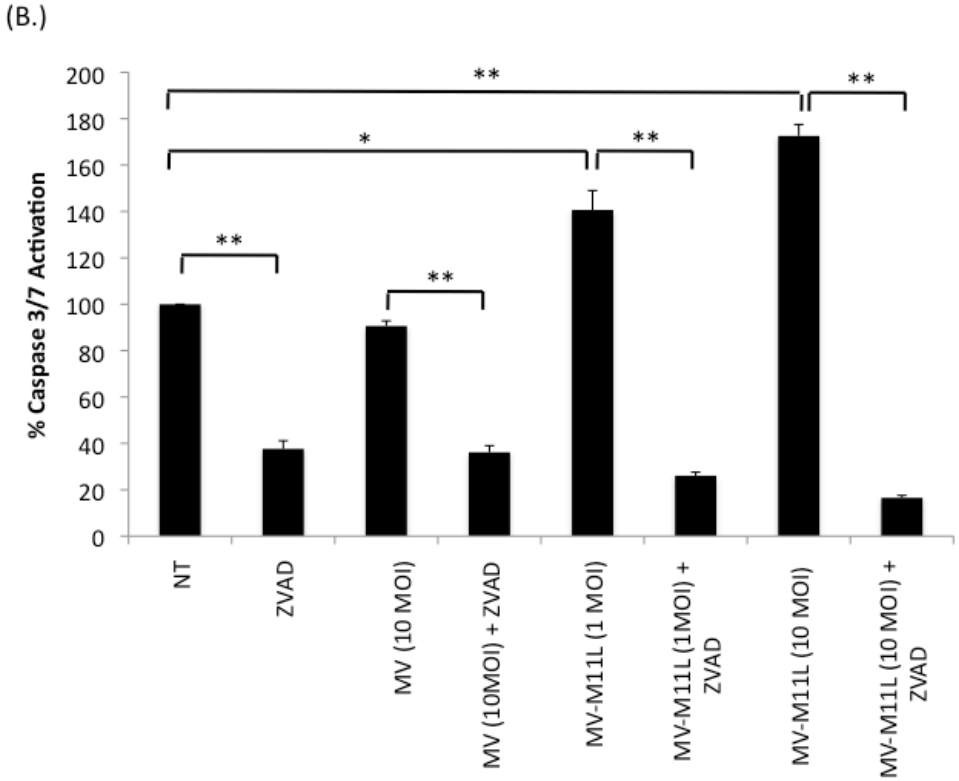
(B.)
% Caspase 3/7 Activation
200
180
160
140
120
100
80
60
40
20
0
**
*
NT
ZVAD
MV (10 MOI)
MV (10MOI) + ZVAD
MV-M11L (1 MOI)
MV-M11L (1MOI) + ZVAD
MV-M11L (10 MOI)
MV-M11L (10 MOI) + ZVAD

Figure 3.8: MyxV-M011L-KO significantly enhances MyxV-induced cell death in BT025 and BT073 through induction of apoptosis

(A) To assess the ability of MyxV-M11L-KO to enhance cell death, cell viability was assessed by Alamar Blue at 48hrs post-infection. MyxV-M011L-KO resulted in significantly ($p<0.05$; *) reduced viability compared to wild-type virus in both BTIC lines tested at 3 and 10 MOI. Data were normalized to untreated controls and presented as mean +/- standard error, each representing two independent trials with six internal replicates. (B) To assess whether this decrease in viability was attributable to the induction of apoptosis, caspase-3/-7 activation was quantified 48 hrs post-infection. Caspase-3/-7 activation was not induced in response to infection with wild-type virus at 10 MOI, but was significantly induced in response to infection with MyxV-M11L-KO at 1 MOI ($p<0.05$; *) and 10 MOI ($p<0.01$; **). In all treatment conditions, pre-treatment with the apoptosis inhibitor ZVAD (1μM, 1hr pre-treatment) significantly ($p<0.01$; **) reduced basal levels of caspase-3/-7 activity. Data are presented as mean +/- standard error and represent two independent trials each with four internal replicates.

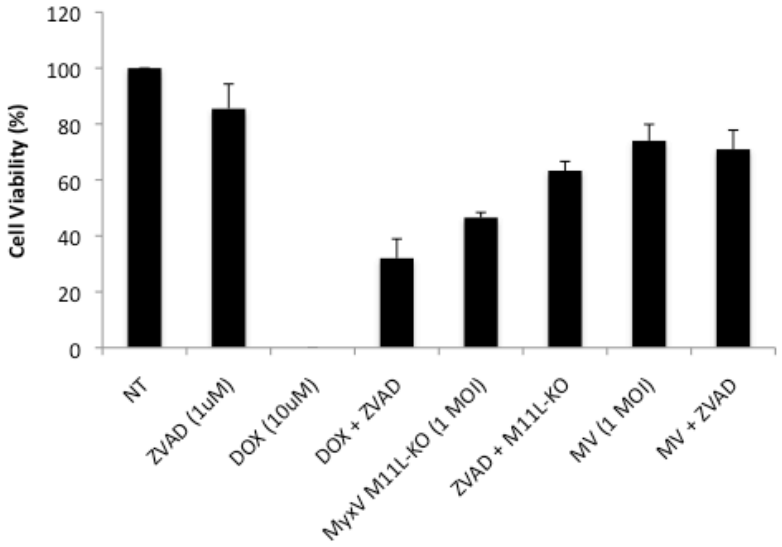

Figure 3.9: Inhibition of caspase activity may partially rescue MyxV-M011L-KO phenotype

To affirm whether MyxV-M011L-KO was killing cells through the induction of apoptosis, BT025 neurospheres were disrupted into single cell suspension and seeded at $1x10^4$ cells/well in a clear-bottomed, black-sided 96-well plate in serum-free neural stem cell media (+EGF, +FGF). Twenty-four hours later, the cells were treated with: media control (NT), the pan-caspase inhibitor ZVAD (1μM), doxorubicin (10μM; positive control for apoptotic cell death), ZVAD + doxorubicin (1hr pretreatment with 1μM ZVAD), 1MOI MyxV-M011L-KO, ZVAD + 1 MOI MyxV-M011L-KO (1hr pretreatment with 1μM ZVAD), 1MOI MyxV, or ZVAD + 1MOI MyxV (1hr pretreatment with 1μM ZVAD). Viability was measured via Alamar blue at 48hrs post-infection and absorbance values normalized to the untreated control. Data are presented as mean +/- standard deviation from a single experiment with six internal replicates.

3.7 Autophagy-related signalling in response to MyxV infection

Under autophagy-promoting conditions, LC3-I is lipidated to produce LC3-II; this lipidated form is detectable as a faster migrating 16kDa band on an immunoblot, as distinct from the 18kDa non-lipidated form[155]. Using rapamycin as a positive control for the induction of autophagy, we sought to test whether MyxV infection induces autophagy in BTICs. As shown in *Figure 3.10*, no bands were detectable in the 16kDa or 18kDa range, in either the positive or negative controls, in either BT025 or BT073. This suggests that either (i) these cells do not express LC3, (ii) LC3 exists in an oligimerized form, (iii) LC3 exists in an alternatively processed form, or (iv) the antibody is not sufficiently sensitive to detect the protein. The presence of other unidentified bands on the immunoblot suggests that an alternatively processed or oligimerized LC3 protein may be present. Nonetheless, no evidence for or against the induction of autophagy by MyxV could be ascertained from these data.

3.8 Summary and significance

In this chapter, we have determined the baseline susceptibility of five BTIC lines to MyxV infection and killing, and demonstrated that the majority of BTICs tested are only moderately susceptibility to MyxV-mediated cell death. Paradoxically, in several lines, this modest susceptibility was observed despite robust infection of the BTIC neurospheres with MyxV. The observation that infection does not predict susceptibility to MyxV-mediated cell death suggested that a non-lytic mechanism of cell death might be at play. To test the hypothesis that MyxV-induced cell death was mediated by apoptosis, we

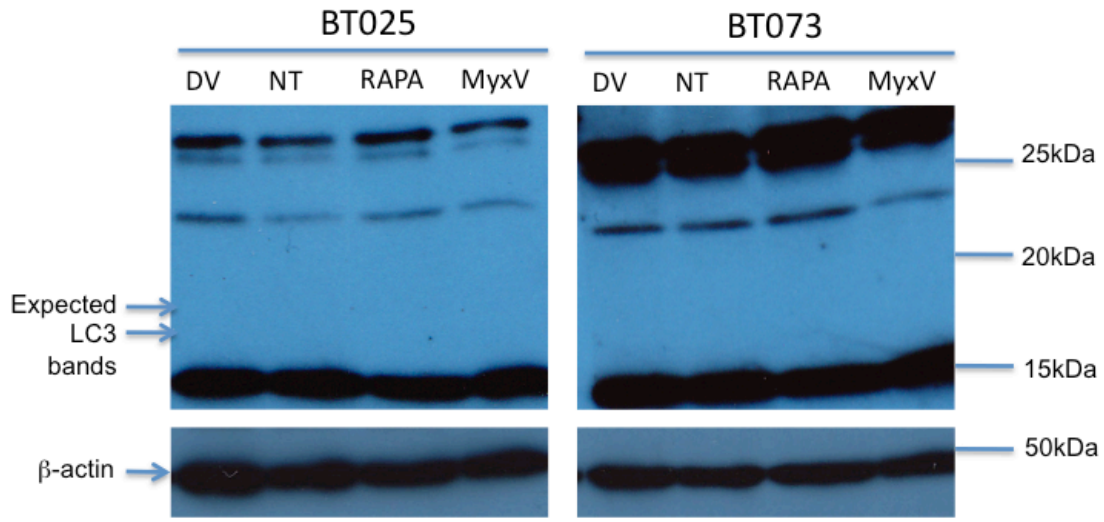

Figure 3.10: Immunoblot for induction of autophagy is inconclusive

To assess the induction of autophagy-related signaling, we examined the conversion of LC3b from its 18kDa to 16kDa forms. BT025 and BT073 were treated with the following: MyxV (10MOI), UV-inactivated virus (DV), rapamycin (1μM; as a positive control for autophagy), or no treatment for 48hrs prior to the preparation of whole cell extracts. Although LC3b is generally considered to be ubiquitously expressed in all cell types, no immunoreactive protein was observed at the 16-18kDa size. Thus no conclusions can be drawn from these data regarding the possible induction of autophagy by MyxV infection.

tested caspase-3/-7 activation as well as caspase and PARP cleavage in multiple BTIC lines. It was demonstrated that MyxV does not induce apoptosis in any BTIC line tested, but rather MyxV infection lowers basal caspase-3/-7 activation in multiple BTIC lines. To test the hypothesis that viral protein MyxV-M011L is mediating anti-apoptotic signalling, the MyxV-M011L-KO virus was tested. This virus dramatically enhanced BTIC cell death compared to wild-type MyxV, and evidence was presented that this increased cell death was attributable to apoptosis.

The significance of this work is two-fold. First, the baseline susceptibility of BTICs to MyxV infection and killing has been established, laying the groundwork for high-throughput screens of pharmacological agents that enhance MyxV-mediated cell death in subsequent chapters. Secondly, the observation that MyxV actively counteracts apoptotic signalling in BTICs suggests putative strategies for improving MyxV efficacy, including the use of modified viruses or the use of pro-apoptotic chemotherapeutics that counteract the anti-apoptotic effects of MyxV.

Chapter Four: Identification of Synergistic Compounds

4.1 Introduction & Rationale

As discussed in Chapter I and examined in Chapter III, many BTICs are only moderately susceptible to MyxV-mediated cell death *in vitro,* despite being infected with the virus. To date, several resistance mechanisms have been elucidated in other models that seek to explain patterns of susceptibility to MyxV. For instance, cells that mount an active Type I IFN response to MyxV are typically resistant to MyxV infection, a phenotype that can be reversed with the use of an inhibitor such as rapamycin, which blunts the antiviral IFN response[94,96,166]. Additionally, Akt activation status can affect viral replication, whereby cells that do not have activated Akt, or which do not demonstrate Akt activation upon MyxV infection, are typically resistant to MyxV, a phenotype that can be partially reversed by rapamycin-mediated Akt activation[93,132].

In the BTIC model, susceptibility to MyxV does not appear to be governed by IFN production, as these cells do not induce Type I IFN signalling following MyxV infection[109]. Furthermore, susceptibility does not appear to correlate with Akt activation, based upon unpublished data from the Forsyth lab. Thus, the two known MyxV resistance mechanisms are inadequate to describe patterns of resistance in BTICs. With the mechanisms governing MyxV resistance in BTICs unknown, strategically developing targeted combination approaches to overcome resistance can be particularly challenging. One approach is to utilize an unbiased screen of small molecule inhibitors to identify

compounds that synergize with MyxV, and thus improve MyxV-mediated cell death in the BTIC model.

In this chapter, a 73-molecule drug library was used in an unbiased screen to identify compounds that synergize with MyxV to enhance BTIC killing. A full list of the drugs and their corresponding numerical codes is provided in *Appendix A*. The objective of this work was to identify agents of potential clinical utility in maximizing the efficacy of oncolytic MyxV therapy. The ChemieTek small molecule inhibitor library was deemed appropriate for this end goal, since the library consists of well-characterized compounds that have demonstrated acceptable toxicity profiles throughout preclinical and clinical testing.

The characterization of baseline BTIC susceptibility to MyxV infection and killing in Chapter III established the framework within which to pursue drug-virus combination studies. In particular, these observations guided both the decision of which BTIC line to screen against the drug library, and the parameters (time point, MOI, etc.) to use for this endeavour. Although the diverse nature of patient-derived BTICs ensures that no single BTIC line is representative of all tumours, it was necessary to identify a single BTIC line to carry forward into the drug screen. BT025 was selected for this purpose, for several reasons: (i) BT025 bears several clinically relevant mutations (p53, PTEN) that might influence drug susceptibility, (ii) BT025 is well-characterized *in vitro* and *in vivo*[31,109] (iii) BT025 is moderately resistant to MyxV-induced cell death (*Figure 3.1*), thus retaining the capacity to be improved pharmacologically and (iv) despite being fairly

resistant to MyxV-induced cell death, BT025 allows for productive infection of MyxV, as indicated by late viral gene expression (*Figure 3.4*), thus permitting sufficient infection for meaningful examination of drug-virus interaction.

The parameters for the 73-drug small molecule inhibitor screen were also informed by data from Chapter III. As illustrated by *Figures 3.1* and *3.4*, the 24hr timepoint is characterized by minimal cell death and little evidence of late viral gene expression. For the purposes of determining synergistic interactions between drug and virus, we wanted to allow sufficient time for a productive viral replication to be established, thus 48hrs was chosen. Compared to previous work investigating synergy of MyxV and rapamycin in BTICs[109], the 48hr timepoint is a relatively early one (compared to 96-144hr timepoints explored in the rapamycin study). This relatively early time point was deemed to be particularly important in this study, since OVs are typically eliminated quickly in patients, and thus there may be a very limited window of time during which a drug can act to improve viral infection or killing before the virus is eliminated. Furthermore, time points longer than 72hrs were not deemed to be of interest due to tissue culture artefacts, such as neurosphere overgrowth and acidification of cell culture media, which can emerge over prolonged time course experiments. Based on the data from Chapter III, an optimal virus concentration for determining synergy also had to be determined. To minimize the effect of the virus while maximizing the opportunity to detect synergy, the dose of 1MOI was chosen. Viral gene expression at 1MOI at 48hrs indicates that some cells are infected, but the number of infected cells is sufficiently low that a compound that improves viral replication and/or spread could be detected.

The basic outline for the drug screen experimental design is shown in *Figure 4.1A*. The validity of the 4hr pre-treatment approach was verified in a high-profile systems approach-based study that examined the importance of timing in the erlotinib-based sensitization of breast cancer cells to DNA damaging agents[167]. The 4hr pre-treatment was shown to result in optimal rewiring of the dynamic oncogenic signalling networks, even though erlotinib itself requires only minutes to inhibit target phosphorylation[167]. Since our approach anticipated that small molecule inhibitors would rewire the BTICs to be more sensitive to MyxV-mediated cell death, we wanted to allow sufficient time for this rewiring to occur. In an oncolytic virus context, the 4hr pretreatment approach was previously validated in a high-throughput pharmacoviral screen of >10,000 molecules, which identified several novel compounds that enhance the efficacy of oncolytic VSV after a 4hr drug pre-treatment[168].

Based upon the parameters outlined above, a first-pass screen of the small molecule inhibitor library was performed. The organization of the experiments following the first-pass screening process is outlined in *Figure 4.1B*.

4.2 First-pass screen reveals eight potential candidates for further characterization

The first-pass screen of BT025 was performed as described in *Figure 4.1*, and graphs of viability generated for all 73 drugs alone and in combination with 1 MOI MyxV (*Appendix A*). As shown in *Figure 4.2*, data were summarized by plotting the difference in viability between combination-treated cells and drug-alone-treated cells on a

(A.) *For each drug in screen:*

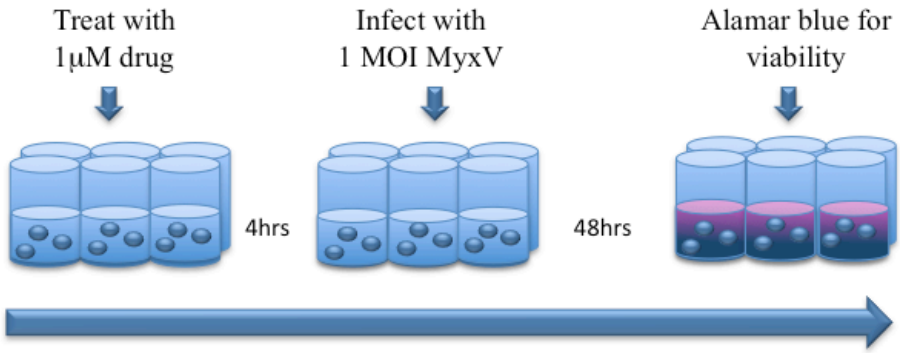

(B.)

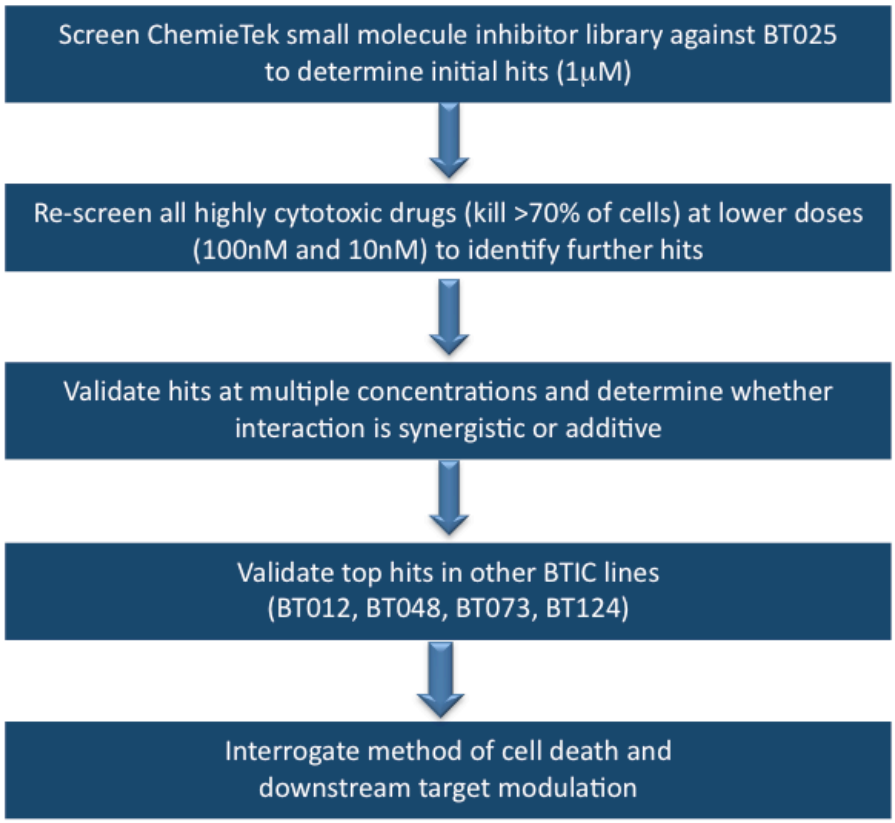

Figure 4.1: Experimental design for 73-compound small molecule inhibitor drug screen

(A) Schematic for combination treatment schedule: BT025 cells were plated at a density of $1x10^4$ cells/well in a 96-well plate. Twenty-four hours later, drugs were added at a concentration of 1μM and cells incubated for four hours. MyxV (1 MOI) was subsequently added to half of the drug-treated wells, for a total of six internal replicates per treatment. No-treatment and virus-only controls were also included. Cells were incubated for an additional 48hrs and viability measured by Alamar blue (B) Schematic for selection of lead compounds: following the first-pass screen of all the drugs at 1 μM, drug combinations that killed cells 20% more effectively than drug alone were selected as candidate compounds for further examination. Drugs that killed >70% of cells in the absence of virus were considered cytotoxic and re-screened at a lower dose (100 nM or 10 nM). Candidate drugs from each of the screens were further characterized by Chou-Talalay analysis for determination of synergy. A single lead synergistic compound was chosen for validation in the panel of BTICs and for mechanistic analysis.

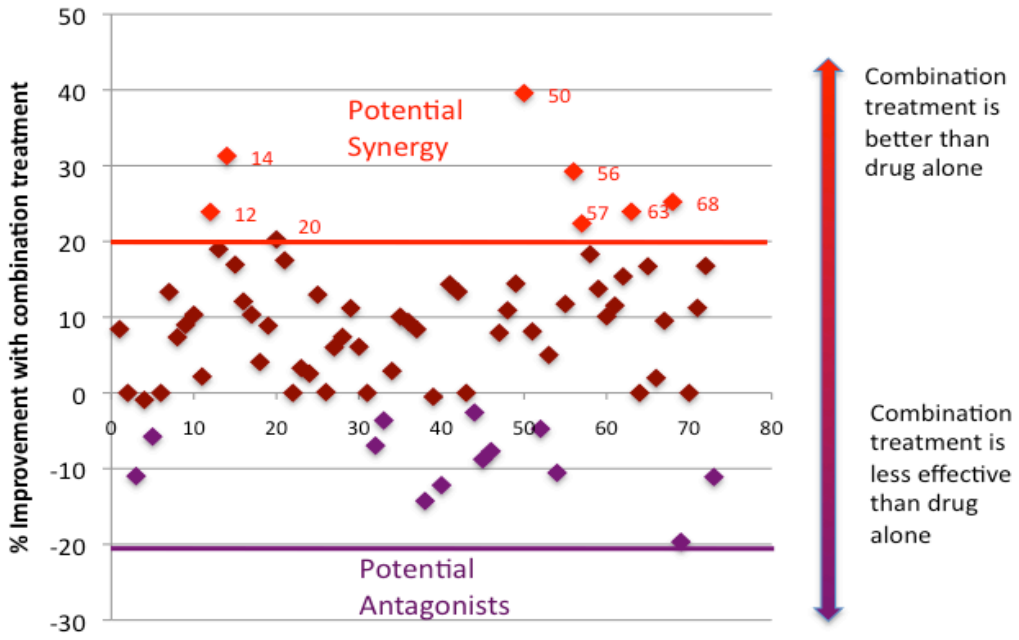

Figure 4.2: Summary data for first-pass screen of BT025 with all 73 drugs, alone and in combination with virus

BT025 cells were plated at a density of $1x10^4$ cells/well in a 96-well plate. Drugs were added at a concentration of 1μM and cells incubated for four hours. MyxV (1 MOI) was subsequently added to half of the drug-treated wells, for a total of six internal replicates per treatment. No-treatment and virus-only controls were also included. Cells were incubated for a further 48hrs and viability measured by Alamar blue. Drugs were numbered sequentially (*Appendix A*) and are represented accordingly along the *x*-axis. Values on the *y*-axis indicate the percent difference in cell viability between drug alone and combination treatment. Since virus alone kills 20% of BT025 cells, combination treatments that killed >20% better than drug alone were considered candidates for further testing (threshold for hits is indicated by solid red line). Eight candidate compounds were identified in this first-pass screen.

scatterplot of all 73 compounds. Drugs in which combination treatment did not enhance killing are clustered around 0%, while combination treatments that were less effective than drug alone are represented as negative values. Since virus alone kills ~20% of cells, combination treatments that killed >20% better than drug alone were considered hits (indicated by the solid red line). Based on this criterion, eight potential candidates were selected for further characterization. As shown in *Figure 4.3A*, all eight inhibitors showed a significant ($p<0.05$, *) combination effect when compared to either drug or virus alone, based upon three independent trials in BT025. These drugs and their primary activities, as indicated by ChemieTek, are listed in *Table 4.1*. Interestingly, these combination effects were only observed when BT025 cells were pre-treated with drug prior to virus infection; concurrent treatment with drug and virus did not significantly enhance cell killing for any of the hits tested (*Figure 4.3B*). To determine whether the combination effect observed following drug pre-treatment was due to an increase in viral infection, MyxV-FLuc, a highly sensitive reporter construct under the control of an early viral promoter, was utilized. Prior to using this construct to test viral infection, several validation experiments were performed. To verify that there were no differences in the behaviour of MyxV-FLuc when compared to MyxV-dsRED, the ability of these two viral strains to induce cell death was compared using the Alamar blue assay (*Figure 4.4A*). Infection of BT025 cells with either viral strain produced comparable decreases in cell viability. It was also verified that luminescence produced by infection with MyxV-FLuc is directly proportional ($R^2=0.998$) to MyxV-FLuc MOI (*Figure 4.4B*), validating the use of this virus as a tool to quantify drug-induced changes in viral infection. To test whether drug treatment caused an increase in viral luminescence (indicative of an increase in viral

(A.)

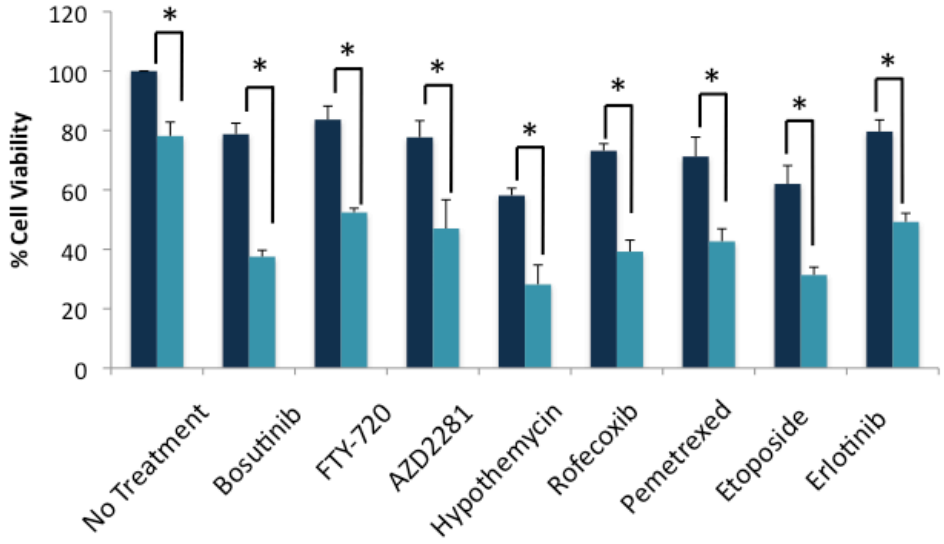
% Cell Viability
120
100
80
60
40
20
0
*
No Treatment
Bosutinib
FTY-720
AZD2281
Hypothemycin
Rofecoxib
Pemetrexed
Etoposide
Erlotinib

(B.)

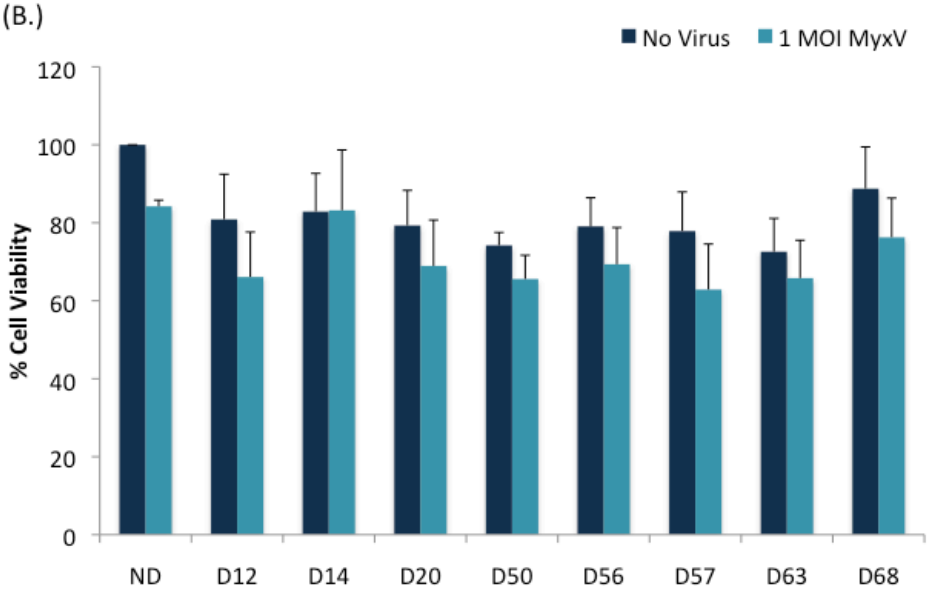
No Virus
1 MOI MyxV
% Cell Viability
120
100
80
60
40
20
0
ND
D12
D14
D20
D50
D56
D57
D63
D68

Figure 4.3: Each of the eight candidate compounds demonstrated a significant combination effect in BT025

(A) To determine whether the eight candidate compounds identified in the first-pass screen demonstrated a significant combination effect in BT025, viability was assessed by Alamar blue using the same conditions as the initial screen. BT025 cells were plated at a density of $1x10^4$ cells/well in a 96-well plate. The eight candidate compounds were added at a concentration of 1 μM and cells incubated for four hours. MyxV (1 MOI) was subsequently added to half of the drug-treated wells. No-treatment and virus-only controls were also included. Cells were incubated for 48hrs and viability measured by Alamar blue. All eight candidate compounds showed a significant ($p<0.05$; *) combination effect, improving cell killing compared to either drug or virus alone. Data are plotted as the mean viability +/- standard error of three independent experiments, each with six internal replicates. (B) To determine whether the combination effect would also be observed upon concurrent treatment with drug and virus, BT025 cells were plated at a density of $1x10^4$ cells/well in a 96-well plate and co-treated with the eight candidate compounds at 1μM in combination with MyxV at 1MOI. Virus-only and drug-only controls were also included. Cells were incubated for 48hrs and viability measured by Alamar blue. None of the eight candidate compounds showed a significant ($p<0.05$) combination effect following co-treatment, indicating that pre-treatment with drug is essential to achieve a combination effect. Data are plotted as the mean viability +/- standard error of three independent experiments, each with six internal replicates. Drug number codes are as follows: D12 = bosutinib; D14 = FTY-720; D20 = AZD2281; D50 = hypothemycin; D56 = rofecoxib; D57 = pemetrexed; D63 = etoposide; D68 = erlotinib.

Table 4.1: Identification of Candidate Compounds (1μM Screen)

Drug	#	Primary Activity
Bosutinib	12	Abl, Src inhibitor
FTY720	14	S1P receptor modulator
AZD2281	20	PARP 1/2 inhibitor
Hypothemycin	50	T cell activation inhibitor, MEK/ERK/PDGFR inhibitor
Rofecoxib	56	COX-2 inhibitor
Pemetrexed	57	nucleic acid synthesis inhibitor, antifolate
Etoposide	63	Topoisomerase II poison
Erlotinib	68	EGF-R inhibitor

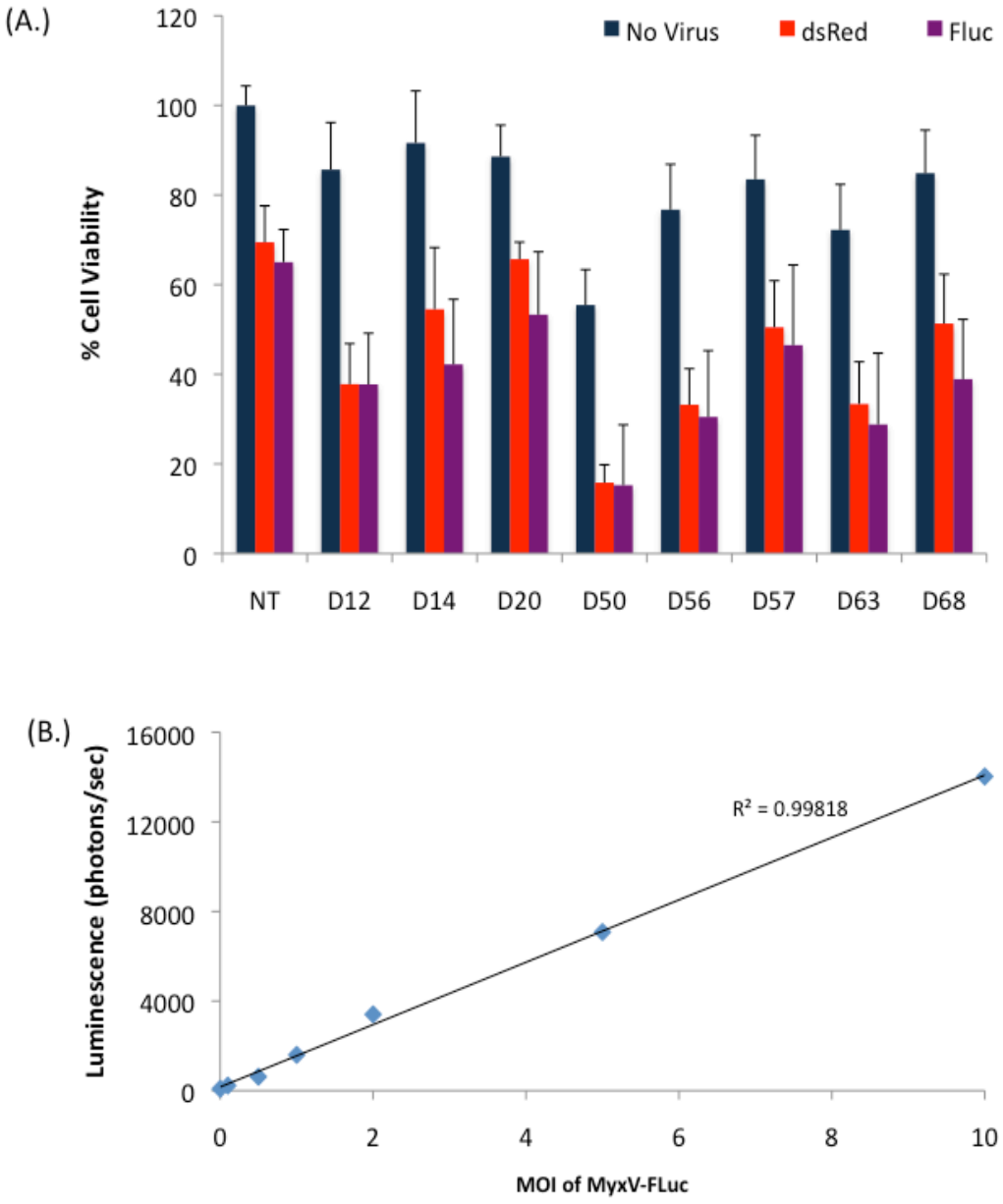
(A.)
No Virus
dsRed
Fluc
% Cell Viability
120
100
80
60
40
20
0
NT
D12
D14
D20
D50
D56
D57
D63
D68
(B.)
Luminescence (photons/sec)
16000
12000
8000
4000
0
R² = 0.99818
0
2
4
6
8
10
MOI of MyxV-FLuc

Figure 4.4: Confirmation of viral luminescence as an appropriate surrogate measure for viral infection

(A) To assess whether the observed combination effect was due to an increase in viral infection, MyxV-FLuc (a luminescent MyxV construct) was utilized. Prior to testing the impact of drug treatment on viral infection, it was necessary to confirm that MyxV-FLuc and MyxV-dsRED had comparable effects on BTIC viability. To test this, a single experiment was performed in which BT025 cells were plated at $1x10^4$ cells/well in a 96-well plate. The eight candidate compounds were added at 1 μM and cells incubated for 4hrs. MyxV-dsRED (1 MOI) was added to one third of the drug-treated wells and MyxV-FLuc (1 MOI) to another third of the drug-treated wells, while the final third comprised the drug-only controls. Six internal replicates were performed per treatment. Cells were incubated for 48hrs and viability measured by Alamar blue. For each of the combination treatments tested, MyxV-dsRED and MyxV-FLuc caused a comparable loss of cell viability. In this experiment, drug number codes are as follows: D12 = bosutinib; D14 = FTY-720; D20 = AZD2281; D50 = hypothemycin; D56 = rofecoxib; D57 = pemetrexed; D63 = etoposide; D68 = erlotinib. Data are plotted as the mean +/- standard deviation of six internal replicates in a single experiment. (B) To validate the use of viral luminescence as a surrogate marker for infection, a dose response of MyxV-FLuc was generated and the correlation between MOI and luminescence determined after 24hrs. In this experiment, BT025 cells were plated at $1x10^4$ cells/well in a black-sided 96-well plate. MyxV-Fluc was subsequently added at the indicated MOI (0.1, 0.5, 1, 5, and 10 MOI, equivalent to $1x10^3$, $5 x 10^3$, $1 x 10^4$, $5 x 10^4$, and $1 x 10^5$ viral particles per well) in

internal replicates of six and incubated for a further 24hrs. At this time, cells were incubated for ten minutes with the luciferase substrate, D-luciferin. Total luminescence (photons/sec) was measured on a SpectraMax plate reader. Data points indicate the mean luminescence of six internal replicates. The coefficient of determination (R^2) between MOI and luminescence was shown to be extremely high (R^2=0.998). Importantly, luminescence is only produced by the transcription of the viral genome, and thus this read-out measures virus particles that have infected cells, not free virus particles in solution. These observations confirmed that luminescence was an effective tool to measure whether viral infection was increased upon treatment with any of the eight lead compounds.

infection), viral luciferase expression was quantified after 24hrs for both combination-treated and virus-alone-treated BTICs. As shown in *Figure 4.5*, none of the eight drugs tested increased early viral gene expression at the 24hr time point, suggesting that the observed combination effect is not due to increased viral infection. It is worth noting, however, that the least efficacious drug combination at 48hrs (MyxV+Drug 20, *Figure 4.4a*) had the lowest relative viral gene expression levels, while the drug combination with the greatest efficacy at 48hrs (MyxV+Drug 50, *Figure 4.4a*) had the highest relative gene expression levels, suggesting that a substantial decrease in viral gene expression may impair the efficacy of the combination treatment.

4.3 Rescreen of twenty-two cytotoxic drugs reveals three more hits

Based on the first pass screen (*Appendix B1*), twenty-two small molecule inhibitors were observed to kill >70% of BT025 cells alone at 1μM and were deemed cytotoxic, obscuring potential combination effects. These drugs are listed in *Table 4.2*. Subsequently, these drugs were re-screened at 100nM in three independent trials. Data for all twenty-two drugs are shown in *Appendix B2.* From this screen at 100nM, three drugs were identified for which combination treatment significantly ($p<0.05$; *) improved cell killing compared to either drug or virus alone (see *Figure 4.6A*). Characteristics of these drugs are listed in *Table 4.3*. To determine whether this combination effect was due to an increase in viral infection, BTICs treated with the three low-dose candidate compounds were infected with MyxV-FLuc and viral luciferase expression was quantified after 24hrs (see *Figure 4.6B*). None of the low-dose hit drugs increased viral gene expression in BT025, indicating that increased viral infection is likely not

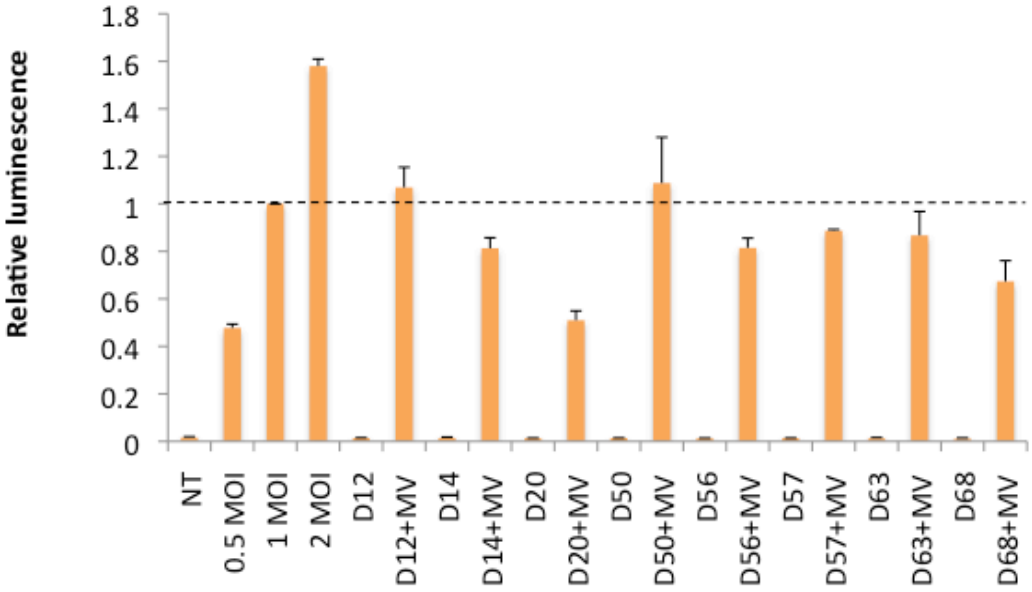
Relative luminescence
1.8
1.6
1.4
1.2
1
0.8
0.6
0.4
0.2
0
NT
0.5 MOI
1 MOI
2 MOI
D12
D12+MV
D14
D14+MV
D20
D20+MV
D50
D50+MV
D56
D56+MV
D57
D57+MV
D63
D63+MV
D68
D68+MV

Figure 4.5: Viral luminescence, a quantitative measure of MyxV infection, does not increase in response to pre-treatment of BT025 with any of the eight candidate compounds

(A) To assess whether the combination effect in *Figure 4.3* was due to an increase in viral infection, luminescence was measured for virus-only and combination-treated BT025 cells at 24hrs post-infection. BT025 cells were plated at $1x10^4$ cells/well in a 96-well plate and the eight candidate compounds were added at 1 μM and cells incubated for four hours. Drug-only controls were included as a control for background luminescence. A viral luminescence dose response (MyxV-FLuc at 0, 0.5, 1, 2 MOI) was also included. After 24 hrs, cells were incubated with the FLuc substrate D-luciferin, and luminescence was measured, with raw luminescence values normalized to 1 MOI (dashed line). None of the eight candidate compounds was shown to significantly (p>0.05) increase viral infection, as indicated by viral luminescence at 24 hrs post-infection. As expected, none of the eight candidates demonstrated any background luminescence. Data are plotted as the mean normalized luminescence, +/- standard error of two independent experiments, each with four internal replicates. Drug number codes are as follows: D12 = bosutinib; D14 = FTY-720; D20 = AZD2281; D50 = hypothemycin; D56 = rofecoxib; D57 = pemetrexed; D63 = etoposide; D68 = erlotinib.

Table 4.2: Cytotoxic Drugs from Drug Library

Drug	#	Primary Activity
Docetaxel	2	Tubulin stabilizer
PIK-75	6	PI-3K inhibitor
Axitinib	8	VEGFR inhibitor
GDC-0941	11	PI-3K inhibitor
BI 2536	22	PLK inhibitor
ZM447439	23	Aurora kinase inhibitor
pp242	24	mTOR inhibitor
LBH-589	26	HDAC inhibitor
MK-2206	28	Akt inhibitor
BMS-754807	31	IGF-1R inhibitor
PF-2341066	34	C-Met-R inhibitor
SN-38	39	Topoisomerase I poison
VX-680	43	Aurora kinase inhibitor
Vorinostat	53	Histone deacetylase inhibitor
Dasatinib	54	Src inhibitor
Gemcitabine	58	nucleic acid synthesis inhibitor
Doxorubicin	59	Topoisomerase II poison
Topotecan	60	Topoisomerase I poison
Bortezomib	64	Proteosome inhibitor
Paclitaxel	69	Tubulin stabilizer
17-DMAG	70	HSP90 inhibitor

(A.)

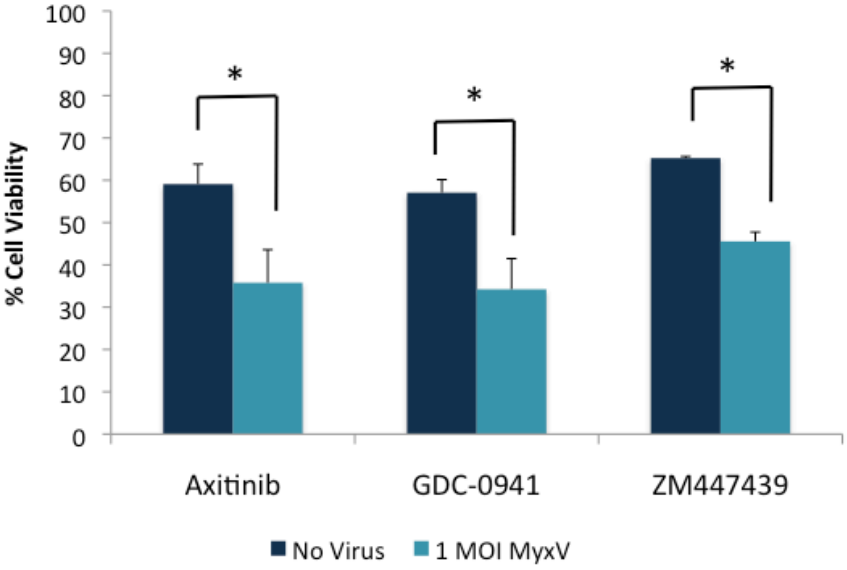
100
90
80
70
60
50
40
30
20
10
0
% Cell Viability
*
*
*
Axitinib
GDC-0941
ZM447439
No Virus
1 MOI MyxV

(B.)

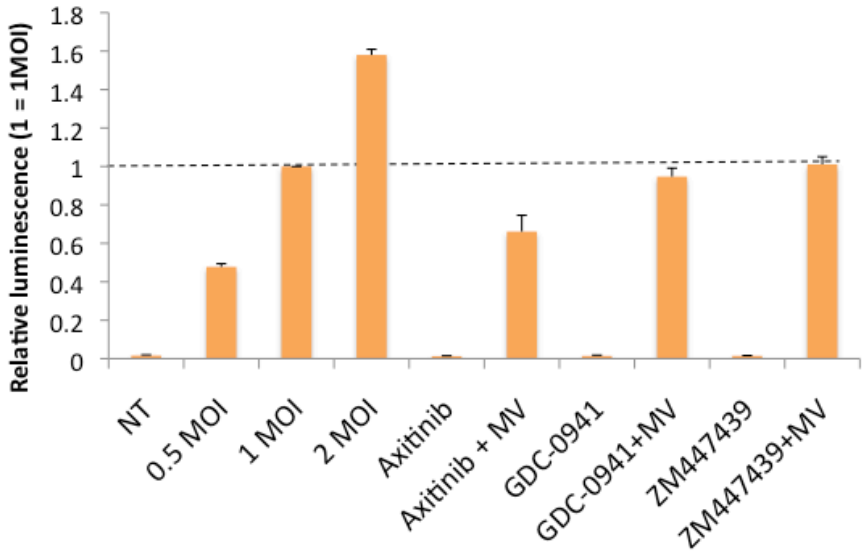
1.8
1.6
1.4
1.2
1
0.8
0.6
0.4
0.2
0
Relative luminescence (1 = 1MOI)
NT
0.5 MOI
1 MOI
2 MOI
Axitinib
Axitinib + MV
GDC-0941
GDC-0941+MV
ZM447439
ZM447439+MV

Figure 4.6: Three of twenty-two cytotoxic drugs show a significant combination effect that is not attributable to an increase in viral infection

(A) Twenty-two cytotoxic drugs (drug alone killed >70% of cells) were re-screened as shown in *Appendix B2*. BT025 cells were plated at a density of $1x10^4$ cells/well in a 96-well plate. The twenty-two cytotoxic compounds were added at a concentration of 100nM and cells incubated for 4hrs. MyxV (1 MOI) was subsequently added to half of the drug-treated wells. No-treatment and virus-only controls were also included. Cells were incubated for 48 hrs and viability measured by Alamar blue. Three candidate compounds were shown to significantly ($p<0.05$; *) improve cell killing compared to either treatment alone. Data are plotted as the mean viability +/- standard error of three independent experiments, each with six internal replicates. (B) To assess whether the combination effect in (A) was due to an increase in viral infection, luminescence was measured for virus-only and combination-treated BT025 cells at 24hrs post-infection. BT025 cells were plated at $1x10^4$ cells/well in a 96-well plate and the three candidate compounds were added at 100nM and cells incubated for four hours prior to infection with MyxV-FLuc. Drug-only controls were included as a control for background luminescence. A viral luminescence dose response (MyxV-FLuc at 0, 0.5, 1, 2 MOI) was also included. After 24 hrs, cells were incubated with the FLuc substrate D-luciferin, and luminescence was measured, with raw luminescence values normalized to 1 MOI. None of the three candidate compounds was shown to significantly increase viral infection ($p>0.05$), as indicated by viral luminescence at 24 hrs post-infection. As expected, none of the three candidates demonstrated any background luminescence. Data are plotted as the mean normalized luminescence, +/- standard error of two independent experiments, each with four internal replicates.

Table 4.3: Identification of Candidate Compounds (100nM Screen)

Drug	#	Activity
Axitinib	8	VEGF-R inhibitor
GDC-0941	11	PI-3K inhibitor
ZM447439	23	Aurora kinase inhibitor

responsible for the observed combination effect. As shown in *Appendix B2*, several drugs were highly cytotoxic even at a relatively low dose of 100nM. These drugs were re-screened in a third-pass screen at 10nM (*Appendix B3*), but no further candidate compounds were identified.

4.4 Six candidate compounds were shown to be synergistic with virus at the lowest dose tested following Chou-Talalay analysis

To determine the nature of the interaction observed with our selected drug-virus combinations, Chou-Talalay analysis was performed. Dose-response curves were generated using drug alone and drug/virus combinations for each of the eleven hits. These are shown in *Appendix C.* Based on these dose-response curves, CI values were calculated for MyxV in combination with each dose of drug. *Figure 4.7* shows the combination indices for the lowest dose tested of each drug. According to the Chou-Talalay method, a drug interaction is considered synergistic if CI <1, additive if CI=1, and antagonistic if CI>1. By this method, six of the original eleven hits were shown to by synergistic with CI<1.

4.5 Summary and significance

In this chapter, a pharmacoviral screening strategy was employed to identify compounds that enhance MyxV-mediated cell death in BTICs. Seventy-three small molecule inhibitors were assessed through several rounds of screening. Of these compounds, eleven were ultimately shown to have a significant combination effect in BT025. Upon

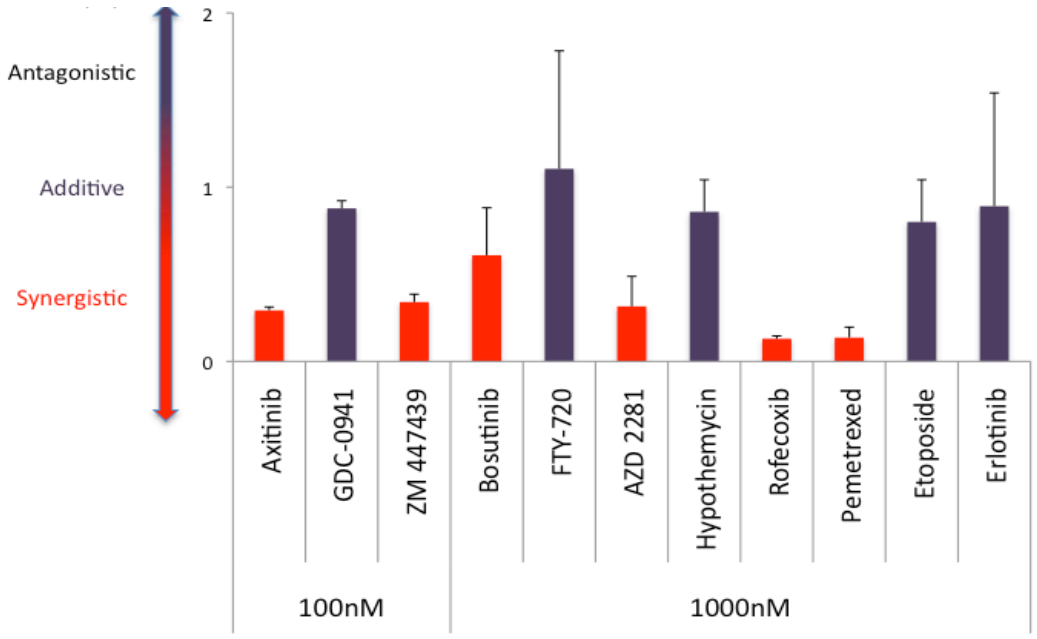

Figure 4.7: Calculation of combination indices reveals that six of eleven candidate compounds are synergistic with MyxV by Chou-Talalay analysis

Combination indices for drug-virus interactions were calculated for all eleven compounds based upon the dose response curves shown in *Appendix C*. BT025 cells were plated at a density of $1x10^4$ cells/well in a 96-well plate. Drug was added at the indicated dose and cells incubated for four hours. MyxV (1 MOI) was subsequently added to half of the drug-treated wells, for a total of eight internal replicates per treatment. No-treatment and virus-only controls were also included. Cells were incubated for an additional 48 hrs and viability measured by Alamar blue (see *Appendix C*). Combination indices were calculated as described in the Methods section and plotted as shown above. According to the Chou-Talalay method, the interaction is considered synergistic when CI<1. As shown above, six of the eleven drugs interact synergistically with virus. Data are plotted as the mean CI for each combination treatment, +/- standard error of two independent CI calculations.

examination of the effect of drug treatment on MyxV infection, none of the compounds was found to significantly increase MyxV infection in BT025. To determine whether the interaction between drug and virus was additive or synergistic in nature, Chou-Talalay analyses were performed, ultimately identifying six agents as synergistic with MyxV. In the next chapter, the strengths and weaknesses of the eleven candidates will be assessed, and a lead compound chosen for further validation.

Chapter Five: Selection and Further Characterization of the Lead Compound Axitinib

5.1 Introduction & Rationale

In Chapter IV, eleven compounds were shown to demonstrate a significant combination effect with MyxV in BT025. Six of these compounds (axitinib, ZM 44734, bosutinib, AZD2281, rofecoxib, and pemetrexed) were shown to synergize with MyxV, following Chou-Talalay analysis. Investigating all of these potential drugs is beyond the scope of this thesis. Nonetheless, it is worth noting that many of these drugs, as well as other members of the represented drug classes, would make excellent candidates for further combination studies in the future.

For this project, a single lead compound was chosen for further characterization. For the purposes of focusing on the most clinically relevant compound, the status of each of the candidate compounds in the drug development pipeline was considered. *Table 5.1* displays the current clinical trial status of each of the eleven compounds according to the National Institute of Health's ClinicalTrials.gov database, as well as the compounds' United States Food and Drug Administration (FDA) approval status if applicable. Compounds that were not listed as having been in clinical trials for GBM (GDC-0941, FTY-720, ZM447439, hypothemycin, and rofecoxib) were eliminated as candidates for further characterization in this study. Of the remaining candidates, drugs that were not FDA approved for any indication (AZD2281) were also eliminated. Axitinib, bosutinib, pemetrexed, etoposide, and erlotinib remained as potential lead compounds, based upon

Table 5.1: Drug Development Status of Candidate Compounds

Drug	#	Alternate Names	Company	Activity	FDA Approved?	Clinical Trials Status	Clinicaltrials.gov ID#
Axitinib	8	AG-013736	Pfizer	VEGFR inhibitor	Yes, for renal cell carcinoma	Phase II GBM Phase III renal cell carcinoma Phase III pancreatic	NCT01508117 NCT00920816 NCT00471146
GDC-0941	11	None	Genentech	PI-3K inhibitor	No	Phase II breast Phase II NSCLC	NCT01437566 NCT01493843
Bosutinib	12	SKI-606	Pfizer	Abl, Src inhibitor	Yes for chronic myelogenous leukemia	Phase II GBM Phase II-III various solid tumours	NCT01331291 NCT00959946
FTY720	14	Fingolimod, Gilenya	Novartis	S1P receptor modulator, PP2A activator	For multiple sclerosis	Phase III/IV MS	NCT01499667
AZD2281	20	Olaparib	AstraZeneca	PARP 1/2 inhibitor	No	Phase I GBM Phase II triple negative breast cancer Phase II NSCLC Phase II ovarian	NCT01390571 NCT01116648 NCT01513174 NCT01081951
ZM447439	23	None	Selleck	Aurora kinase inhibitor	No	None	NA
Hypothemycin	50	None	Off patent	T cell activation inhibitor, MEK/ERK/ PDGFR inhibitor	No	None for cancer	None
Rofecoxib	56	Vioxx	Merck	COX-2 inhibitor	Withdrawn for arthritis	Phase II NSCLC Phase III colorectal adenomas	NCT00385606 NCT00282386
Pemetrexed	57	Alimta	Eli Lilly	Nucleic acid synthesis inhibitor, antifolate	For non-small cell lung cancer (NSCLC)	Phase II GBM Phase III pancreatic	NCT00276783 NCT00035035
Etoposide	63	VePesid, Toposar	Off patent	Topoisomerase II poison	For testicular cancer and small cell lung cancer	Phase II GBM	NCT00612430
Erlotinib	68	Tarceva	OSI Pharmaceuticals	EGFR inhibitor	For NSCLC and pancreatic	Phase II GBM	NCT00525525

their current clinical status. Since the long-term goal of this study was to identify compounds that could in future be used clinically in combination with MyxV, it was crucial to eliminate any compounds that were too early in development. Nonetheless, as mentioned previously, the drugs that were eliminated as candidate compounds early in this study may prove instrumental in identifying other novel classes of drugs that synergize with MyxV.

In addition to considering the clinical status of these drugs, the relative ability of each of the candidate compounds to kill BTICs in combination with MyxV was also considered. *Table 5.2* lists the synergistic compounds and compares their ability to kill BTICs according to the minimum cell viability achieved with combination therapy after 48hrs (raw data shown in *Appendix C*) and the drug dose required to achieve this efficacy. Of the candidates listed in *Table 5.2*, the only candidates remaining after the elimination step above were axitinib, bosutinib, and pemetrexed. Comparing the performance of these three compounds, bosutinib kills BTICs reasonably well (13.3% of viable BTICs remaining) with pemetrexed less so (28.3% of viable BTICs remaining), both at a dose of 10μM in combination with 10 MOI MyxV. By comparison, axitinib achieves complete cell killing (0% viable BTICs remaining) at a tenth of the dose (1μM) with the same MOI of virus.

Table 5.2: Performance Summary of Synergistic Candidate Compounds

Drug	#	Synergistic with MyxV?	Dose of drug at which synergy was observed	Minimum cell viability achieved with combination therapy	Dose of drug required to achieve maximum observed effect	Dose of virus required to achieve maximum observed effect
Axitinib	8	Yes	100nM	0%	1μM	10 MOI
ZM447439	23	Yes	100nM	12.9%	1μM	10 MOI
Bosutinib	12	Yes	1μM	13.3%	10μM	10 MOI
AZD2281	20	Yes	1μM	15.2%	3μM	10 MOI
Rofecoxib	56	Yes	1μM	27.4%	10μM	10 MOI
Pemetrexed	57	Yes	1μM	28.3%	10μM	10 MOI

To summarize, axitinib was chosen as the lead compound in this investigation based upon both its pre-clinical *in vitro* efficacy with MyxV, as determined in this project, and for its favourable clinical profile. Axitinib demonstrated synergy with MyxV at a low, clinically achievable doses (100nM) and demonstrated substantial cell killing at 48hrs in BT025, with ~95% killing observed following a combination treatment with 300nM axitinib and 10 MOI MyxV, and ~100% killing at 1μM with 10 MOI MyxV (*Appendix C*). Importantly, this dose of axitinib falls within the range of clinically attainable plasma concentrations[169]. Depending upon dosing regimen and food intake status, the mean steady-state plasma concentration of axitinib on Day 15 of treatment has been shown to range from 20ng/ml to 160ng/ml[169,170], or 71.7nM- 414nM. Thus, our observation of synergy at 100nM falls within a pharmacologically relevant drug concentration. Of course, in addition to plasma concentration, it is imperative that the lead compound has demonstrated the ability to penetrate the blood-brain barrier. Ongoing Phase II clinical trials of axitinib in high-grade gliomas (e.g. NCT01562197 and NCT01508117) will yield insight into whether axitinib reaches therapeutically relevant doses in brain tumours. Importantly, axitinib is FDA-approved (for renal cell carcinoma) and is in clinical trials for a vast array of solid tumours including gliomas. In these trials, axitinib has been demonstrated to have an acceptable toxicity profile, with the most common adverse reactions including nausea, fatigue, anorexia, diarrhea, and hypertension[169]. Axitinib's potential to have anti-angiogenic effects in addition to synergizing with MyxV could be an additional benefit in a clinical setting. This combination of qualities led to the selection of axitinib as a lead compound for further characterization.

5.2 Axitinib in combination with MyxV leads to substantial cell killing in multiple BTIC lines

The panel of genetically distinct BTICs characterized in Chapter III was revisited in order to determine whether the MyxV-axitinib combination effect observed with BT025 would be observed in different genetic backgrounds. As shown in *Figure 5.1*, BT012, BT073, and BT124 show a high degree of susceptibility to the combination treatment, with 300nM axitinib in combination with 10MOI MyxV leading to almost complete BTIC killing. BT048 was slightly more resistant to combination treatment, which appeared to be the result of reduced susceptibility to MyxV rather than reduced susceptibility to axitinib (since axitinib alone killed BT048 with similar efficacy as it did in BT025 and BT012, in the absence of virus). Interestingly, BT124 was the least susceptible to axitinib alone, but remained susceptible to the combination therapy, indicating that susceptibility to combination treatment may be dictated by baseline susceptibility to MyxV rather than baseline susceptibility to axitinib.

5.3 Axitinib in combination with MyxV leads to substantial cell killing in conventional glioma cell lines

Three human glioma cell lines whose susceptibility to MyxV has been previously characterized[92] were tested to determine *in vitro* susceptibility to combination treatment. These cells ranged from the fairly susceptible U87 to the more resistant U118. As

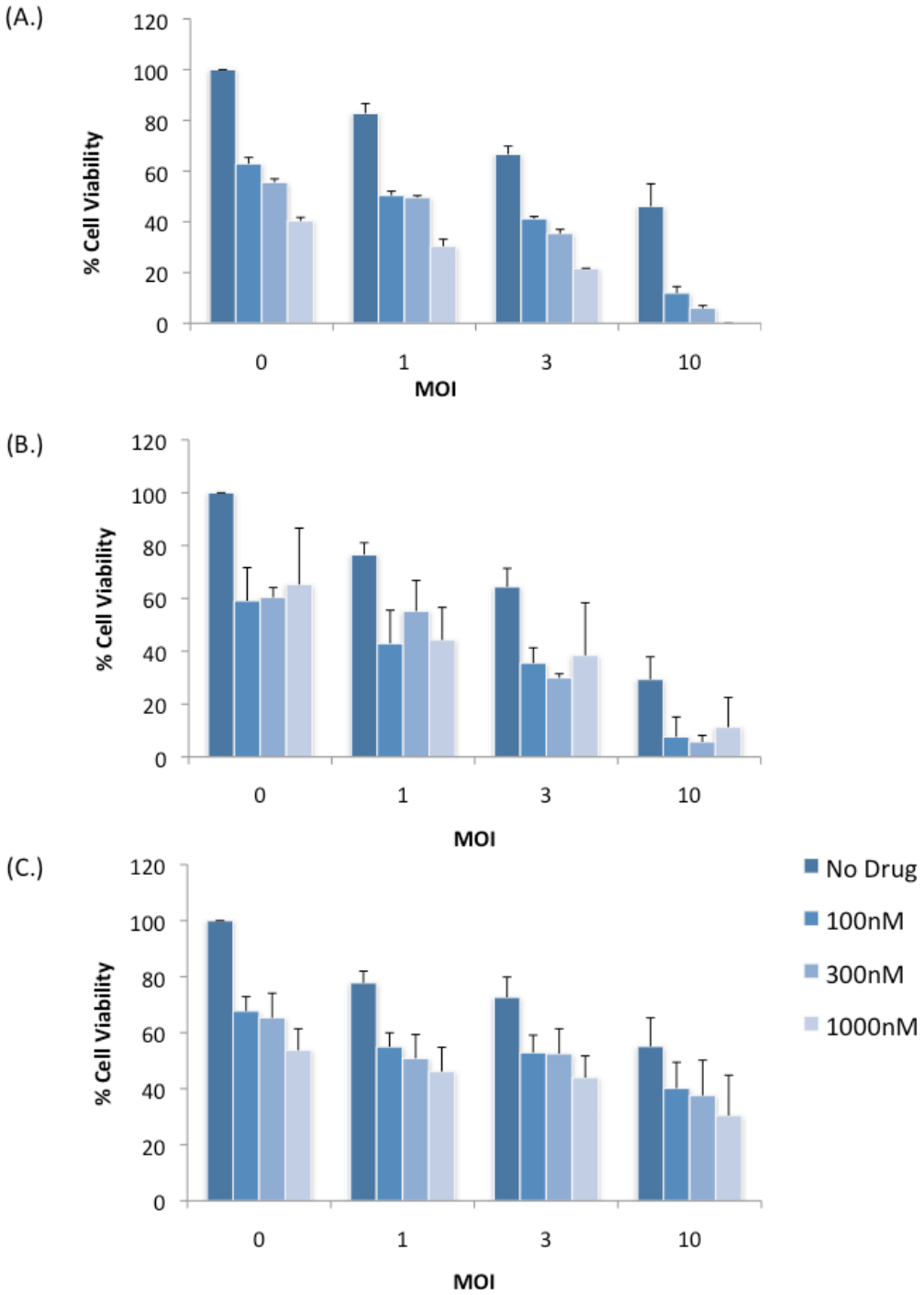
(A.)
120
100
80
60
40
20
0
% Cell Viability
0
1
3
10
MOI
(B.)
120
100
80
60
40
20
0
% Cell Viability
0
1
3
10
MOI
(C.)
120
100
80
60
40
20
0
% Cell Viability
0
1
3
10
MOI
No Drug
100nM
300nM
1000nM

(D.)

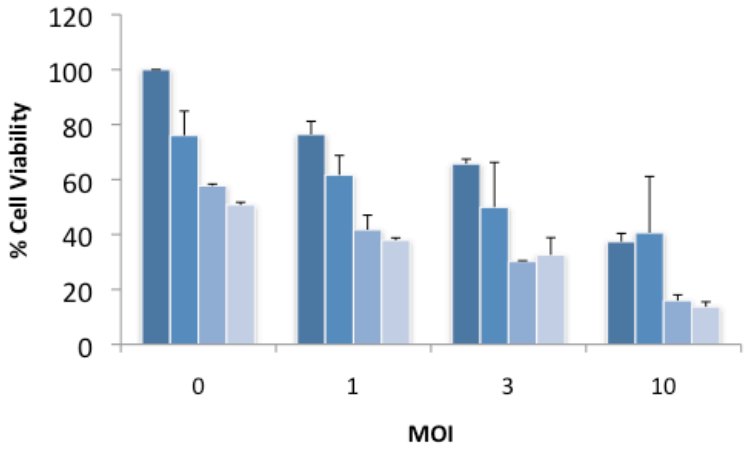
120
100
80
60
40
20
0
% Cell Viability
0
1
3
10
MOI

(E.)

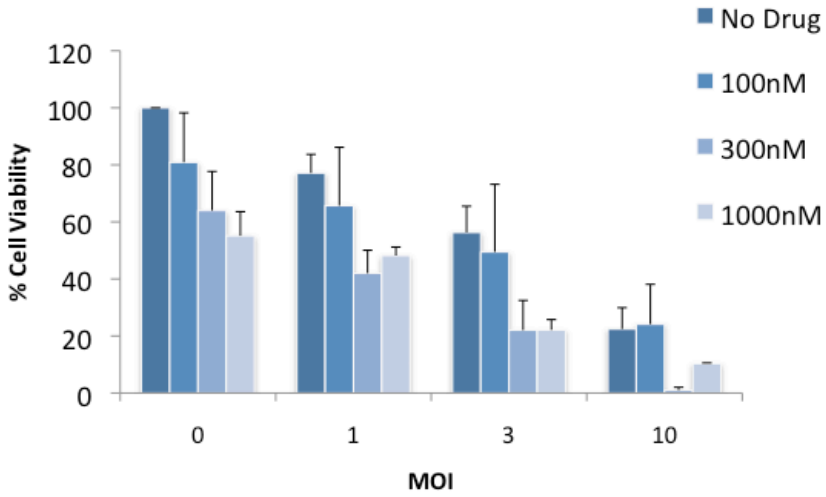
No Drug
100nM
300nM
1000nM
120
100
80
60
40
20
0
% Cell Viability
0
1
3
10
MOI

Figure 5.1: Axitinib administration with MyxV is an effective combination in multiple BTIC lines

Five BTIC lines were each disrupted into single cell suspension and seeded at $1x10^4$ cells/well in a 96-well plate in serum-free neural stem cell media (+EGF,+FGF). Twenty-four hours later, drugs were added at the indicated concentration and cells incubated for four hours. MyxV was subsequently added to half of the drug-treated wells, for a total of eight internal replicates per treatment. No-treatment, drug-only, and virus-only controls were included. Cells were incubated for an additional 48hrs and viability measured by Alamar blue: (A) BT025 (B) BT012 (C) BT048 (D) BT073 (E) BT124. Data are plotted as mean viability, +/- standard error of two independent experiments.

demonstrated in *Figure 5.2*, virtually complete cell killing was observed in all cell lines tested at 300nM axitinib and 10MOI MyxV.

5.4 Axitinib treatment alone or in combination with MyxV does not induce apoptosis

To determine whether axitinib alone or in combination with MyxV induces apoptotic signalling in BTIC lines, we examined caspase-3/-7 activation in BT025. Cells were treated with 10 MOI MyxV, 300nM axitinib, or 10 MOI + 300nM axitinib. As shown in *Figure 5.3A*, no evidence of caspase activation was observed 48hrs post-infection, from axitinib alone or in combination-treated cells. To validate these observations, immunoblots were performed to probe for PARP cleavage as a result of axitinib treatment (alone or in combination with MyxV) after 48hrs. Doxorubicin was included as a positive control for apoptosis. As shown in *Figure 5.3B*, no evidence of PARP cleavage was observed following treatment with axitinib, alone or in combination with MyxV, while PARP cleavage was readily observed following treatment with doxorubicin.

5.5 Axitinib modulates downstream signalling pathways

To investigate downstream targets affected by axitinib treatment in BT025, a PathScan™ Multiplex immunoblot was performed. BT025 cells were treated with 0-1000nM axitinib for 2hrs and whole cell extracts (prepared in the presence of phosphatase inhibitors) were immunoblotted using the Multiplex Western Cocktail™, which includes monoclonal antibodies against phospho-p90RSK(Ser380), phospho-Akt (Ser 473), phospho-Erk1/2 (Thr202/Tyr204), phospho-S6 ribosomal protein (Ser235/236), and the loading control

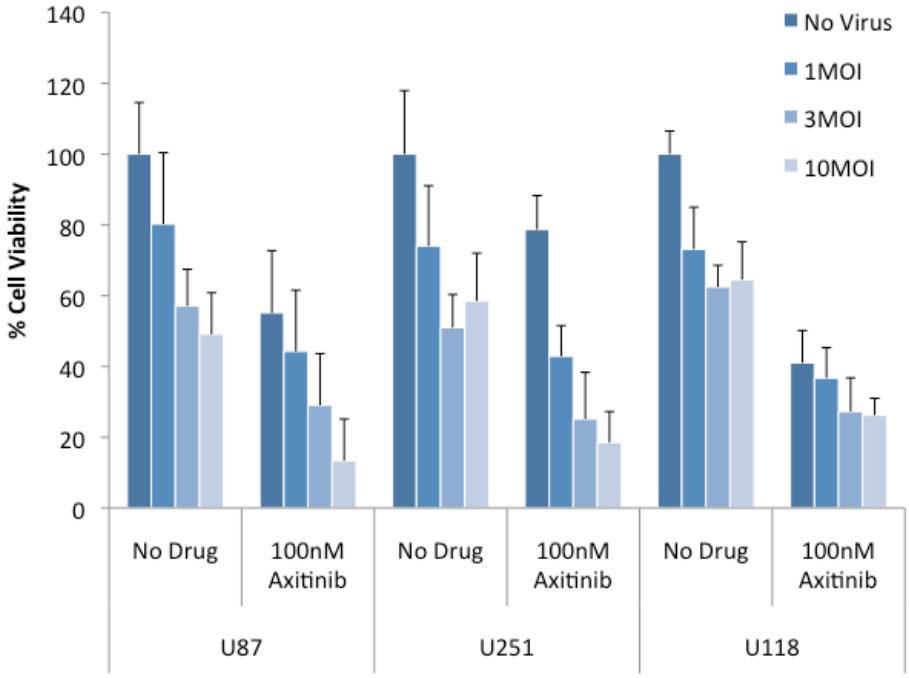

Figure 5.2: Axitinib administration with MyxV is an effective combination in multiple human glioma cell lines

Cells were harvested and plated at a density of $5x10^3$ cells/well in a 96-well plate. Axitinib was added at the indicated concentrations and cells incubated for four hours. MyxV was subsequently added to half of the drug-treated wells, for a total of eight internal replicates per treatment. No-treatment, virus-only, and drug-only controls were also included. Cells were incubated for an additional 48hrs and viability measured by Alamar blue. Data are plotted as the mean viability +/- standard deviation from a single experiment.

(A.)

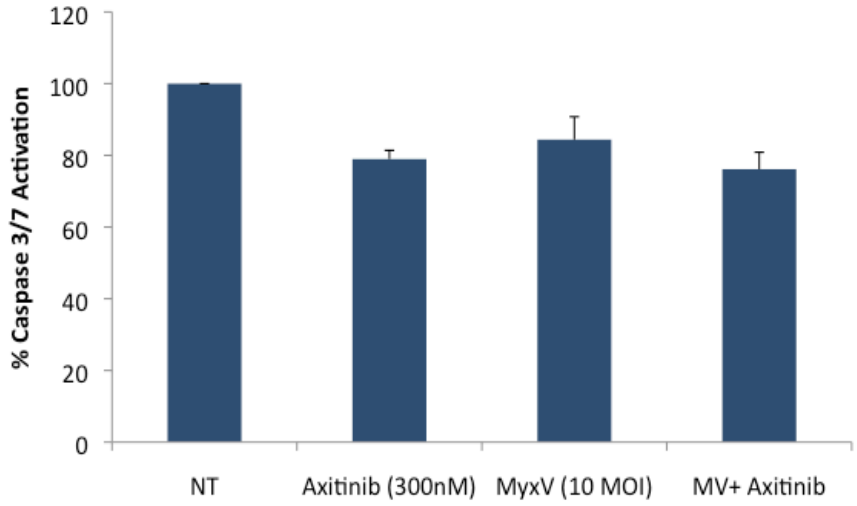
120
100
80
60
40
20
0
% Caspase 3/7 Activation
NT
Axitinib (300nM)
MyxV (10 MOI)
MV+ Axitinib

(B.)

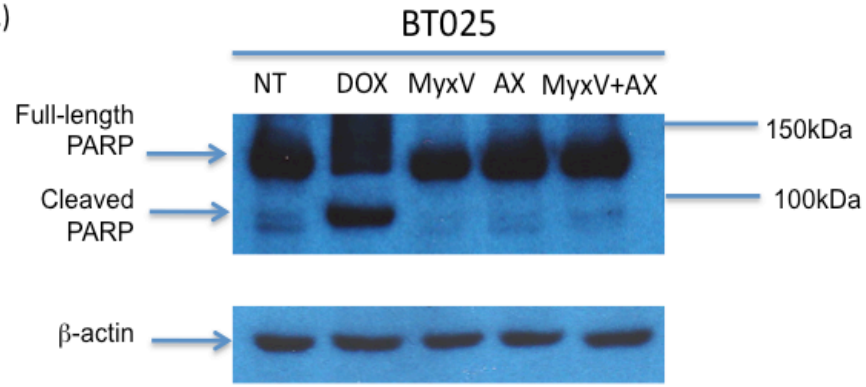
BT025
NT
DOX
MyxV
AX
MyxV+AX
Full-length PARP
Cleaved PARP
150kDa
100kDa
β-actin

Figure 5.3: Axitinib administration with MyxV does not induce apoptosis

(A) BT025 neurospheres were disrupted into single cell suspension and seeded at $1x10^4$ cells/well in a clear-bottomed, black-sided 96-well plate in serum-free neural stem cell media (+EGF, +FGF). Twenty-four hours later, cells were treated with axitinib (300nM) and cells incubated for four hours. MyxV (10 MOI) was subsequently added. Cells were incubated for 48hrs and caspase-3/-7 activation measured by the Caspase-Glo™ luminescent assay. Axitinib alone and in combination with virus does not induce caspase-3/-7 activation. Data are presented as mean +/- standard error and represent two independent experiments, each with four internal replicates. (B) To validate the observation that axitinib does not induce caspase-3/-7 activation, BT025 cells were treated with doxorubicin (1μM), MyxV (10 MOI), axitinib (300nM) or MyxV with axitinib (10MOI MyxV pre-treated with 300nM axitinib for 4hrs) and incubated for 48hrs prior to preparation of whole cell extracts and immunoblotting. BT025 extracts were immunoblotted for PARP. Cleavage of PARP from its full-length (116 kDa) to cleaved (89kDa) product is indicative of apoptosis. In BT025 cells, PARP cleavage is not induced in response to axitinib treatment, with or without pre-treatment with virus.

Rab11 (*Figure 5.4*). This time point was chosen based on the observation in previous reports that axitinib target modulation is apparent as early as one hour post-treatment[171]. Compared to the untreated control, phospho-Akt levels modestly decline with the addition of axitinib, which is consistent with previous reports on axitinib[171]. Although Akt activation has been shown in the literature to favour MyxV replication, activation of the pro-survival PI-3K-Akt/mTOR axis could also function to prevent cell death upon viral infection. Thus, axitinib-mediated attenuation of Akt signalling may function to promote cell death, potentially at the expense of further viral replication. This hypothesis will be discussed further in Chapter VI.

Interestingly, phospho-Erk1/2 increases with the addition of axitinib. This may reflect the possibility that the diminished signalling through the PI-3K/Akt pathway triggers a compensatory increase in the activation of the MEK/Erk pathway in this model. Additional experiments will be required to determine whether the activation of this pathway is a consequence of axitinib treatment, and the effect this signalling has on MyxV-mediated cell death. Phospho-S6 and phospho-P90RSK do not appear to be affected by axitinib treatment at 2hrs post-infection, although they may be affected at a later time point.

5.6 Summary and significance

In this chapter, axitinib was rationally selected from a list of eleven candidate compounds as the lead compound in this investigation. Axitinib was shown to be effective in

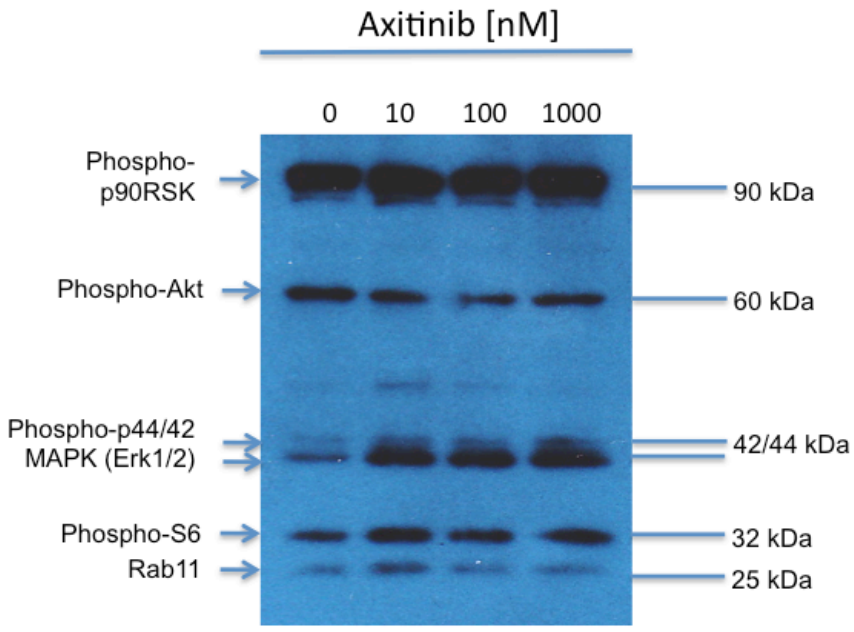

Figure 5.4: Axitinib treatment moderately reduces Akt phosphorylation

To determine downstream targets affected by axitinib treatment in BT025, a PathScan™ Multiplex immunoblot was performed. BT025 cells were treated with 0, 10, 100, or 1000nM axitinib for 2hrs prior to preparation of whole cell extracts and immunoblotting. BT025 extracts were immunoblotted using the Multiplex Western Cocktail™, which includes monoclonal antibodies against phospho-p90RSK(Ser380), phospho-Akt (Ser 473), phospho-Erk1/2 (Thr202/Tyr204), phospho-S6 ribosomal protein (Ser235/236), and the loading control Rab11. Compared to the untreated cells (0nM, far left), phospho-Akt levels are modestly attenuated by treatment with axitinib, while phospho-Erk1/2 levels increase upon exposure to axitinib. Phospho-S6 and phospho-p90RSK are not affected by axitinib treatment.

combination with MyxV in a panel of genetically distinct BTIC lines, as well as in three immortalized glioma cell lines. Several observations were also made concerning the mechanism of interaction between MyxV and axitinib. Firstly, it was shown using caspase-3/-7 activation and PARP cleavage immunoblots that axitinib alone or in combination with MyxV does not induce apoptosis. Secondly, it was demonstrated that axitinib treatment leads to a moderate decrease in Akt phosphorylation, suggesting a possible point of molecular interaction between MyxV and axitinib. Although these investigations into the mechanism driving MyxV-axitinib synergy are preliminary, these observations provide useful direction for further studies of the mechanism for synergy. These future directions will be outlined in Chapter VI.

Chapter Six: Discussion

MyxV is an experimental OV that has shown substantial promise in preclinical glioma models, curing orthotopic xenograft gliomas with a single intracranial injection[92]. However, despite promising results in conventional glioma cell lines, MyxV has been shown to be less effective in BTIC models, leading to only modest increases in survival[109]. In this investigation, we sought to interrogate and enhance MyxV-mediated cell death in patient-derived BTICs using a pharmacoviral approach. After interrogating the mechanism of MyxV-mediated cell death, we utilized a pharmacoviral screen of 73 small molecule inhibitors to identify eleven compounds that demonstrated a significant combination effect with MyxV, and verified the efficacy of the lead compound, axitinib, in a panel of BTIC lines. Mechanism of cell death and downstream target modulation were also investigated.

As many experimental OVs are currently making the transition from preclinical to clinical testing, it is of the utmost importance that preclinical studies realistically assess the limitations of OVs as monotherapies, and attempt to address these limitations through intelligent combination therapy approaches. Although an *in vivo* drug screen would be the ideal approach to identify compounds that synergize with virus, the cost and logistics for the purposes of this study were prohibitive. In this *in vitro* investigation, we have elucidated several possible approaches for optimizing MyxV therapy in the future, including pharmacoviral treatments with various small molecule inhibitors. As a consequence of our investigations into the mechanism of MyxV-induced cell death, the

intriguing possibility of using knock-out viruses with altered mechanisms of host cell killing was also brought forward. These exciting possibilities will be addressed in further detail below.

6.1 Characterization of MyxV-induced Cell Killing

In Chapter III, it was demonstrated that most BTICs were infected with MyxV, yet were only modestly susceptible to MyxV-induced cell death. This observation adds a layer of complexity to the original paradigm of OV therapy, which envisioned that a productive infection must ultimately culminate in cell lysis and the release of viral progeny[62]. The observation that infection does not necessarily result in cell death raises the possibility that MyxV infection is not in itself lethal to BTICs. When one considers that MyxV encodes a plethora of proteins, such as anti-apoptotic proteins and growth factor homologues, designed to sustain host cell viability, it becomes increasingly unlikely that MyxV-infected BTICs die through direct viral oncolysis. As discussed in Chapter I, infected cells are frequently capable of eliciting apoptosis and/or autophagy as a programmed self-defence mechanism against replicating viruses. The induction of apoptosis as a mechanism of oncolytic virus-induced killing has been previously documented[172-174]. These observations led to the hypothesis that MyxV-mediated cell death is mediated by a programmed cell death response that is triggered upon viral infection. Variations in the intrinsic resistance to programmed cell death might then account for differences in susceptibility to MyxV between different genetically distinct BTIC lines.

To test the hypothesis that BTICs die through MyxV-triggered apoptosis, apoptotic signalling following infection was measured using a functional caspase-3/-7 activation assay, and the results confirmed in a subset of cell lines using immunoblots for cleavage of caspase-3, caspase-7, and PARP. The executioner caspases-3 and -7 were strategically chosen as the focus of this work because both the intrinsic and extrinsic pathways converge upon the activation of the executioner caspases, whereas the intiator caspases (caspase-8, -9, etc.) are activated under a more narrow set of circumstances[138]. Since viruses have been shown to elicit apoptosis through both intrinsic and extrinsic pathways, the measurement of caspase-3 and -7 activation ensured that the induction of apoptosis by either mechanism would be revealed by our assay.

In all BTICs tested, apoptosis assays revealed no evidence for the induction of apoptosis following viral infection, and in several BTIC lines, viral infection appeared to lower basal levels of caspase-3 and -7 activation (*Figure 3.6*). The fact that some basal level of caspase-3/-7 activation was present in culture is not unusual, as apoptotic signalling in neurospheres has been previously documented in neural stem cell cultures[175,176]. This low-level signalling may be the result of apoptosis of cells in the center of the growing neurospheres; this hypothesis could be tested using immunostaining of intact spheres for caspase-3/-7. In our BTIC neurospheres, addition of the pan-caspase inhibitor ZVAD was shown to abrogate basal levels of caspase-3/-7 signalling, with no significant effect on survival (*Figures 3.6 and 3.9*).

However, the observation that virus infection also lowered basal levels of caspase-3/-7 signalling in some cell lines was both intriguing and unexpected. Upon further examination of the literature, the observation seems consistent with the fact that MyxV encodes the Bcl-2 structural homologue M011L for the specific purpose of inhibiting mitochondrial apoptosis[108,150,151]. The observation that MyxV only lowered basal caspase activity in a subset of BTIC lines may be indicative of the intrinsic resistance of those cell lines to apoptosis. It is possible that BTICs that already exist in a highly anti-apoptotic state are most susceptible to the down-regulation of caspase activity by virus. However, no work has yet been done, to our knowledge, examining the relative levels of pro- (e.g. BAK, BAX, BID, BAD, and PUMA) and anti- (e.g. Bcl-2, Mcl-1) apoptotic proteins in these BTICs; such a study would be highly informative in predicting the anti-apoptotic action of MyxV in BTIC lines. Upon initial examination, and bearing in mind the caveat of a very small sample size, p53 status does not seem to determine this phenotype: BT012 and BT073, in which MyxV partially abrogates basal caspase activity, are p53 wild-type and p53 mutant respectively.

Based upon previous reports stating that MyxV actively prevents apoptosis through the expression of MyxV-M011L[108,149-152], we hypothesized that MyxV-induced cell death could be enhanced through the deletion of this viral gene. MyxV-M011L-KO virus was shown to dramatically enhance cell killing compared to wild-type virus in both cell lines tested, and to significantly increase pro-apoptotic signalling following infection, an effect that was abrogated by the pan-caspase inhibitor, Z-VAD (*Figure 3.8*). This inhibitor also

partially abrogated MyxV-M011LKO-mediated cell death, highlighting that MyxV-M011L-KO-induced cell death involves apoptosis, yet is ultimately multi-factorial.

This is the first indication, to our knowledge, that a MyxV mutant that has been modified to promote apoptosis has been shown to be a more efficacious oncolytic agent than wildtype virus. Typically, a swift apoptotic response is thought to inhibit effective viral replication, as apoptosis is considered to be an evolutionary mechanism to prevent viral replication and spread[144]. The only examination of MyxV-M011L-KO in the oncolytic setting, to our knowledge, was an examination of the replicative potential of various MyxV mutants in glioma cell lines; since MyxV-M011L-KO promotes apoptosis, typically at the expense of viral replication, it was not identified as a candidate for further study[153]. Our demonstration that MyxV-M011L-KO drastically improves cell killing when compared to wild-type virus *in vitro* challenges the popular assumption that maximizing viral replication is the most appropriate strategy to maximize efficacy. Our observations, though warranting additional investigation, support the possibility that modified OVs could be used as highly targeted pro-apoptotic agents, "oncotropic" rather than "oncolytic" viruses in the traditional sense.

Additional investigations of MyxV-M011L-KO across the full panel of BTIC lines, including the most resistant BT048, are needed to validate its improved efficacy compared to wild-type virus. The inclusion of new, low-passage patient samples in this panel, preferably including samples from each of the newly identified major sub-groups of GBM[24], would be an asset for confirming clinical applicability. Since the mutant virus

currently bears no fluorescent or luminescent reporters to facilitate its use in experimental settings, virus titres must also be performed to quantify viral replication, while infection can be further validated through immunoblots of early and late MyxV proteins. Confirmation of the M011L knock-out should be performed in our hands using either reverse transcriptase polymerase chain reaction (RT-PCR) for M011L or immunoblot analysis using M011L antibodies previously described[151]. In order to further validate our preliminary conclusion that MyxV-M011L-KO kills through apoptosis, multi-channel flow cytometry could be performed in which detection of viral markers is combined with annexin/propidium iodide analysis. This would not only provide further evidence for apoptosis as a means of cell death, but also elucidate whether bystander apoptosis is induced in non-infected cells, as has been shown previously with viruses such as oncolytic HSV[172].

It is noteworthy that MyxV-M011L-KO was more effective in BT025 then BT073, which may be related to the intrinsic levels of pro- and anti-apoptotic proteins in these BTIC lines. When combined with data from other BTIC lines, it would interesting to investigate whether susceptibility to MyxV-M011L-KO-induced killing could be correlated to the expression of such proteins. If the expression of a specific protein, such as Bcl-2, were correlated with greater resistance to virally-induced cell death, it may be possible to strategically combine this virus with a targeted small molecule inhibitor (such as the Bcl-2 inhibitors ABT-737 or ABT-263) in order to tip the balance of signalling in favour of a pro-apoptotic response. Clinically, the use of a highly tumour-selective pro-apoptotic agent (MyxV-M011L-KO) in combination with a less selective pro-apoptotic agent (Bcl-

2 inhibitor) would ideally lower the dose of small molecule inhibitor necessary to achieve therapeutic efficacy, thus minimizing side-effects traditionally associated with systemically administered pro-apoptotic therapy. Of course, specificity for tumour cells must be confirmed with MyxV-M011L-KO to ensure its safety.

Despite these exciting observations and opportunities, it must be noted that the manner of MyxV-mediated cell death induced in BTICs by wild-type MyxV was still not fully elucidated in this work. No evidence was obtained for apoptosis as a mechanism of cell death, and preliminary autophagy assays were inconclusive, thus leaving open the possibility that MyxV-mediated autophagy is responsible for cell death in BTICs. Though our initial attempts to detect LC3β processing by immunoblot were unsuccessful, it was not determined whether the antibody failed to detect LC3β in the BTICs tested, whether LC3β is under-expressed in these cells, or whether LC3β exists in an oligomer of a different size. Confirmation of LC3β expression at the mRNA level would be an important first step in trouble-shooting this assay, as would the inclusion of a positive control with known levels of LC3 expression in future experiments.

Several other assays are available for confirming or refuting the involvement of autophagy in MyxV-mediated cell death (extensively reviewed elsewhere[177-179]). For instance, detection of autophagosomes by electron microscopy is a commonly used approach. Assuming that LC3 expression is confirmed in one or more BTICs, immunofluorescence could also be used to determine whether LC3 is incorporated into

autophagosome membranes. However, one limitation to these approaches is that they are static; any observed increase in autophagosome production or LC3 processing may be attributed to either an induction in autophagy or a blockade in late-stage autophagosomal degradation, creating a backlog of autophagosomes[155]. Thus, the gold standard for measuring autophagy is the quantification of autophagic flux, that is the passage of protein substrates through the autophagic degradation pathway[155]. In order to verify that autophagy is acting as a cell death and not a cell survival mechanism under the stress of viral infection, it is necessary to perform siRNA-mediated knock-down studies in which crucial autophagy regulating genes (such as ATG5 or Beclin-1) are silenced. The abrogation of cell death by the silencing of autophagy genes would suggest that the virus is killing through autophagy; an increase or no change in cell death would indicate that autophagy is not responsible for cell death, but rather may be acting as a survival mechanism under conditions of viral infection.

One of the challenges when faced with determining whether viral infection results in autophagic cell death is the confounding factor that certain viruses can deliberately induce autophagy for the purpose of facilitating the maturation of virions[154]. In such cases, autophagy is not a programmed cell death response to viral infection, but rather a strategy co-opted by the virus to facilitate its replication. Such subtle differences are very difficult to ascertain experimentally, as the abrogation of autophagic signalling may cause reduced cell death in either case. It is worth noting that in addition to apoptosis and autophagy, a multitude of other subsets of programmed cell death have been identified, including necroptosis, pyroptosis, and lysosome-mediated programmed cell death,

amongst others[180]; these were not addressed in this study. According to the Nomenclature Committee on Cell Death 2009, up to twelve distinct cell death modalities have been identified[181]. These pathways often cross-talk with each other and with apoptotic and autophagic cell death pathways, making the delineation of distinct, non-overlapping death pathways difficult[180]. In determining the mechanism of cell death that results from viral infection, the task becomes further complicated by the manipulation of cell death pathways by viral proteins[144]. This observation has led leading members of the OV field to recently suggest that existing concepts of cell death are inadequate to describe the complex nature of OV-mediated cell death[79]. In spite of this observation, attempts to characterize cell death following OV infection may yield clinically useful insights into how the virus may be optimized, either genetically or through combination therapy, to maximize efficacy.

There are several technical limitations worth discussing for this initial work. Firstly, in chapter III, we elected to quantify late viral gene expression as a surrogate for viral titres. Although viral titres are unquestionably the gold standard for confirming viral infection, previous work in our lab has repeatedly confirmed the release of viral progeny in several of these BTIC lines. Since viral replication was not a major endpoint in this study, late viral gene expression was deemed an appropriate surrogate for confirming productive viral infection. It is worth noting that the sensitivity of the RFP reporter is somewhat confounded by the high background fluorescence (~46 fluorescence units). Despite this, an increase in reporter expression over time was confirmed for all BTICs tested, indicating that late viral gene expression was achieved in all five BTIC lines.

It is also worth noting that our initial characterization of cell viability relied upon the Alamar blue assay, which provides a colorimetric indication of mitochondrial viability. This assay was utilized for several reasons. Firstly, the colorimetric approach (as opposed to fluorescence or luminescence) ensured that viral fluorescent and/or luminescent reporters would not interfere with viability read-outs. Secondly, other assays that indicate cell proliferation as opposed to viability, such as bromodeoxyuridine (BrdU) incorporation assays, might be confounded by the presence of viral genomic double-stranded DNA, biasing the results towards false positives. The colorimetric readout of Alamar blue was not known to be confounded in any way by the virus, although the fluorescent read-out of this assay was avoided due to overlapping emission wavelengths with the dsRED viral reporter. Although Alamar blue is extremely well-validated in the literature, confirmation of the initial BTIC susceptibility assays could be performed using alternative, non-mitochondrial viability assays, such as neutral red[182].

6.2 Small Molecule Inhibitor Drug Screen

Given that wild-type MyxV cytotoxicity appears inherently limited in BTICs, identifying chemotherapeutics that enhance MyxV-mediated cell death was proposed as an effective strategy to optimize cell killing. An *in vitro* screen of 73 small molecule inhibitors in BT025, alone and in combination with MyxV, was performed to identify compounds that might ultimately synergize with MyxV. Eleven initial candidate compounds with the potential to synergize with MyxV were identified. We verified that combination therapy at the indicated dose significantly enhanced BTIC killing compared to either

monotherapy in all eleven hits (p<0.05). Four of the initial hit compounds were inhibitors of the PI-3K pathway (either targeting PI-3K itself or upstream receptor tyrosine kinases); various inhibitors of this pathway have previously been shown to enhance the efficacy of OVs[93,135,136]. In addition, our list of hits included the topoisomerase II poison etoposide, which has been shown in the literature to synergize with oncolytic HSV in a glioma stem cell model[125]. The identification of signalling pathways with known potential to synergize with OVs provided confidence in the validity of this approach.

Using Chou-Talalay analysis, we verified that six candidate compounds were synergistic with MyxV in BT025 cells. In particular, axitinib was shown to be synergistic with MyxV at low, therapeutically relevant doses, and to kill ~100% of the cells at a dose of 1000nM in combination with 10 MOI MyxV. Combined with its favourable clinical profile, these observations led to the selection axitinib, a relatively specific inhibitor of VEGFR1, 2, and 3, as the lead compound for mechanistic characterization.

6.2.1 The Drug Screen Approach: Benefits and Limitations

Unbiased high-throughput approaches that generate vast amounts of data are becoming increasingly popular in modern cancer research. Some examples include drug discovery screens, whereby previously uncharacterized molecules are tested for the ability to induce a specific cellular response[183]; cellular interaction screens, whereby stromal cells are co-cultured with cancer cells to elucidate trends in drug resistance[184]; and synergy screens, whereby various combinations of drugs are tested to elucidate synergistic interactions[185]. Such screens are often automated, which allows for vast datasets to be generated with

high efficiency. In this project, no automation was possible, and thus the screen was somewhat more directed in scope than the vast high-throughput drug arrays often described in the literature.

The drug library utilized in this study consisted of 73 small molecule inhibitors, all of which are in preclinical or clinical development (or FDA-approved) for cancer or other conditions. Although previous pharmacoviral screens have been much larger in nature (>10,000 drugs), these screens included vast numbers of previously uncharacterized compounds[168]. By contrast, our approach eliminated drugs with unknown or prohibitive toxicity profiles, and ensured all of our candidates were well characterized in either preclinical or clinical trials. We initially tested this drug library in a single BTIC line (BT025), at one concentration, at one time point, in combination with one concentration of MyxV. Although these parameters were rationally selected (as described in detail in Chapter IV), this approach biases the system towards false negatives; it is possible that compounds other than those identified in our screen would demonstrate synergy at different concentrations of drug and/or virus, at different time points, or in different in BTIC lines. Some of these issues were circumvented through re-testing of more potent drugs at lower concentrations (100 and 10nM), which yielded three further candidate compounds, and by testing candidate compounds at multiple concentrations. Nonetheless, it is possible that some drugs with the potential to synergize with MyxV were overlooked due to the parameters of the initial screen. If the initial screen had not yielded such successful candidates for synergy, it would have been possible to widen the test parameters.

Although this method was prone to false negatives, the initial screen had no false positives; all eight drugs initially identified as putative hit compounds at 1μM were later shown to have a statistically significant combination effect when repeated in three independent trials (*Figure 4.3*). Although not all of these proved to be synergistic combinations, this increases our confidence in the validity of the initial parameters and the established benchmark (20% improvement in killing over each monotherapy) for the candidate compounds. Interestingly, our screen identified several novel drug classes that had not been shown previously to synergize with OVs *in vitro*, including COX2 inhibitors and VEGFR inhibitors. These drug classes would be excellent candidates for future targeted studies investigating novel pharmacoviral therapies.

When considering the results of this investigation, an important caveat is that the *in vitro* BTIC drug screen system does not accurately recapitulate many elements of the glioma microenvironment, such as hypoxia and immune infiltration. It is possible, and in fact extremely likely, that mRNA and protein expression profiles of these cells would be vastly different *in vivo* than *in vitro*. As a result, some of the candidate compounds we identified may not be effective *in vivo*, and conversely, some drugs that were not identified in this study may be excellent synergistic compounds *in vivo.* This highlights the necessity to test putative hits in *in vivo* systems, and ideally, to develop drug screen approaches that can be pragmatically performed *in vivo.*

6.3 Chou-Talalay Analysis

The use of the Chou-Talalay analysis to determine whether the interaction between the two treatments is synergistic or additive is one of the most well-validated approaches in the literature[186]. Initially developed in 1984, and based on several decades of research, the Chou-Talalay analysis is a simple yet powerful tool for elucidating whether the interaction between two compounds may be characterized as additive, synergistic, or antagonistic[162,187,188]. Though the mathematical basis of the Chou-Talalay analysis will not be discussed in detail here, it is worth noting the overall approach is based on the concept of the median effect, the idea that the median is a useful reference point around which to organize an analysis of drug interactions[186]. In practical terms, this may be understood as the notion that comparing the observed IC_{50}'s of drugs in combination against their predicted IC_{50}'s in combination is a useful framework to establish the nature of their interactions. The Chou-Talalay analysis provides a numerical indication of drug interactions, called the combination index (CI), whereby values <1 indicate synergy, values =1 indicate additive effects, and values >1 indicate antagonism. A combined effect that exceeds the effect of either drug alone does not necessarily indicate synergism, as such an interaction may be additive or even mildly antagonistic[186].

There are a variety of benefits to the Chou-Talalay analysis. For instance, a putative mechanism for synergy is unnecessary in this analysis[186], making it ideally suited for high-throughput combination studies and for novel combinatorial studies where mechanisms of drug interaction may be unknown or impossible to predict. Furthermore, a specific pattern of drug kinetics (first-order, second-order, etc.) is not required; the only

requirement is that the dose response of each drug in isolation be determined prior to examining the combination effect[186]. Additionally, the Chou-Talalay analysis is quantitative, allowing for differentiation between highly synergistic and moderately synergistic interactions[186]. This quantification can be performed at various doses of each agent, allowing one to determine the concentrations of each drug at which the synergistic interaction is most pronounced. Multiple studies have established that the use of Chou-Talalay analysis is applicable to pharmacoviral interactions[129,135,168], as well as more traditional drug-drug interactions, making it ideally suited for the current study.

One limitation of the Chou-Talalay analysis is that it does not provide a read-out of overall efficacy of the drugs in combination. As highlighted in Chapter V, certain combinations may be highly synergistic but may not necessarily result in highly efficient cell killing. Thus, when choosing lead combinations for further characterization, it is necessary to examine the raw dose response curves to determine whether optimal cell death is indeed achieved.

6.4 Improved viral infection as a mechanism of synergy

In Chapter IV, improved viral infection was investigated as a mechanism of interaction between each of the eleven drug candidates and MyxV at the 24hr timepoint (*Figure 4.5*). Although no suggestion of improved viral infection was seen at this timepoint, it is possible that immediate viral infection (6-12hrs) may have been transiently affected, which would not have been detected by our 24hr assay. Conversely, in order to determine whether viral replication, as opposed to infection, was improved through combination

treatment, it would be necessary to examine later time points following infection with a low dose of virus to determine whether replication and/or spread through the BTIC culture is improved through drug treatment. These are important experiments to pursue in the future in order to fully elucidate the interaction between hit drugs and virus.

6.5 Characterization of the Lead Compound: Axitinib

In this investigation, we demonstrated that the VEGFR/PDGFR/cKIT inhibitor axitinib enhances the efficacy of MyxV therapy in multiple genetically distinct BTIC lines (*Figure 5.1*), as well as in conventional glioma cell lines such as U87, U251 and U118 (*Figure 5.2*). This is the first time, to our knowledge, that axitinib has been shown to synergize with an OV. It was demonstrated, using caspase-3/-7 activation assays and PARP cleavage immunoblots, that this enhancement of cell death did not appear to be caused by the induction of apoptosis (*Figure 5.3*), as is often the case when chemotherapeutic agents and OV therapies are combined (see Chapter I). Given the anti-apoptotic qualities of MyxV described in Chapter III, this result is not surprising. Bearing in mind that autophagy may be triggered when apoptosis is inhibited, examination of autophagy using the methods delineated earlier appears to be a logical next step in elucidating the cell death mechanism resulting from combination therapy.

As discussed in Chapter V, axitinib was chosen as a lead compound for a number of reasons, including but not limited to: (i) its high degree of synergy with MyxV in BT025 (ii) its ability kill~100% of BT025 cells after 48hrs in combination with MyxV (iii) the observation of synergy at doses that correspond to clinically achievable plasma

concentrations (iv) the presence of ongoing clinical GBM trials to determine blood-brain barrier penetration in humans, (v) its acceptable toxicity profile as an FDA-approved chemotherapeutic for other cancer types, and (vi) its oral bioavailability.

As shown in *Figure 6.1*, axitinib and other VEGFR inhibitors act upon the receptors' intracellular kinase domains, thus preventing downstream signalling. Traditionally, in glioma and other cancers, VEGFR inhibitors have been thought to act upon endothelial cells in order to reduce angiogenesis and/or normalize tumour vasculature to improve delivery of systemic chemotherapeutics. In our system, axitinib exerted a direct anti-tumour effect upon the BTICs, both alone and in combination with MyxV. Based upon a multiplex immunoblot analysis, it was shown that the PI-3K/Akt pathway was modulated by axitinib treatment (*Figure 5.4*). Since all of the tyrosine kinase receptors that axitinib is known to act upon (VEGFR1/2/3, PDGFR, cKIT) can signal through this pathway, it currently remains unclear through which receptor axitinib is acting. Based upon microarray gene expression data (Weiss lab, unpublished data), it appears that BT025, BT012, BT073, and BT048 express very low levels, if any, of VEGFR2 (KDR) and VEGFR3 (FLT4), and no data are available examining VEGFR1 expression. Based on the same gene expression array, the BTICs express very little if any VEGFC (which signals through VEGFR2/3[189]) but do express moderate levels of VEGFA (which signals through VEGFR1/2[189]) and VEGFB (which signals exclusively through VEGFR1[189]). The fact that all four of these BTICs produce relatively high levels of VEGFB in culture, and that VEGFB signals exclusively through VEGFR1[190], suggests that this receptor might be present on these BTICs and may

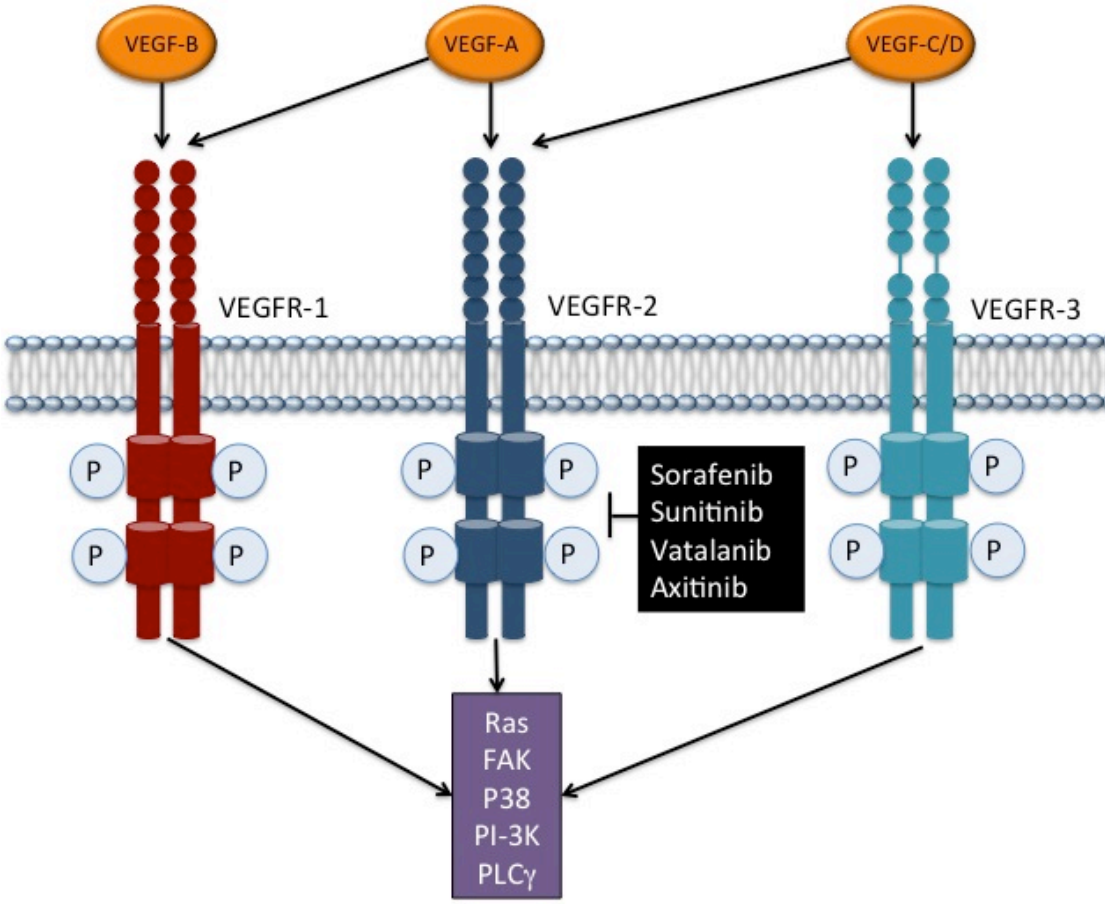

Figure 6.1: Overview of VEGF signalling and downstream effectors

represent a key avenue by which axitinib modulates intracellular signalling. Additional evidence that supports this hypothesis, based on unpublished data from the Forsyth lab, is the observation that multiple BTICs with moderate MyxV sensitivity (BT025, BT042, BT048) can release high levels of VEGF when infected with MyxV. It is possible that autocrine signalling by this growth factor may be driving cellular survival in the face of viral infection. Blockade of autocrine VEGF signalling by axitinib during MyxV treatment may abrogate cell survival signals and push the cells towards a cell death pathway.

While this putative mechanism is at present merely educated speculation, it would be reasonably straightforward to test this hypothesis. First and foremost, the presence of the VEGFR1 receptor could be confirmed at the level of mRNA and protein. If this receptor is absent, this would suggest that axitinib is acting through one of its alternative receptors (discussed in more detail below). If this receptor is present, then the use of VEGFR1-specific blocking antibodies could be utilized to verify whether blocking VEGFR1 signalling enhances MyxV-mediated cell death. Alternatively, the VEGF-mediated autocrine signalling pathway could be interrupted through the use of VEGF-binding antibodies (such as bevacizumab, which targets the VEGFR1 ligand[169]) in combination with MyxV, which would then be predicted to have the same effect as axitinib. Although other pharmacological VEGFR inhibitors could be tested to see whether synergy is recapitulated, it is worth noting that axitinib is one of the most potent and specific VEGFR inhibitors available[169], and thus other VEGFR inhibitors may be of limited experimental utility. Ultimately, siRNA knockdown of VEGFR1 or VEGF itself could be

used to determine with a high degree of specificity whether disruption of the VEGF autocrine signalling network is sufficient to enhance MyxV efficacy; however, if VEGF is a dominant growth factor in these *in vitro* BTIC systems, it is possible that the growth and viability of this siRNA knock-down would be severely compromised, even in the absence of virus, making a transient knock-down an attractive experimental approach.

If axitinib's mechanism of synergy is traced to its ability to inhibit VEGF autocrine signalling, then the question emerges as to why other tyrosine kinase inhibitors that inhibit VEGFR, such as sunitinib and sorafenib, did not emerge as hit compounds in the current investigation. The most likely explanation for this is the relative specificity and potency of axitinib compared to sunitinib and sorafenib. For instance, axitinib has IC_{50} values *in vitro* of 0.1nM, 0.2nM and 0.2nM for VEGFR1, 2, and 3 respectively; by comparison, sunitinib has IC_{50} values *in vitro* of 2nM, 10nM, and 17nM respectively for VEGFR1,2, and 3. Although both drugs inhibit effectively at nanomolar concentrations, VEGFR is >20-fold more potent than sunitinib. Sorafenib is even less potent, with an IC_{50} values *in vitro* of 90nM for VEGFR2 and 20nM for VEGFR3[169]. Thus, although sunitinib and sorafenib were not identified as candidates for synergy in this screen, they may prove to be effective candidate compounds in combination with MyxV at higher doses.

Though considered highly specific for VEGFR1/2/3, axitinib can also inhibit PDGFRβ (IC_{50}=1.6nM) and cKIT (IC_{50} = 1.7nM) as well. Levels of cKIT expression in BTICs appear to be very low or non-existent based upon the previously described gene

expression profiling data (Weiss lab, unpublished data). However, PDGFRα and β appear to be expressed at moderate levels in all four BTIC lines for which data are available, suggesting that PDGFR blockade may be an alternative mechanism by which axitinib is modulating downstream signalling. Interestingly, one of the other eight drugs initially shown to improve MyxV-mediated cell death, hypothemycin, has also been shown to inhibit PDGFR, indicating that PDGFR inhibition may be an important mechanism for enhancing MyxV efficacy.

Regardless of the specific mechanism by which axitinib is inducing downstream target modulation, any combination therapy with axitinib is likely to have various beneficial clinical effects besides enhancing OV efficacy. For example, as a VEGFR inhibitor, axitinib may confer therapeutically beneficial anti-angiogenic or vascular normalizing effects. Axitinib itself has been shown in other solid tumours to improve the intratumoural concentration of other drugs (e.g. cyclophosphamide) through normalization of the tumour vasculature[191]. Importantly, however, vascular normalizing agents can actually decrease uptake of systemically administered OVs under certain circumstances[192], highlighting the need for efficacious preclinical models to elucidate these complex interactions. Alternatively, intratumoral administration of the virus may circumvent this difficulty altogether.

One of the benefits of axitinib versus other VEGFR inhibitors is its relative specificity for VEGFR1/2/3. Whereas axitinib only affects PDGFRβ and cKIT in addition to VEGFR, other multi-tyrosine kinase inhibitors such as pazopanib also target FGFR1/2,

PDGFRα/β, cKIT, LTK, LCK, and cFMS in addition to VEGFR[169]. The more narrow specificity for VEGFR1/2/3 means that axitinib is associated with fewer off-target effects than other VEGFR inhibitors[169]. The milder toxicity profile makes axitinib a more favourable option if VEGFR inhibition is shown to be an optimal approach for pursuing synergy with MyxV.

These favourable characteristics, in combination with the results of this study, suggest that axitinib should be further pursued in preclinical studies with MyxV, using *in vivo* studies of BTIC xenografts and eventually syngeneic glioma models to optimize synergy.

6.6 Limitations of the Cancer Stem Cell Hypothesis and the BTIC model

In this investigation, we have utilized BTICs grown under neurosphere-promoting conditions as an *in vitro* model for high-grade glioma. However, much controversy remains about the relevance of BTICs and their stem-like characteristics *in vitro*. Although the intratumoural heterogeneity of GBMs has long been understood, the conceptualization of this heterogeneity as a hierarchal organization, with stem-like cells at the apex, is relatively recent and still under debate. The nuanced nature of the cancer stem cell hypothesis, and the lack of uniform terminology to adequately describe it, has contributed to the debate. The original incarnation of the stem cell hypothesis, which few individuals still endorse fully, postulated that the cell of origin in brain tumours is a stem cell; that this stem cell gives rise to other stem cells and the differentiated tumour bulk; that this stem cell is inherently treatment resistant; that this stem cell leads to recurrence; and that this stem cell population can be easily identified by somatic stem cell markers.

As a corollary to these tenets, it was also postulated that stem cells would be prognostic indicators of clinical aggressiveness, and that targeting stem cells would enable tumour eradication. Many in the field now endorse a somewhat revised version of the hypothesis, and it is widely acknowledged that certain limitations to the hypothesis remain.

For the purposes of this project, our understanding of the brain tumour stem cell hypothesis and its associated corollaries is as follows. Firstly, patient tumours are highly heterogeneous, and contain sub-populations of cells with distinctive characteristics, such as enhanced tumorigenic capacity or drug resistance. Whether these sub-populations arise from differentiation, mutation, or both cannot be determined empirically in patients, and thus we must rely upon *in vivo* GBM models of increasing sophistication to answer such questions. Secondly, various *in vitro* methods exist to enrich patient-derived GBMs for cells that resemble somatic stem cells in their genotypic and phenotypic characteristics. Certain phenotypes, such as enhanced tumorigenic capacity or drug resistance, may be associated with these stem-like cells compared to non-enriched populations, but their characteristics in culture following many manipulations (dissociation, selection, transplantation, etc.) may bear limited resemblance to sub-populations of interest in the parent tumour. Thirdly, no single stem cell marker can unequivocally identify stem-like populations, though a multi-gene signature may eventually emerge and prove useful at identifying stem-like sub-populations. Lastly, the presence of stem-like cells in a tumour does not indicate that the tumour arose from a stem cell, and many models have demonstrated that the transformation of more differentiated cells, such as oligodendrocyte precursor cells[193], can lead to tumorigenesis.

In the current study, patient-derived BTICs were deemed an appropriate model for several reasons. Firstly, they form highly infiltrative, vascularised, aggressive tumours in intracranial models, which mimic the primary clinical features of GBMs[31,109]. These phenotypes are in contrast to the conventional GBM cell lines at our disposal (such as U87, U251), which form large but well-circumscribed tumours[194]. Whether this more highly invasive phenotype is due to stem-like characteristics is not of substantial interest in this study – the ability of the model to mimic patient gliomas in later *in vivo* studies is of primary importance. Since it is important to evaluate the ability of OVs to target distant cells and to spread within large tumours, the aggressive phenotype is particularly relevant in preclinical OV studies. Additionally, many of the BTIC lines have been shown to be resistant to TMZ, suggesting that they may resemble TMZ-resistant populations in the parent tumour. TMZ-resistant populations are important preclinical models, since early stage clinical trials will invariably include patients who have failed the standard of care treatment regimen of surgery, radiation, and TMZ. Since the mechanisms of TMZ resistance have not been fully elucidated, despite being extensively studied, it is possible that the molecular features that contribute to TMZ resistance (such as expression of trans-membrane drug transporters) may also confer resistance to certain small molecule inhibitors of interest in our studies. Lastly, BTICs grown in neurosphere conditions have been shown to preserve the parental gene expression signature with higher fidelity than traditional cell culture methods[56].

Critics present the well-reasoned argument that BTICs cultured over the long term change in response to selective pressure *in vitro*, and thus no longer accurately represent the parent tumour. These criticisms are valid, yet not unique to BTICs; conventional cell lines face the same limitations. The optimal approach is to use freshly cultured, low-passage GBM samples whenever possible. While the high-throughput nature of drug screens often requires cells to be vastly expanded and thus passaged many times, it is important to consider testing drug candidates of interest in low-passage samples prior to further preclinical testing. It may also be of interest for labs to compare gene expression data of cultured BTICs to parent tumour samples to identify whether pathways of interest have changed substantially from the parent tumour. Although all cells are expected to change in culture over time, it has been shown that the neurosphere culture conditions preserve the heterogeneity of the parent tumour more accurately than traditional culture methods[56].

6.7 Implications of anti-apoptotic MyxV signalling on pharmacoviral therapy

It has been repeatedly highlighted throughout this investigation that MyxV exerts an anti-apoptotic effect on infected BTICs. Such an observation has important implications for combination therapy. For example, when combining MyxV with agents that can kill through apoptosis, such as TMZ, one must ensure that MyxV's anti-apoptotic effects are not negatively impacting the efficacy of the chemotherapeutic agent. If a mild antagonistic effect between TMZ and MyxV were observed, several strategies are possible, including co-administration with an additional pro-apoptotic agent (such as a

Bcl-2 inhibitor) or alternatively the use of a virus whose anti-apoptotic mechanisms are impaired, such as the MyxV-M011L-KO virus.

If MyxV is capable of inhibiting the efficacy of pro-apoptotic agents, this might explain why many agents in our small molecule inhibitor drug screen were not improved further by MyxV or in some cases, why combination treatment was of equal or lesser efficacy than drug alone. It is also possible that agents such as the Bcl-2 inhibitors, which were not hits at 1μM, may be valuable candidates for combination therapy at higher doses. A drug screen using very low dose MyxV-M011L-KO virus would also be highly informative to answer these questions and to provide the opportunity for discovery of novel drug-virus interactions in the BTIC system.

6.8 Future Directions

A plethora of ideas for future experiments have been provided in this chapter, and thus only a subset of these experiments will be summarized here. Firstly, the mechanism of wildtype MyxV-mediated cell death should be fully elucidated. As shown with MyxV-M011L-KO, modified viruses that alter the virus-host cell interactions to favour cell death rather than cell survival can lead to vastly improved oncolysis. MyxV is also known to encode other genes that prevent alternative cell death mechanisms (such as M013, which prevents inflammasome-mediated cell death[195]); modified viruses lacking genes such as M013 may prove to be potent oncolytic agents and could be investigated in the future. In the meantime, MyxV-M011L-KO should be fully characterized *in vitro* and *in vivo*, and its lack of toxicity to normal cells verified. If specificity for malignant cells is

maintained, MyxV-M011L-KO may be a more appropriate candidate than wild-type MyxV for future clinical trials. Further mechanistic characterization of axitinib in combination with MyxV is also required, in order to determine the molecular basis for synergy and to determine whether any of the modified MyxV constructs (such as MyxV-M011L-KO) would further enhance the efficacy of pharmacoviral therapy.

As mentioned previously, all of the candidate compounds identified in this study, and other small molecule inhibitors of the same classes, could be the subject of further investigations. Several classes of drugs that had not previously been known to synergize with OV's *in vitro* were identified in this study, including COX2 inhibitors and VEGF signalling inhibitors; although these drug classes have shown synergy with OVs *in vivo*, this was attributable to effects on the immune system[119] and vasculature[196] respectively. This is the first time, to our knowledge, that such compounds have been shown to synergize with OVs through direct action on tumour cells. Further characterization of these drug classes in combination with OVs would be an exciting avenue to pursue for future studies.

6.9 Conclusions & Significance

In this investigation, we explored the mechanism of MyxV-induced cell death in BTICs and suggest that wildtype MyxV does not kill through apoptosis in the BTIC model. We also demonstrated that abrogation of the anti-apoptotic viral protein M011L dramatically enhances cell death through apoptosis. This provides the first example, to our knowledge, of a MyxV mutant that improves BTIC killing through the active induction of apoptosis.

Although still in its preliminary stages, this work establishes a precedent for manipulating the cell death response to viral infection, thus establishing a framework to investigate MyxV-M011L-KO as a targeted pro-apoptotic agent.

As a means towards further improving MyxV efficacy, we screened 73 small molecule inhibitors for synergy with MyxV, and established a list of eleven hits that may be of interest to other investigators. We validated axitinib as the lead compound and demonstrated modulation of intracellular signalling pathways in response to axitinib treatment. Our results lay the groundwork for establishing an effective pharmacoviral treatment regimen, which, following *in vivo* validation, may eventually be translated to clinical trials with MyxV.

References

1. Kanu, O.O.*, et al.* Glioblastoma multiforme: a review of therapeutic targets. *Expert Opinion on Therapeutic Targets* **13**, 701-718 (2009).
2. Chen, J., McKay, R.M. & Parada, L.F. Malignant glioma: lessons from genomics, mouse models, and stem cells. *Cell* **149**, 36-47 (2012).
3. Wen, P.Y. & Kesari, S. Malignant gliomas in adults. *The New England Journal of Medicine* **359**, 492-507 (2008).
4. Furnari, F.B.*, et al.* Malignant astrocytic glioma: genetics, biology, and paths to treatment. *Genes & Development* **21**, 2683-2710 (2007).
5. Maher, E.A.*, et al.* Marked genomic differences characterize primary and secondary glioblastoma subtypes and identify two distinct molecular and clinical secondary glioblastoma entities. *Cancer Research* **66**, 11502-11513 (2006).
6. Stupp, R.*, et al.* Radiotherapy plus concomitant and adjuvant temozolomide for glioblastoma. *The New England Journal of Medicine* **352**, 987-996 (2005).
7. Demuth, T. & Berens, M.E. Molecular mechanisms of glioma cell migration and invasion. *Journal of Neuro-Oncology* **70**, 217-228 (2004).
8. Mason, W.P. & Cairncross, J.G. Drug Insight: temozolomide as a treatment for malignant glioma--impact of a recent trial. *Nature Clinical Practice. Neurology* **1**, 88-95 (2005).
9. Hegi, M.E.*, et al.* MGMT gene silencing and benefit from temozolomide in glioblastoma. *The New England Journal of Medicine* **352**, 997-1003 (2005).
10. Esteller, M.*, et al.* Inactivation of the DNA-repair gene MGMT and the clinical response of gliomas to alkylating agents. *The New England Journal of Medicine* **343**, 1350-1354 (2000).
11. Al-Lazikani, B., Banerji, U. & Workman, P. Combinatorial drug therapy for cancer in the post-genomic era. *Nature Biotechnology* **30**, 679-692 (2012).
12. Sellers, W.R. A blueprint for advancing genetics-based cancer therapy. *Cell* **147**, 26-31 (2011).
13. Druker, B.J.*, et al.* Efficacy and safety of a specific inhibitor of the BCR-Abl tyrosine kinase in chronic myeloid leukemia. *The New England Journal of Medicine* **344**, 1031-1037 (2001).
14. Siegel, R., Ward, E., Brawley, O. & Jemal, A. Cancer statistics, 2011: the impact of eliminating socioeconomic and racial disparities on premature cancer deaths. *CA: A Cancer Journal for Clinicians* **61**, 212-236 (2011).
15. Al-Lazikani, B., Banerji, U. & Workman, P. Combinatorial drug therapy for cancer in the post-genomic era. *Nature Biotechnology* **30**, 679-692 (2012).
16. Mok, T.S.*, et al.* Gefitinib or carboplatin-paclitaxel in pulmonary adenocarcinoma. *The New England Journal of Medicine* **361**, 947-957 (2009).
17. Chapman, P.B.*, et al.* Improved survival with vemurafenib in melanoma with BRAF V600E mutation. *The New England Journal of Medicine* **364**, 2507-2516 (2011).
18. Kanu, O.O.*, et al.* Glioblastoma multiforme oncogenomics and signaling pathways. *Clinical Medicine. Oncology* **3**, 39-52 (2009).

19. Bogler, O. & Sawaya, R. Biomarkers and cancer stem cells in primary brain tumors. Foreword. *Current Problems in Cancer* **32**, 95-96 (2008).
20. Parsons, D.W.*, et al.* An integrated genomic analysis of human glioblastoma multiforme. *Science* **321**, 1807-1812 (2008).
21. Huang, T.T., Sarkaria, S.M., Cloughesy, T.F. & Mischel, P.S. Targeted therapy for malignant glioma patients: lessons learned and the road ahead. *Neurotherapeutics* **6**, 500-512 (2009).
22. Yamanaka, R. & Saya, H. Molecularly targeted therapies for glioma. *Annals of Neurology* **66**, 717-729 (2009).
23. Verhaak, R.G.*, et al.* Integrated genomic analysis identifies clinically relevant subtypes of glioblastoma characterized by abnormalities in PDGFRA, IDH1, EGFR, and NF1. *Cancer Cell* **17**, 98-110 (2010).
24. Phillips, H.S.*, et al.* Molecular subclasses of high-grade glioma predict prognosis, delineate a pattern of disease progression, and resemble stages in neurogenesis. *Cancer Cell* **9**, 157-173 (2006).
25. De Witt Hamer, P.C. Small molecule kinase inhibitors in glioblastoma: a systematic review of clinical studies. *Neuro-Oncology* **12**, 304-316 (2010).
26. Szerlip, N.J.*, et al.* Intratumoral heterogeneity of receptor tyrosine kinases EGFR and PDGFRA amplification in glioblastoma defines subpopulations with distinct growth factor response. *Proceedings of the National Academy of Sciences of the United States of America* **109**, 3041-3046 (2012).
27. Snuderl, M.*, et al.* Mosaic amplification of multiple receptor tyrosine kinase genes in glioblastoma. *Cancer Cell* **20**, 810-817 (2011).
28. Chen, R.*, et al.* A hierarchy of self-renewing tumor-initiating cell types in glioblastoma. *Cancer Cell* **17**, 362-375 (2010).
29. Venere, M., Fine, H.A., Dirks, P.B. & Rich, J.N. Cancer stem cells in gliomas: identifying and understanding the apex cell in cancer's hierarchy. *Glia* **59**, 1148-1154 (2011).
30. Dirks, P.B. Brain tumor stem cells: the cancer stem cell hypothesis writ large. *Molecular Oncology* **4**, 420-430 (2010).
31. Kelly, J.J.*, et al.* Proliferation of human glioblastoma stem cells occurs independently of exogenous mitogens. *Stem Cells* **27**, 1722-1733 (2009).
32. Lapidot, T., *et al*. A cell initiating human acute myeloid leukaemia after transplantation into SCID mice. *Nature* **367**, 645-648 (1994).
33. Al-Hajj, M., Wicha, M.S., Benito-Hernandez, A., Morrison, S.J. & Clarke, M.F. Prospective identification of tumorigenic breast cancer cells. *Proceedings of the National Academy of Sciences of the United States of America* **100**, 3983-3988 (2003).
34. Collins, A.T., Berry, P.A., Hyde, C., Stower, M.J. & Maitland, N.J. Prospective identification of tumorigenic prostate cancer stem cells. *Cancer Research* **65**, 10946-10951 (2005).
35. Fang, D.*, et al.* A tumorigenic subpopulation with stem cell properties in melanomas. *Cancer Research* **65**, 9328-9337 (2005).
36. Li, C.*, et al.* Identification of pancreatic cancer stem cells. *Cancer Research* **67**, 1030-1037 (2007).

37. Ricci-Vitiani, L.*, et al.* Identification and expansion of human colon-cancer-initiating cells. *Nature* **445**, 111-115 (2007).
38. Li, C., Lee, C.J. & Simeone, D.M. Identification of human pancreatic cancer stem cells. *Methods in Molecular Biology* **568**, 161-173 (2009).
39. O'Brien, C.A., Pollett, A., Gallinger, S. & Dick, J.E. A human colon cancer cell capable of initiating tumour growth in immunodeficient mice. *Nature* **445**, 106-110 (2007).
40. Ignatova, T.N.*, et al.* Human cortical glial tumors contain neural stem-like cells expressing astroglial and neuronal markers in vitro. *Glia* **39**, 193-206 (2002).
41. Singh, S.K.*, et al.* Identification of a cancer stem cell in human brain tumors. *Cancer Research* **63**, 5821-5828 (2003).
42. Singh, S.K.*, et al.* Identification of human brain tumour initiating cells. *Nature* **432**, 396-401 (2004).
43. Son, M.J., Woolard, K., Nam, D.H., Lee, J. & Fine, H.A. SSEA-1 is an enrichment marker for tumor-initiating cells in human glioblastoma. *Cell Stem Cell* **4**, 440-452 (2009).
44. Mao, X.G.*, et al.* Brain tumor stem-like cells identified by neural stem cell marker CD15. *Translational Oncology* **2**, 247-257 (2009).
45. Lathia, J.D.*, et al.* Integrin alpha 6 regulates glioblastoma stem cells. *Cell Stem Cell* **6**, 421-432 (2010).
46. Ogden, A.T.*, et al.* Identification of A2B5+CD133- tumor-initiating cells in adult human gliomas. *Neurosurgery* **62**, 505-514; discussion 514-505 (2008).
47. Gilbert, C.A. & Ross, A.H. Cancer stem cells: cell culture, markers, and targets for new therapies. *Journal of Cellular Biochemistry* **108**, 1031-1038 (2009).
48. Rich, J.N. The implications of the cancer stem cell hypothesis for neuro-oncology and neurology. *Future Neurology* **3**, 265-273 (2008).
49. Beier, D.*, et al.* CD133(+) and CD133(-) glioblastoma-derived cancer stem cells show differential growth characteristics and molecular profiles. *Cancer Research* **67**, 4010-4015 (2007).
50. Joo, K.M.*, et al.* Clinical and biological implications of CD133-positive and CD133-negative cells in glioblastomas. *Laboratory Investigation* **88**, 808-815 (2008).
51. Zeppernick, F.*, et al.* Stem cell marker CD133 affects clinical outcome in glioma patients. *Clinical Cancer Research* **14**, 123-129 (2008).
52. Beier, D.*, et al.* CD133 expression and cancer stem cells predict prognosis in high-grade oligodendroglial tumors. *Brain Pathology* **18**, 370-377 (2008).
53. Zhang, M.*, et al.* Nestin and CD133: valuable stem cell-specific markers for determining clinical outcome of glioma patients. *Journal of Experimental and Clinical Cancer Research* **27**, 85 (2008).
54. Laks, D.R.*, et al.* Neurosphere formation is an independent predictor of clinical outcome in malignant glioma. *Stem Cells* **27**, 980-987 (2009).
55. Singh, S.K., Clarke, I.D., Hide, T. & Dirks, P.B. Cancer stem cells in nervous system tumors. *Oncogene* **23**, 7267-7273 (2004).

56. Lee, J.*, et al.* Tumor stem cells derived from glioblastomas cultured in bFGF and EGF more closely mirror the phenotype and genotype of primary tumors than do serum-cultured cell lines. *Cancer Cell* **9**, 391-403 (2006).
57. Bao, S.*, et al.* Glioma stem cells promote radioresistance by preferential activation of the DNA damage response. *Nature* **444**, 756-760 (2006).
58. Liu, G.*, et al.* Analysis of gene expression and chemoresistance of CD133+ cancer stem cells in glioblastoma. *Molecular Cancer* **5**, 67 (2006).
59. Blough, M.D.*, et al.* Sensitivity to temozolomide in brain tumor initiating cells. *Neuro-Oncology* **12,** 756-760 (2010).
60. Blough, M.D., Beauchamp, D.C., Westgate, M.R., Kelly, J.J. & Cairncross, J.G. Effect of aberrant p53 function on temozolomide sensitivity of glioma cell lines and brain tumor initiating cells from glioblastoma. *Journal of Neurooncology* **102**, 1-7 (2011).
61. Mahoney, D.J. & Stojdl, D.F. Fighting fire with fire: rewiring tumor cells for oncolytic virotherapy. *Future Oncology* **8**, 219-221 (2012).
62. Wollmann, G., Ozduman, K. & van den Pol, A.N. Oncolytic virus therapy for glioblastoma multiforme: concepts and candidates. *Cancer Journal* **18**, 69-81 (2012).
63. Stanford, M.M. & McFadden, G. Myxoma virus and oncolytic virotherapy: a new biologic weapon in the war against cancer. *Expert Opinion on Biologic Therapy* **7**, 1415-1425 (2007).
64. Kelly, E. & Russell, S.J. History of oncolytic viruses: genesis to genetic engineering. *Molecular Therapy* **15**, 651-659 (2007).
65. Hammill, A.M., Conner, J. & Cripe, T.P. Oncolytic virotherapy reaches adolescence. *Pediaticr Blood Cancer* **55**, 1253-1263 (2010).
66. Bierman, H.R.*, et al.* Remissions in leukemia of childhood following acute infectious disease: staphylococcus and streptococcus, varicella, and feline panleukopenia. *Cancer* **6**, 591-605 (1953).
67. Southam, C.M. & Moore, A.E. Clinical studies of viruses as antineoplastic agents with particular reference to Egypt 101 virus. *Cancer* **5**, 1025-1034 (1952).
68. Asada, T. Treatment of human cancer with mumps virus. *Cancer* **34**, 1907-1928 (1974).
69. Cassel, W.A. & Garrett, R.E. Newcastle disease virus as an antineoplastic agent. *Cancer* **18**, 863-868 (1965).
70. Southam, C.M. & Moore, A.E. Induced immunity to cancer cell homografts in man. *Annals of the New York Academy of Science* **73**, 635-653 (1958).
71. Moore, A.E., Rhoads, C.P. & Southam, C.M. Homotransplantation of human cell lines. *Science* **125**, 158-160 (1957).
72. Bischoff, J.R.*, et al.* An adenovirus mutant that replicates selectively in p53-deficient human tumor cells. *Science* **274**, 373-376 (1996).
73. Khuri, F.R.*, et al.* a controlled trial of intratumoral ONYX-015, a selectively-replicating adenovirus, in combination with cisplatin and 5-fluorouracil in patients with recurrent head and neck cancer. *Nature Medicine* **6**, 879-885 (2000).
74. Nemunaitis, J.*, et al.* Selective replication and oncolysis in p53 mutant tumors with ONYX-015, an E1B-55kD gene-deleted adenovirus, in patients with

advanced head and neck cancer: a phase II trial. *Cancer Research* **60**, 6359-6366 (2000).
75. Garber, K. China approves world's first oncolytic virus therapy for cancer treatment. *Journal of the National Cancer Institute* **98**, 298-300 (2006).
76. Liu, T.C., Galanis, E. & Kirn, D. Clinical trial results with oncolytic virotherapy: a century of promise, a decade of progress. *Nature Clinincal Practice Oncology* **4**, 101-117 (2007).
77. Tedcastle, A., Cawood, R., Di, Y., Fisher, K.D. & Seymour, L.W. Virotherapy--cancer targeted pharmacology. *Drug Discovery Today* **17**, 215-220 (2012).
78. Kim, J.H.*, et al.* Systemic armed oncolytic and immunologic therapy for cancer with JX-594, a targeted poxvirus expressing GM-CSF. *Molecular Therapy* **14**, 361-370 (2006).
79. Russell, S.J., Peng, K.W. & Bell, J.C. Oncolytic virotherapy. *Nature Biotechnology* **30**, 658-670 (2012).
80. Strong, J.E., Coffey, M.C., Tang, D., Sabinin, P. & Lee, P.W. The molecular basis of viral oncolysis: usurpation of the Ras signaling pathway by reovirus. *EMBO Journal* **17**, 3351-3362 (1998).
81. Martuza, R.L. Conditionally replicating herpes vectors for cancer therapy. *Journal of Clinical Investigation* **105**, 841-846 (2000).
82. Kanai, R., Wakimoto, H., Cheema, T. & Rabkin, S.D. Oncolytic herpes simplex virus vectors and chemotherapy: are combinatorial strategies more effective for cancer? *Future Oncology* **6**, 619-634 (2010).
83. Sova, P.*, et al.* A tumor-targeted and conditionally replicating oncolytic adenovirus vector expressing TRAIL for treatment of liver metastases. *Molecular Therapy* **9**, 496-509 (2004).
84. Martuza, R.L., Malick, A., Markert, J.M., Ruffner, K.L. & Coen, D.M. Experimental therapy of human glioma by means of a genetically engineered virus mutant. *Science* **252**, 854-856 (1991).
85. Rampling, R.*, et al.* Toxicity evaluation of replication-competent herpes simplex virus (ICP 34.5 null mutant 1716) in patients with recurrent malignant glioma. *Gene Therapy* **7**, 859-866 (2000).
86. Papanastassiou, V.*, et al.* The potential for efficacy of the modified (ICP 34.5(-)) herpes simplex virus HSV1716 following intratumoural injection into human malignant glioma: a proof of principle study. *Gene Therapy* **9**, 398-406 (2002).
87. Harrow, S.*, et al.* HSV1716 injection into the brain adjacent to tumour following surgical resection of high-grade glioma: safety data and long-term survival. *Gene Therapy* **11**, 1648-1658 (2004).
88. Chiocca, E.A.*, et al.* A phase I open-label, dose-escalation, multi-institutional trial of injection with an E1B-Attenuated adenovirus, ONYX-015, into the peritumoral region of recurrent malignant gliomas, in the adjuvant setting. *Molecular Therapy* **10**, 958-966 (2004).
89. Forsyth, P.*, et al.* A phase I trial of intratumoral administration of reovirus in patients with histologically confirmed recurrent malignant gliomas. *Molecular Therapy* **16**, 627-632 (2008).

90. Freeman, A.I., *et al.* Phase I/II trial of intravenous NDV-HUJ oncolytic virus in recurrent glioblastoma multiforme. *Molecular Therapy* **13**, 221-228 (2006).
91. Zemp, F.J., Corredor, J.C., Lun, X., Muruve, D.A. & Forsyth, P.A. Oncolytic viruses as experimental treatments for malignant gliomas: using a scourge to treat a devil. *Cytokine and Growth Factor Reviews* **21**, 103-117 (2010).
92. Lun, X., *et al.* Myxoma virus is a novel oncolytic virus with significant antitumor activity against experimental human gliomas. *Cancer Research* **65**, 9982-9990 (2005).
93. Lun, X.Q., *et al.* Targeting human medulloblastoma: oncolytic virotherapy with myxoma virus is enhanced by rapamycin. *Cancer Research* **67**, 8818-8827 (2007).
94. Lun, X., *et al.* Myxoma virus virotherapy for glioma in immunocompetent animal models: optimizing administration routes and synergy with rapamycin. *Cancer Research* **70**, 598-608 (2010).
95. Kirn, D.H. & Thorne, S.H. Targeted and armed oncolytic poxviruses: a novel multi-mechanistic therapeutic class for cancer. *Nature Reviews Cancer* **9**, 64-71 (2009).
96. Wang, F., *et al.* Disruption of Erk-dependent type I interferon induction breaks the myxoma virus species barrier. *Nature Immunology* **5**, 1266-1274 (2004).
97. Wang, F., *et al.* RIG-I mediates the co-induction of tumor necrosis factor and type I interferon elicited by myxoma virus in primary human macrophages. *PLoS Pathogens* **4**, e1000099 (2008).
98. Wang, G., *et al.* Infection of human cancer cells with myxoma virus requires Akt activation via interaction with a viral ankyrin-repeat host range factor. *Proceedings of the National Academy of Sciences of the United States of America* **103**, 4640-4645 (2006).
99. Cameron, C., *et al.* The complete DNA sequence of myxoma virus. *Virology* **264**, 298-318 (1999).
100. Senzer, N.N., *et al.* Phase II clinical trial of a granulocyte-macrophage colony-stimulating factor-encoding, second-generation oncolytic herpesvirus in patients with unresectable metastatic melanoma. *Journal of Clinical Oncology* **27**, 5763-5771 (2009).
101. Mastrangelo, M.J., *et al.* Intratumoral recombinant GM-CSF-encoding virus as gene therapy in patients with cutaneous melanoma. *Cancer Gene Therapy* **6**, 409-422 (1999).
102. Heo, J., *et al.* Sequential therapy with JX-594, a targeted oncolytic poxvirus, followed by sorafenib in hepatocellular carcinoma: preclinical and clinical demonstration of combination efficacy. *Molecular Therapy* **19**, 1170-1179 (2011).
103. Seet, B.T., *et al.* Poxviruses and immune evasion. *Annual Reviews in Immunology* **21**, 377-423 (2003).
104. Barrett, J.W., Cao, J.X., Hota-Mitchell, S. & McFadden, G. Immunomodulatory proteins of myxoma virus. *Seminars in Immunology* **13**, 73-84 (2001).
105. Everett, H. & McFadden, G. Poxviruses and apoptosis: a time to die. *Current Opinions in Microbiology* **5**, 395-402 (2002).

106. Johnston, J.B. & McFadden, G. Poxvirus immunomodulatory strategies: current perspectives. *Journal of Virology* **77**, 6093-6100 (2003).
107. Wang, S. & El-Deiry, W.S. TRAIL and apoptosis induction by TNF-family death receptors. *Oncogene* **22**, 8628-8633 (2003).
108. Su, J.*, et al.* Myxoma virus M11L blocks apoptosis through inhibition of conformational activation of Bax at the mitochondria. *Journal of Virology* **80**, 1140-1151 (2006).
109. Lun, X.*, et al.* Treating brain tumour initiating cells using a combination of Myxoma virus and rapamycin. *Neuro-Oncology* **Submitted** (2012).
110. Emadi, A., Jones, R.J. & Brodsky, R.A. Cyclophosphamide and cancer: golden anniversary. *Nature Reviews Clinical Oncology* **6**, 638-647 (2009).
111. Kottke, T.*, et al.* Improved systemic delivery of oncolytic reovirus to established tumors using preconditioning with cyclophosphamide-mediated Treg modulation and interleukin-2. *Clinical Cancer Research* **15**, 561-569 (2009).
112. Qiao, J.*, et al.* Cyclophosphamide facilitates antitumor efficacy against subcutaneous tumors following intravenous delivery of reovirus. *Clinical Cancer Research* **14**, 259-269 (2008).
113. Fulci, G.*, et al.* Cyclophosphamide enhances glioma virotherapy by inhibiting innate immune responses. *Proceedings of the National Academy of Sciences of the United States of America* **103**, 12873-12878 (2006).
114. Thomas, M.A.*, et al.* Immunosuppression enhances oncolytic adenovirus replication and antitumor efficacy in the Syrian hamster model. *Molecular Therapy* **16**, 1665-1673 (2008).
115. Peng, K.W.*, et al.* Using clinically approved cyclophosphamide regimens to control the humoral immune response to oncolytic viruses. *Gene Therapy* (2012).
116. Lun, X.Q.*, et al.* Efficacy of systemically administered oncolytic vaccinia virotherapy for malignant gliomas is enhanced by combination therapy with rapamycin or cyclophosphamide. *Clinical Cancer Research* **15**, 2777-2788 (2009).
117. Ikeda, K.*, et al.* Oncolytic virus therapy of multiple tumors in the brain requires suppression of innate and elicited antiviral responses. *Nature Medicine* **5**, 881-887 (1999).
118. Cerullo, V.*, et al.* Immunological effects of low-dose cyclophosphamide in cancer patients treated with oncolytic adenovirus. *Molecular Therapy* **19**, 1737-1746 (2011).
119. Chang, C.L., Ma, B., Pang, X., Wu, T.C. & Hung, C.F. Treatment with cyclooxygenase-2 inhibitors enables repeated administration of vaccinia virus for control of ovarian cancer. *Molecular Therapy* **17**, 1365-1372 (2009).
120. Ottolino-Perry, K., Diallo, J.S., Lichty, B.D., Bell, J.C. & McCart, J.A. Intelligent design: combination therapy with oncolytic viruses. *Molecular Therapy* **18**, 251-263 (2010).
121. Nguyen, T.L.*, et al.* Chemical targeting of the innate antiviral response by histone deacetylase inhibitors renders refractory cancers sensitive to viral oncolysis. *Proceedings of the National Academy of Sciences of the United States of America* **105**, 14981-14986 (2008).

122. Katsura, T.*, et al.* The effects of trichostatin A on the oncolytic ability of herpes simplex virus for oral squamous cell carcinoma cells. *Cancer Gene Therapy* **16**, 237-245 (2009).
123. Otsuki, A.*, et al.* Histone deacetylase inhibitors augment antitumor efficacy of herpes-based oncolytic viruses. *Molecular Therapy* **16**, 1546-1555 (2008).
124. Amici, C.*, et al.* Herpes simplex virus disrupts NF-kappaB regulation by blocking its recruitment on the IkappaBalpha promoter and directing the factor on viral genes. *Journal of Biological Chemistry* **281**, 7110-7117 (2006).
125. Cheema, T.A.*, et al.* Enhanced antitumor efficacy of low-dose Etoposide with oncolytic herpes simplex virus in human glioblastoma stem cell xenografts. *Clinical Cancer Research* **17**, 7383-7393 (2011).
126. Graat, H.C.*, et al.* Different susceptibility of osteosarcoma cell lines and primary cells to treatment with oncolytic adenovirus and doxorubicin or cisplatin. *British Journal of Cancer* **94**, 1837-1844 (2006).
127. Skelding, K.A., Barry, R.D. & Shafren, D.R. Enhanced oncolysis mediated by Coxsackievirus A21 in combination with doxorubicin hydrochloride. *Investigational New Drugs* **30**, 568-581 (2012).
128. Schache, P.*, et al.* VSV virotherapy improves chemotherapy by triggering apoptosis due to proteasomal degradation of Mcl-1. *Gene Therapy* **16**, 849-861 (2009).
129. Lin, S.F.*, et al.* Synergy of a herpes oncolytic virus and paclitaxel for anaplastic thyroid cancer. *Clinical Cancer Research* **14**, 1519-1528 (2008).
130. Passer, B.J.*, et al.* Oncolytic herpes simplex virus vectors and taxanes synergize to promote killing of prostate cancer cells. *Cancer Gene Therapy* **16**, 551-560 (2009).
131. Yu, D.C.*, et al.* Antitumor synergy of CV787, a prostate cancer-specific adenovirus, and paclitaxel and docetaxel. *Cancer Research* **61**, 517-525 (2001).
132. Stanford, M.M., Barrett, J.W., Nazarian, S.H., Werden, S. & McFadden, G. Oncolytic virotherapy synergism with signaling inhibitors: Rapamycin increases myxoma virus tropism for human tumor cells. *Journal of Virology* **81**, 1251-1260 (2007).
133. Yokoyama, T.*, et al.* Autophagy-inducing agents augment the antitumor effect of telerase-selve oncolytic adenovirus OBP-405 on glioblastoma cells. *Gene Therapy* **15**, 1233-1239 (2008).
134. Alonso, M.M.*, et al.* Delta-24-RGD in combination with RAD001 induces enhanced anti-glioma effect via autophagic cell death. *Molecular Therapy* **16**, 487-493 (2008).
135. Kanai, R., Wakimoto, H., Martuza, R.L. & Rabkin, S.D. A novel oncolytic herpes simplex virus that synergizes with phosphoinositide 3-kinase/Akt pathway inhibitors to target glioblastoma stem cells. *Clinical Cancer Research* **17**, 3686-3696 (2011).
136. Mahller, Y.Y.*, et al.* Oncolytic HSV and erlotinib inhibit tumor growth and angiogenesis in a novel malignant peripheral nerve sheath tumor xenograft model. *Molecular Therapy* **15**, 279-286 (2007).

137. Kanai, R.*, et al.* Oncolytic virus-mediated manipulation of DNA damage responses: synergy with chemotherapy in killing glioblastoma stem cells. *Journal of the National Cancer Institute* **104**, 42-55 (2012).
138. Taylor, R.C., Cullen, S.P. & Martin, S.J. Apoptosis: controlled demolition at the cellular level. *Nature Reviews Molecular Cell Biology* **9**, 231-241 (2008).
139. Riedl, S.J. & Shi, Y. Molecular mechanisms of caspase regulation during apoptosis. *Nature Reviews Molecular Cell Biology* **5**, 897-907 (2004).
140. Earnshaw, W.C., Martins, L.M. & Kaufmann, S.H. Mammalian caspases: structure, activation, substrates, and functions during apoptosis. *Annual Reviews of Biochemistry* **68**, 383-424 (1999).
141. Luthi, A.U. & Martin, S.J. The CASBAH: a searchable database of caspase substrates. *Cell Death and Differentiation* **14**, 641-650 (2007).
142. Hanahan, D. & Weinberg, R.A. Hallmarks of cancer: the next generation. *Cell* **144**, 646-674 (2011).
143. Hanahan, D. & Weinberg, R.A. The hallmarks of cancer. *Cell* **100**, 57-70 (2000).
144. Kaminskyy, V. & Zhivotovsky, B. To kill or be killed: how viruses interact with the cell death machinery. *Journal of Internal Medicine* **267**, 473-482 (2010).
145. Chawla-Sarkar, M.*, et al.* Apoptosis and interferons: role of interferon-stimulated genes as mediators of apoptosis. *Apoptosis* **8**, 237-249 (2003).
146. Arnoult, D.*, et al.* Cytomegalovirus cell death suppressor vMIA blocks Bax- but not Bak-mediated apoptosis by binding and sequestering Bax at mitochondria. *Proceedings of the National Academy of Sciences of the United States of America* **101**, 7988-7993 (2004).
147. Scheffner, M., Huibregtse, J.M., Vierstra, R.D. & Howley, P.M. The HPV-16 E6 and E6-AP complex functions as a ubiquitin-protein ligase in the ubiquitination of p53. *Cell* **75**, 495-505 (1993).
148. Graham, K.A., Opgenorth, A., Upton, C. & McFadden, G. Myxoma virus M11L ORF encodes a protein for which cell surface localization is critical in manifestation of viral virulence. *Virology* **191**, 112-124 (1992).
149. Douglas, A.E., Corbett, K.D., Berger, J.M., McFadden, G. & Handel, T.M. Structure of M11L: A myxoma virus structural homolog of the apoptosis inhibitor, Bcl-2. *Protein Science* **16**, 695-703 (2007).
150. Everett, H.*, et al.* M11L: a novel mitochondria-localized protein of myxoma virus that blocks apoptosis of infected leukocytes. *Journal of Experimental Medicine* **191**, 1487-1498 (2000).
151. Everett, H.*, et al.* The myxoma poxvirus protein, M11L, prevents apoptosis by direct interaction with the mitochondrial permeability transition pore. *Journal of Experimental Medicine* **196**, 1127-1139 (2002).
152. Wang, G.*, et al.* Myxoma virus M11L prevents apoptosis through constitutive interaction with Bak. *Journal of Virology* **78**, 7097-7111 (2004).
153. Barrett, J.W.*, et al.* Identification of host range mutants of myxoma virus with altered oncolytic potential in human glioma cells. *Journal of Neurovirology* **13**, 549-560 (2007).
154. Jordan, T.X. & Randall, G. Manipulation or capitulation: virus interactions with autophagy. *Microbes and Infection* **14**, 126-139 (2012).

155. Kimmelman, A.C. The dynamic nature of autophagy in cancer. *Genes and Development* **25**, 1999-2010 (2011).
156. Debnath, J., Baehrecke, E.H. & Kroemer, G. Does autophagy contribute to cell death? *Autophagy* **1**, 66-74 (2005).
157. Kanzawa, T.*, et al.* Role of autophagy in temozolomide-induced cytotoxicity for malignant glioma cells. *Cell Death and Differentiation* **11**, 448-457 (2004).
158. Daido, S.*, et al.* Pivotal role of the cell death factor BNIP3 in ceramide-induced autophagic cell death in malignant glioma cells. *Cancer Research* **64**, 4286-4293 (2004).
159. Kanzawa, T.*, et al.* Arsenic trioxide induces autophagic cell death in malignant glioma cells by upregulation of mitochondrial cell death protein BNIP3. *Oncogene* **24**, 980-991 (2005).
160. Reynolds, B.A. & Weiss, S. Generation of neurons and astrocytes from isolated cells of the adult mammalian central nervous system. *Science* **255**, 1707-1710 (1992).
161. Smallwood, S.E., Rahman, M.M., Smith, D.W. & McFadden, G. Myxoma virus: propagation, purification, quantification, and storage. *Current Protocols in Microbiology* **Chapter 14**, Unit 14A 11 (2010).
162. Chou, T.C. & Talalay, P. Quantitative analysis of dose-effect relationships: the combined effects of multiple drugs or enzyme inhibitors. *Advances in Enzyme Regulation* **22**, 27-55 (1984).
163. Zhang, K.X.*, et al.* Down-regulation of type I interferon receptor sensitizes bladder cancer cells to vesicular stomatitis virus-induced cell death. *International Journal of Cancer* **127**, 830-838 (2010).
164. Stanziale, S.F.*, et al.* Infection with oncolytic herpes simplex virus-1 induces apoptosis in neighboring human cancer cells: a potential target to increase anticancer activity. *Clinical Cancer Research* **10**, 3225-3232 (2004).
165. Tazawa, H.*, et al.* Genetically engineered oncolytic adenovirus induces autophagic cell death through an E2F1-microRNA-7-epidermal growth factor receptor axis. *International Journal of Cancer* **131**, 2939-2950 (2012).
166. Bartee, E., Mohamed, M.R., Lopez, M.C., Baker, H.V. & McFadden, G. The addition of tumor necrosis factor plus beta interferon induces a novel synergistic antiviral state against poxviruses in primary human fibroblasts. *Journal of Virology* **83**, 498-511 (2009).
167. Lee, M.J.*, et al.* Sequential application of anticancer drugs enhances cell death by rewiring apoptotic signaling networks. *Cell* **149**, 780-794 (2012).
168. Diallo, J.S.*, et al.* A high-throughput pharmacoviral approach identifies novel oncolytic virus sensitizers. *Molecular Therapy* **18**, 1123-1129 (2010).
169. Patson, B., R, B.C. & Olszanski, A.J. Pharmacokinetic evaluation of axitinib. *Expert Opinion on Drug Metabolism & Toxicology* **8**, 259-270 (2012).
170. Rugo, H.S.*, et al.* Phase I trial of the oral antiangiogenesis agent AG-013736 in patients with advanced solid tumors: pharmacokinetic and clinical results. *Journal of Clinical Oncology* **23**, 5474-5483 (2005).
171. Hu-Lowe, D.D.*, et al.* Nonclinical antiangiogenesis and antitumor activities of axitinib (AG-013736), an oral, potent, and selective inhibitor of vascular

endothelial growth factor receptor tyrosine kinases 1, 2, 3. *Clinical Cancer Research* **14**, 7272-7283 (2008).
172. Fu, X., Tao, L. & Zhang, X. An HSV-2-based oncolytic virus deleted in the PK domain of the ICP10 gene is a potent inducer of apoptotic death in tumor cells. *Gene Therapy* **14**, 1218-1225 (2007).
173. Cary, Z.D., Willingham, M.C. & Lyles, D.S. Oncolytic vesicular stomatitis virus induces apoptosis in U87 glioblastoma cells by a type II death receptor mechanism and induces cell death and tumor clearance in vivo. *Journal of Virology* **85**, 5708-5717 (2011).
174. van Rikxoort, M.*, et al.* Oncolytic effects of a novel influenza A virus expressing interleukin-15 from the NS reading frame. *PLoS One* **7**, e36506 (2012).
175. Milosevic, J., Storch, A. & Schwarz, J. Spontaneous apoptosis in murine free-floating neurospheres. *Experimental Cell Research* **294**, 9-17 (2004).
176. Lobo, M.V.*, et al.* Cellular characterization of epidermal growth factor-expanded free-floating neurospheres. *Journal of Histochemistry and Cytochemistry* **51**, 89-103 (2003).
177. Mizushima, N. Methods for monitoring autophagy. *International Journal of Biochemistry and Cell Biology* **36**, 2491-2502 (2004).
178. Mizushima, N., Yoshimori, T. & Levine, B. Methods in mammalian autophagy research. *Cell* **140**, 313-326 (2010).
179. Klionsky, D.J.*, et al.* Guidelines for the use and interpretation of assays for monitoring autophagy in higher eukaryotes. *Autophagy* **4**, 151-175 (2008).
180. Kreuzaler, P. & Watson, C.J. Killing a cancer: what are the alternatives? *Nature Reviews Cancer* **12**, 411-424 (2012).
181. Kroemer, G.*, et al.* Classification of cell death: recommendations of the Nomenclature Committee on Cell Death 2009. *Cell Death and Differentiation* **16**, 3-11 (2009).
182. Repetto, G., del Peso, A. & Zurita, J.L. Neutral red uptake assay for the estimation of cell viability/cytotoxicity. *Nature Protocols* **3**, 1125-1131 (2008).
183. Carmody, L.C.*, et al.* Phenotypic high-throughput screening elucidates target pathway in breast cancer stem cell-like cells. *Journal of Biomolecular Screens* **17**, 1204-1210 (2012).
184. Straussman, R.*, et al.* Tumour micro-environment elicits innate resistance to RAF inhibitors through HGF secretion. *Nature* **487**, 500-504 (2012).
185. Booth, N.L.*, et al.* A cell-based high-throughput screen to identify synergistic TRAIL sensitizers. *Cancer Immunology and Immunotherapy* **58**, 1229-1244 (2009).
186. Chou, T.C. Drug combination studies and their synergy quantification using the Chou-Talalay method. *Cancer Research* **70**, 440-446 (2010).
187. Chou, T.C. Preclinical versus clinical drug combination studies. *Leukemia and Lymphoma* **49**, 2059-2080 (2008).
188. Chou, T.C. Theoretical basis, experimental design, and computerized simulation of synergism and antagonism in drug combination studies. *Pharmacological Reviews* **58**, 621-681 (2006).

189. Azam, F., Mehta, S. & Harris, A.L. Mechanisms of resistance to antiangiogenesis therapy. *European Journal of Cancer* **46**, 1323-1332 (2010).
190. Ivy, S.P., Wick, J.Y. & Kaufman, B.M. An overview of small-molecule inhibitors of VEGFR signaling. *Nature Reviews Clinical Oncology* **6**, 569-579 (2009).
191. Ma, J., Chen, C.S., Blute, T. & Waxman, D.J. Antiangiogenesis enhances intratumoral drug retention. *Cancer Research* **71**, 2675-2685 (2011).
192. Eshun, F.K.*, et al.* VEGF blockade decreases the tumor uptake of systemic oncolytic herpes virus but enhances therapeutic efficacy when given after virotherapy. *Gene Therapy* **17**, 922-929 (2010).
193. Liu, C.*, et al.* Mosaic analysis with double markers reveals tumor cell of origin in glioma. *Cell* **146**, 209-221 (2011).
194. Johnston, A.L.*, et al.* The p75 neurotrophin receptor is a central regulator of glioma invasion. *PLoS Biology* **5**, e212 (2007).
195. Rahman, M.M. & McFadden, G. Myxoma virus lacking the pyrin-like protein M013 is sensed in human myeloid cells by both NLRP3 and multiple Toll-like receptors, which independently activate the inflammasome and NF-kappaB innate response pathways. *Journal of Virology* **85**, 12505-12517 (2011).
196. Kottke, T.*, et al.* Antiangiogenic cancer therapy combined with oncolytic virotherapy leads to regression of established tumors in mice. *Journal of Clinical Investigation* **120**, 1551-1560 (2010).

Appendix A:

Chemietek Small Molecule Inhibitor Drug Library

A.1. Characteristics of small molecule inhibitor drug library

To identify compounds that enhance MyxV-mediated cell death, a screen of 73 small molecule inhibitors was performed in BT025. These small molecule inhibitors were part of a drug library assembled by ChemieTek, and were a kind gift to the Forsyth Lab for this study by Dr. Aru Narendran. To facilitate an unbiased screen, drugs have been assigned a numeric identifier, listed below. The drug function, as indicated by ChemieTek, is also provided. It is worth noting that many of the compounds may have additional activities beyond those listed here.

Table A.1: Characteristics of ChemieTek Small Molecule Inhibitor Drug Library

Drug #	Drug Name	Drug Activity
1	CP-690550	JAK3 inhibitor
2	Docetaxel	Tubulin stabilizer
3	TGX-221	PI3K inhibitor
4	Lapatinib	Tyrosine kinase inhibitor
5	PD 0325901	MEK inhibitor
6	PIK-75, Hydrochloride	PI3K inhibitor
7	ABT-263	Bcl-2 inhibitor
8	Axitinib (AG-013736	VEGF-R inhibitor
9	AZD05030 (Saracatinib)	Src inhibitor
10	Canertinib (CI-1033)	ErbB-R inhibitor
11	GDC-0941	PI3K inhibitor
12	Bosutinib (SKI-606)	Abl, Src inhibitor
13	Nilotinib	Bcr-Abl inhibitor
14	FTY720, Hydrochloride	Immunosuppressant
15	ABT-888	PARP inhibitor
16	BIBW 2992 (Tovok)	Receptor tyrosine kinase inhibitor
17	GDC-0449	Hedgehog pathway inhibitor
18	Vandetanib (Zactima)	Receptor tyrosine kinase inhibitor
19	Vatalanib Dihydrochloride	Receptor tyrosine kinase inhibitor
20	AZD 2281 (Olaparib)	PARP inhibitor
21	Bicalutamide (Caso dex)	Androgen receptor inhibitor
22	BI 2536	PLK inhibitor
23	ZM 447439	Aurora kinase inhibitor
24	Pp242	mTOR inhibitor
25	OSI-906	IGF-1R inhibitor
26	LBH-589 (Panobinostat)	HDAC inhibitor
27	Laropiprant	PGD2-R antagonist
28	MK-2206	Akt inhibitor
29	Ramatroban (Bay u3405)	CRTH2-R antagonist
30	BMS-599626	Receptor tyrosine kinase inhibitor
31	BMS-754807	IGF-1R inhibitor
32	Raltegravir	HIV integrase inhibitor
33	RDEA119	MEK inhibitor
34	PF-2341066	c-Met-R inhibitor
35	AZD 6244 (ARRY-142886)	MEK inhibitor
36	Odanacatib (MK-0822)	Cathepsin inhibitor
37	MS-275	HDAC inhibitor
38	NVP-TAE684	NPM-ALK inhibitor

Drug #	Drug Name	Drug Activity
39	SN-38	Topoisomerase I poison
40	VX702	p38 MAPK inhibitor
41	MGCD0103	HDAC inhibitor
42	Maraviroc (UK-427857)	CCR5 antagonist
43	VX-680	Aurora kinase inhibitor
44	AN2728	PDE4 inhibitor
45	Bexarotene (Targretin)	RXR activator
46	Capecitabine (Xeloda)	Nucleic acid synthesis inhibitor
47	CVT-6883	Adenosine receptor antagonist
48	Motesanib (AMG-706)	Receptor tyrosine kinase inhibitor
49	Imatinib	Tyrosine kinase inhibitor
50	Hypothemycin	T cell activation inhibitor
51	Dimebolin Hydrochloride	Antihistamine
52	FK-506	Immunosuppressant
53	Vorinostat (SAHA)	HDAC inhibitor
54	Dasatinib	Src inhibitor
55	Montelukast Sodium	LTR antagonist
56	Rofecoxib (Vioxx)	COX-2 inhibitor
57	Pemetrexed Disodium (Alimta)	Nucleic acid synthesis inhibitor
58	Gemcitabine (Gemzar)	Nucleic acid synthesis inhibitor
59	Doxorubicin (Adriamycin)	Topoisomerase II poison
60	Topotecan (Hycamtin)	Topoisomerase I poison
61	TM30089	CRTH2-R antagonist
62	Gefitinib (Iressa)	Tyrosine kinase inhibitor
63	Etoposide	Topoisomerase II poison
64	Bortezomib (Velcade)	Proteasome inhibitor
65	ABT-737	Bcl-2 inhibitor
66	Sorafenib	Tyrosine kinase inhibitor
67	Rapamycin (Sirolimus)	mTOR inhibitor
68	Erlotinib, Hydrochloride	EGF-R inhibitor
69	Paclitaxel (Taxol)	Tubulin stabilizer
70	17-DMAG	HSP 90 inhibitor
71	Sunitinib	Tyrosine kinase inhibitor
72	Tandutinib	Receptor tyrosine kinase inhibitor
73	17-AAG	HSP 90 inhibitor

Appendix B:

Pharmacoviral Screen of Small Molecule Inhibitors

B.1. Screen of 73 Small Molecule Inhibitors (1μM)

To identify compounds that enhance MyxV-mediated cell death, a screen of 73 small molecule inhibitors (listed numerically in Appendix A) was performed in BT025. For the initial screen shown here, BT025 was treated with 1μM of each drug alone or in combination with 1 MOI MyxV. Viability was measured 48hrs post-infection with Alamar blue. Eight initial candidate compounds were identified, based on >20% improvement in cell killing compared to drug alone, and targeted for further validation. These compounds are indicated in red. Data are represented as mean +/- standard deviation for a single screen with six internal replicates.

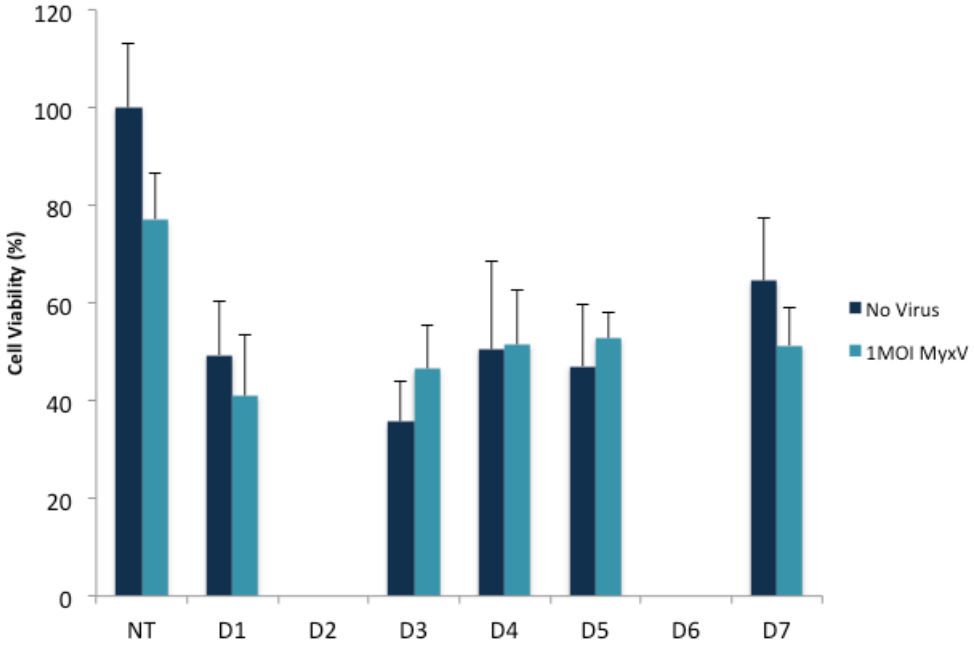
120
100
80
60
40
20
0
Cell Viability (%)
NT
D1
D2
D3
D4
D5
D6
D7
No Virus
1MOI MyxV

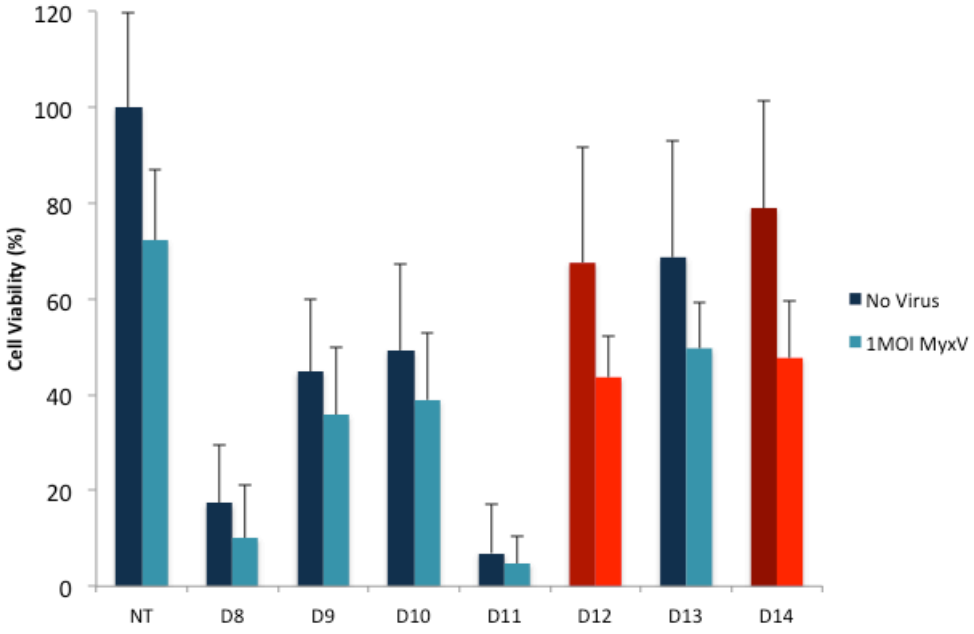
120
100
80
60
40
20
0
Cell Viability (%)
NT
D8
D9
D10
D11
D12
D13
D14
No Virus
1MOI MyxV

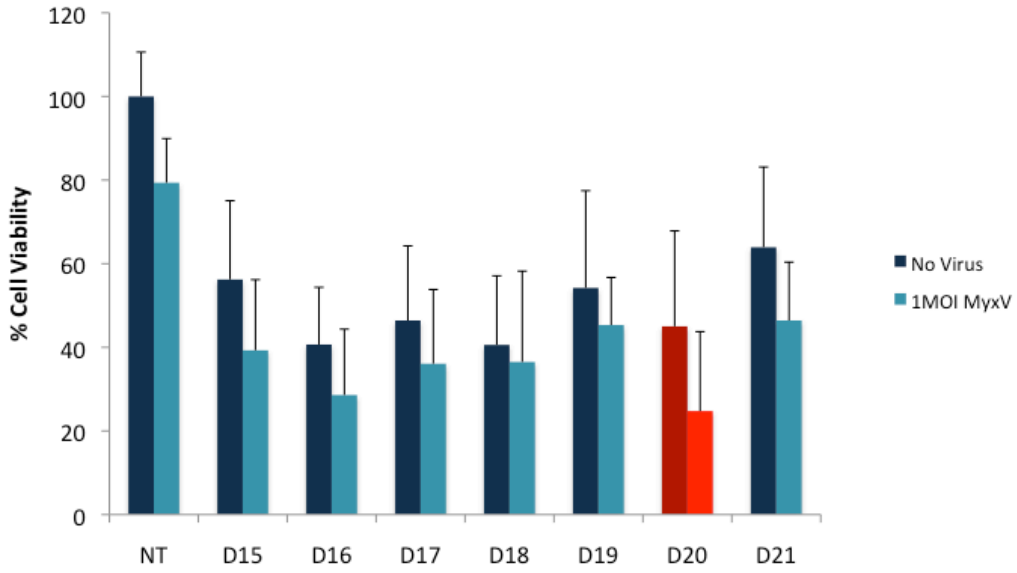
120
100
80
60
40
20
0
% Cell Viability
NT
D15
D16
D17
D18
D19
D20
D21
No Virus
1MOI MyxV

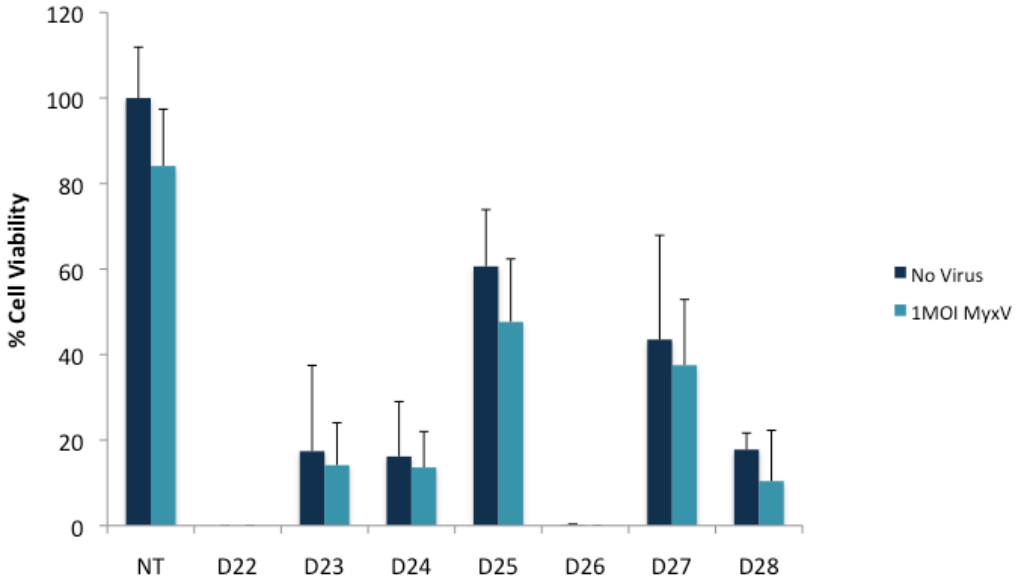
120
100
80
60
40
20
0
% Cell Viability
NT
D22
D23
D24
D25
D26
D27
D28
No Virus
1MOI MyxV

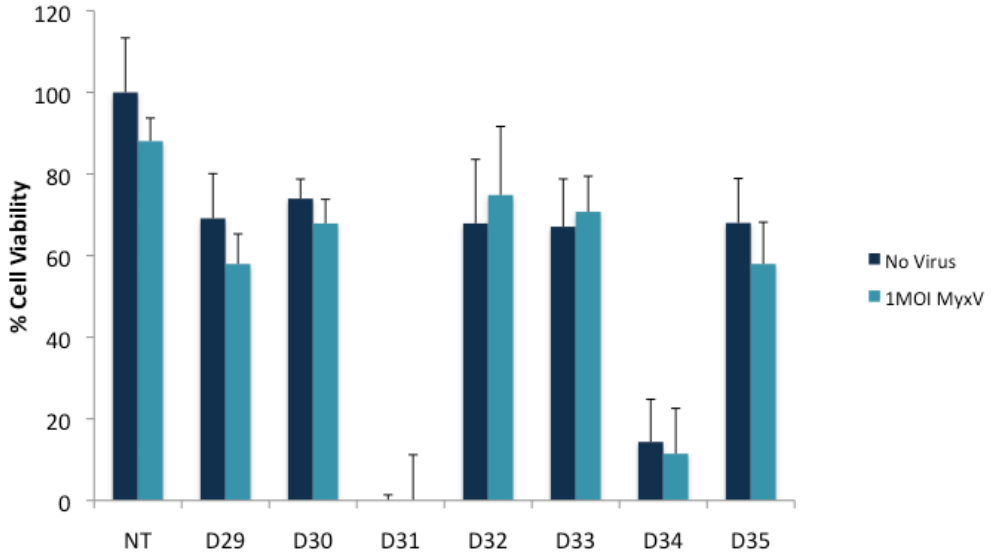
120
100
80
60
40
20
0
% Cell Viability
NT
D29
D30
D31
D32
D33
D34
D35
No Virus
1MOI MyxV

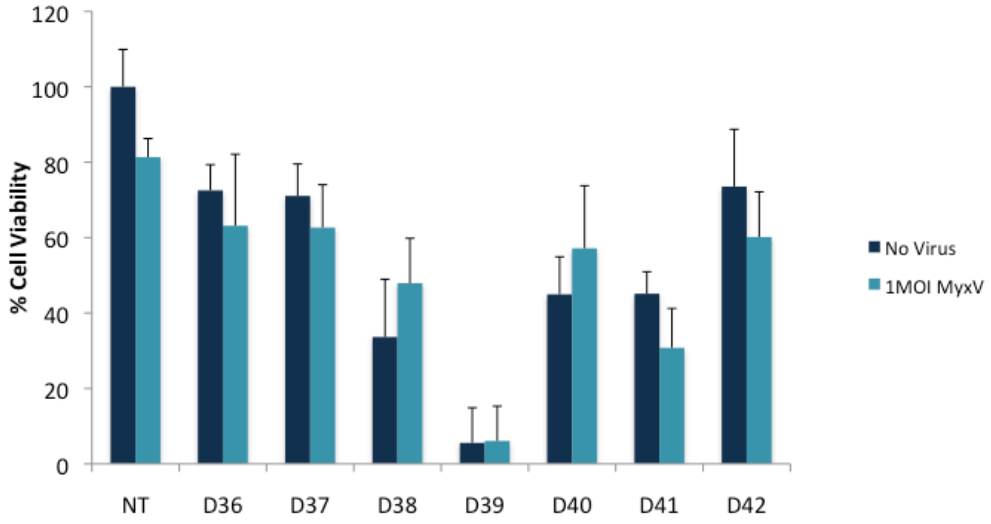
120
100
80
60
40
20
0
% Cell Viability
NT
D36
D37
D38
D39
D40
D41
D42
No Virus
1MOI MyxV

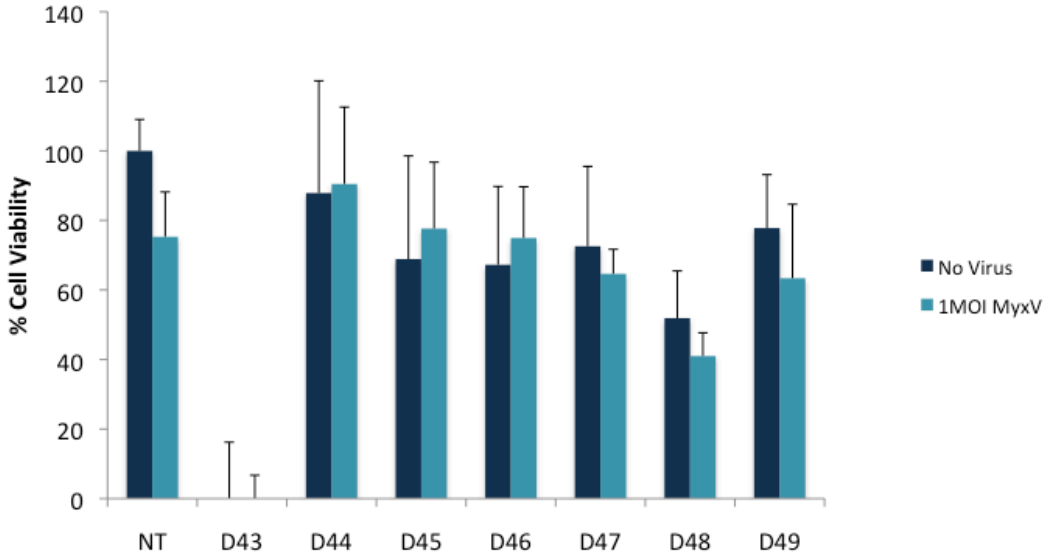
140
120
100
80
60
40
20
0
% Cell Viability
NT
D43
D44
D45
D46
D47
D48
D49
No Virus
1MOI MyxV

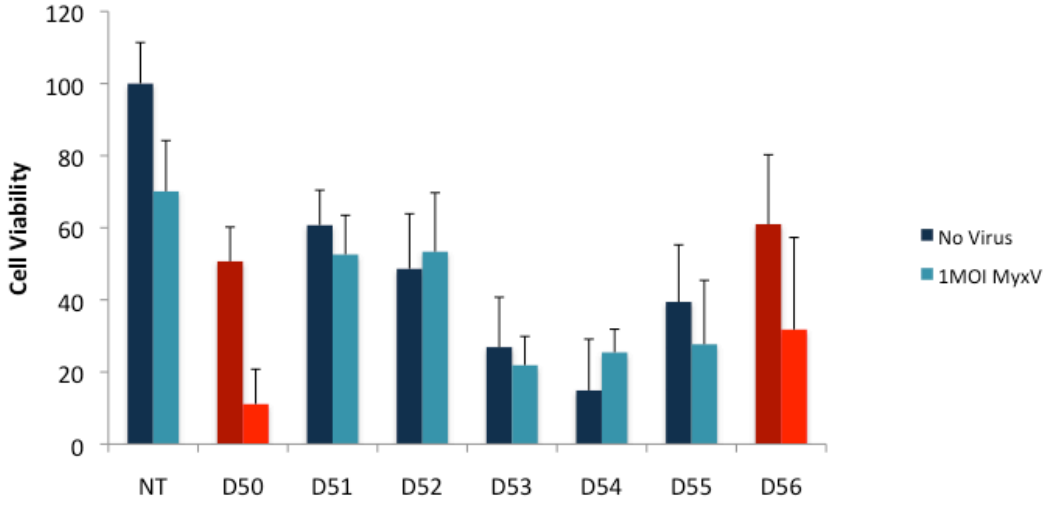
120
100
80
60
40
20
0
Cell Viability
NT
D50
D51
D52
D53
D54
D55
D56
No Virus
1MOI MyxV

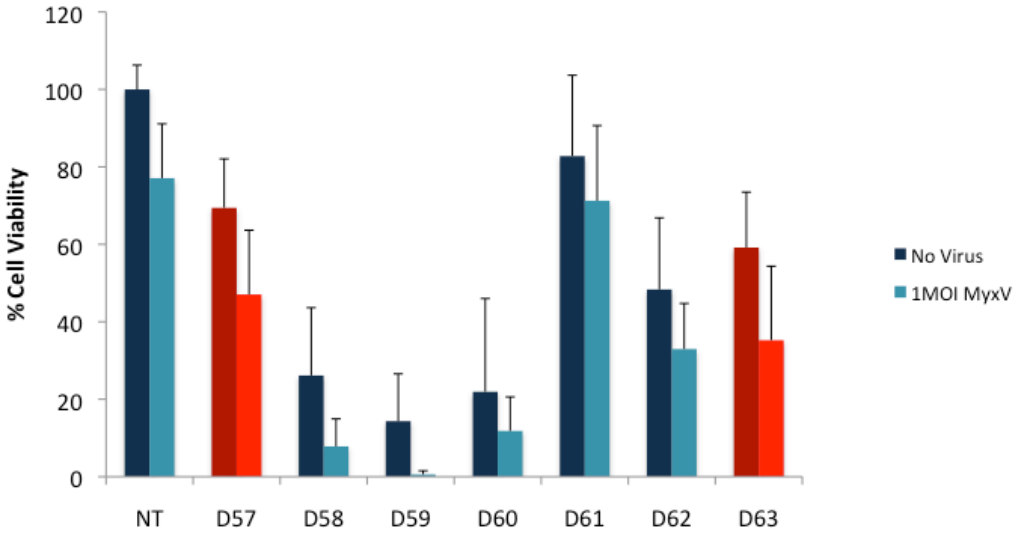
120
100
80
60
40
20
0
% Cell Viability
NT
D57
D58
D59
D60
D61
D62
D63
No Virus
1MOI MyxV

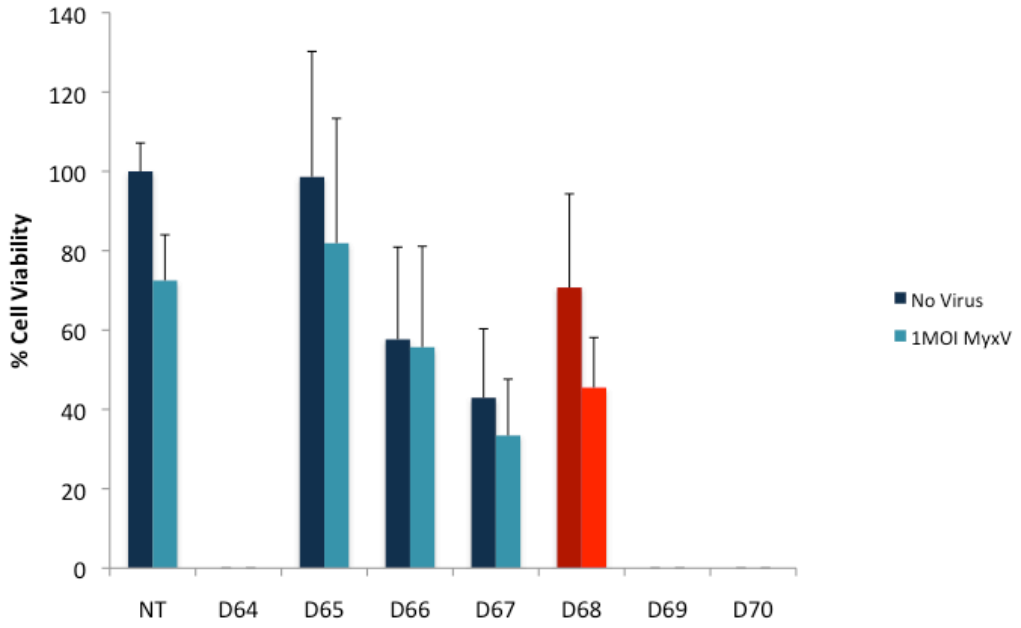
140
120
100
80
60
40
20
0
% Cell Viability
NT
D64
D65
D66
D67
D68
D69
D70
No Virus
1MOI MyxV

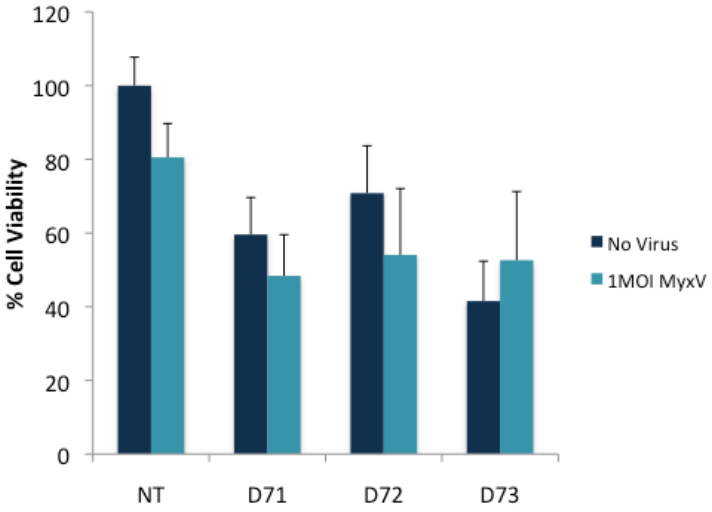
120
100
80
60
40
20
0
% Cell Viability
NT
D71
D72
D73
No Virus
1MOI MyxV

B.2. Additional Screen of 22 Cytotoxic Drugs at 100nM

In the initial screen, 22 drugs were identified that killed >70% of cells in the absence of virus. The cytotoxic nature of these drugs made it impossible to detect evidence of a drug-virus combination effect at the relatively high dose of 1μM, and thus these 22 drugs were re-screened at a lower dose (100nM), alone and in combination with 1 MOI MyxV. Viability was measured 48hrs post-infection with Alamar blue. Three candidate compounds were identified that significantly improved cell killing compared to either treatment alone ($p<0.05$; *). Data are presented as mean +/- standard error of three independent trials, each with six internal replicates.

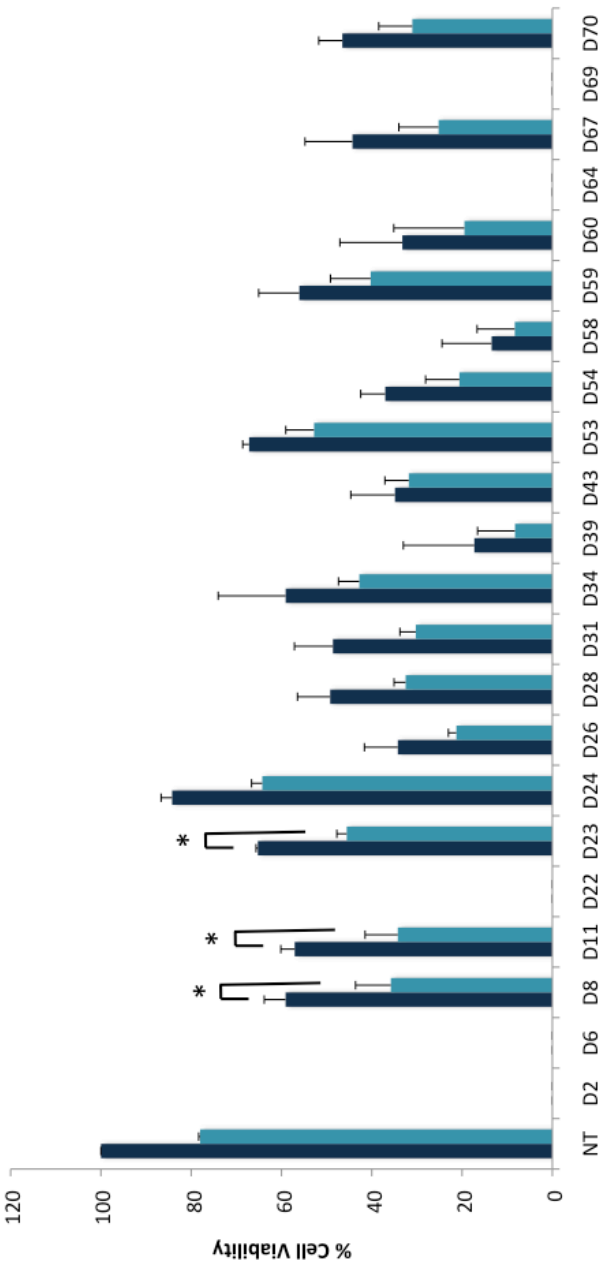
% Cell Viability
120
100
80
60
40
20
0
NT
D2
D6
D8
D11
D22
D23
D24
D26
D28
D31
D34
D39
D43
D53
D54
D58
D59
D60
D64
D67
D69
D70
*
*
*

B.3. Additional Screen of Six Very Highly Cytotoxic Drugs at 10nM

Six of the twenty-two cytotoxic compounds caused >70% reduction in cell viability at 100nM, thus preventing any evidence of a drug-virus combination effect from being observed. These drugs were screened a third time, at 10nM, both alone and in combination with 1 MOI MyxV, and viability measured at 48hrs post-infection with Alamar blue. No further hits were identified at this dose. Data represent mean +/- standard error of three independent experiments with six internal replicates.

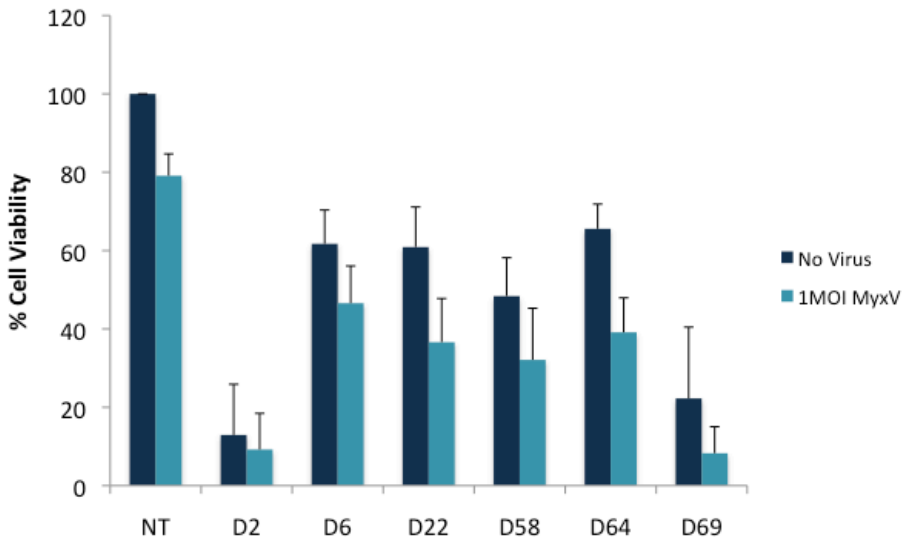
120
100
80
60
40
20
0
% Cell Viability
NT
D2
D6
D22
D58
D64
D69
No Virus
1MOI MyxV

Appendix C:

Dose Response of Candidate Compounds with Myxoma Virus

C.1. Dose response characterization of candidate compounds

Eight high-dose (1μM) and three low dose (100nM) candidate compounds were identified in the initial set of screens, and validated in independent experiments as shown in Chapter IV. In order to conduct a Chou-Talalay analysis of synergy on the drug-virus interaction, dose response characterization was performed for each of the eleven candidate compounds, alone and in combination with three different doses of virus (1, 3, and 10 MOI). High-dose candidate compounds identified in the 1μM screen were tested at 0, 1, 3, and 10μM. Low-dose candidate compounds identified in the 100nM screen were tested at 0, 100, 300, and 1000 nM. The normalized viability data (Alamar blue) for these dose responses is shown below for the following eleven candidate compounds: (A) axitinib (B) GDC-0941 (C) ZM447439 (D) bosutinib (E) FTY720 (F) AZD2281 (G) hypothemycin (H) rofecoxib (I) pemetrexed (J) etoposide (K) erlotinib. Data represent the mean +/- standard error of two independent experiments.

(A.)

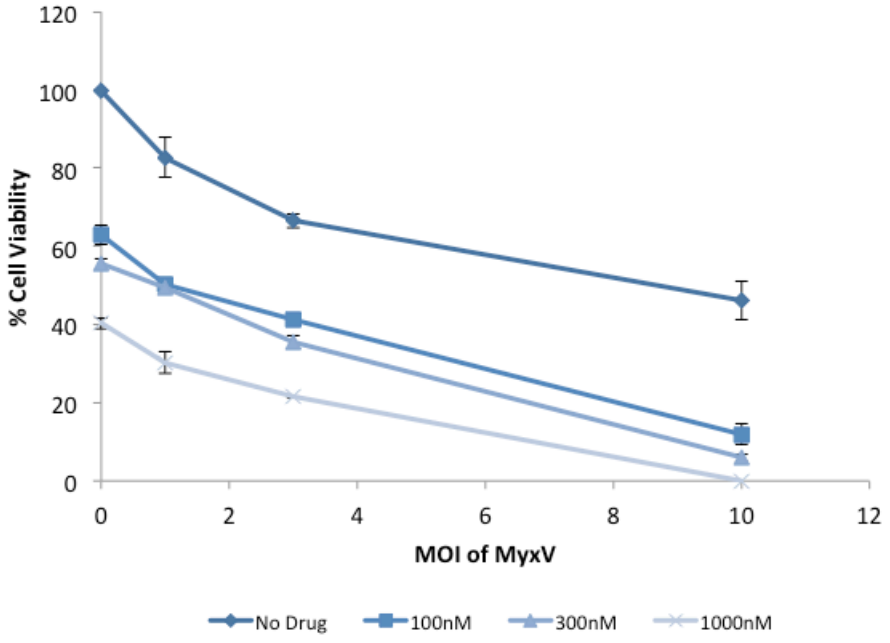
120
100
80
60
40
20
0
% Cell Viability
0
2
4
6
8
10
12
MOI of MyxV
No Drug
100nM
300nM
1000nM

(B.)

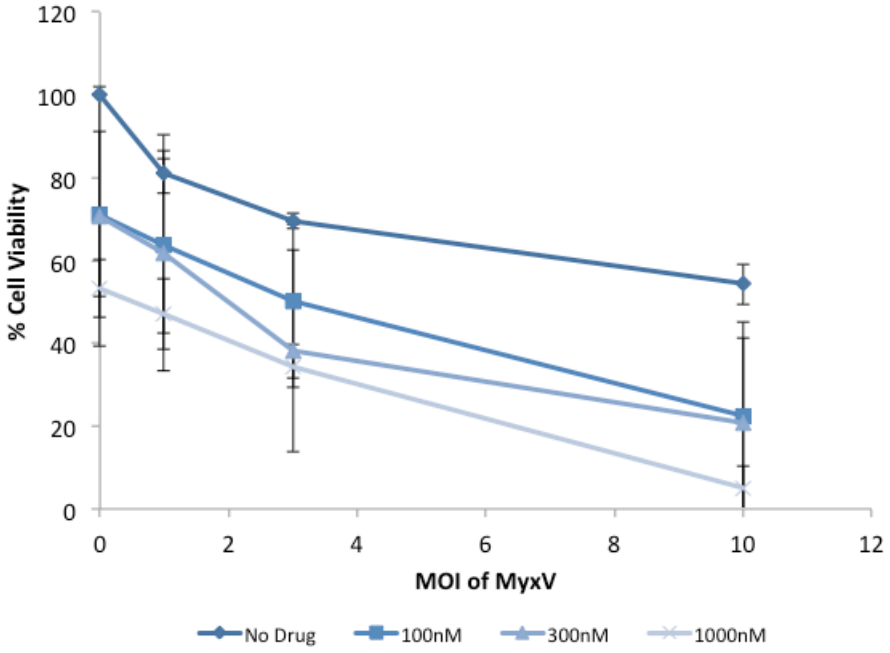
120
100
80
60
40
20
0
% Cell Viability
0
2
4
6
8
10
12
MOI of MyxV
No Drug
100nM
300nM
1000nM

(C.)

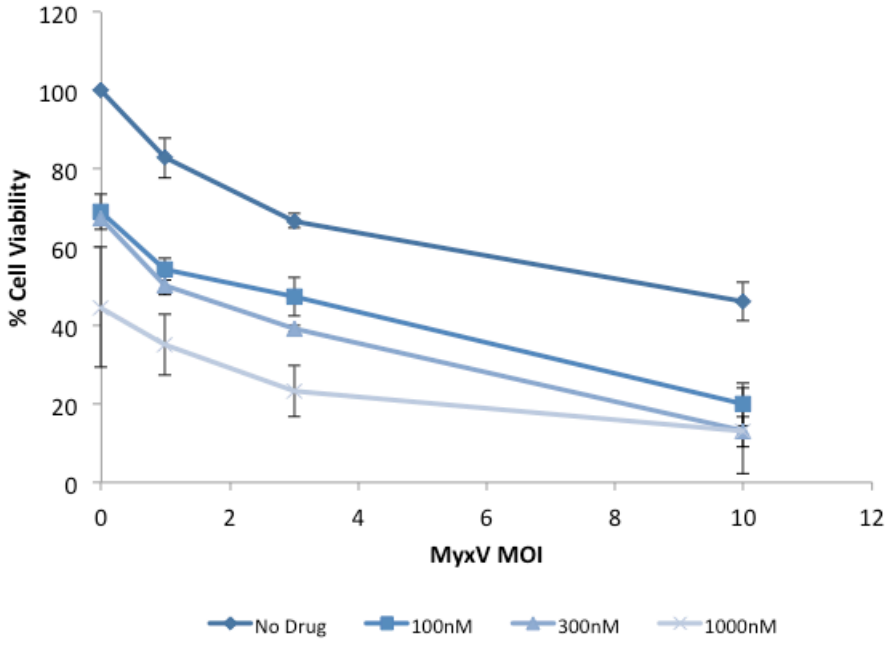
120
100
80
60
40
20
0
% Cell Viability
0
2
4
6
8
10
12
MyxV MOI
No Drug
100nM
300nM
1000nM

(D.)

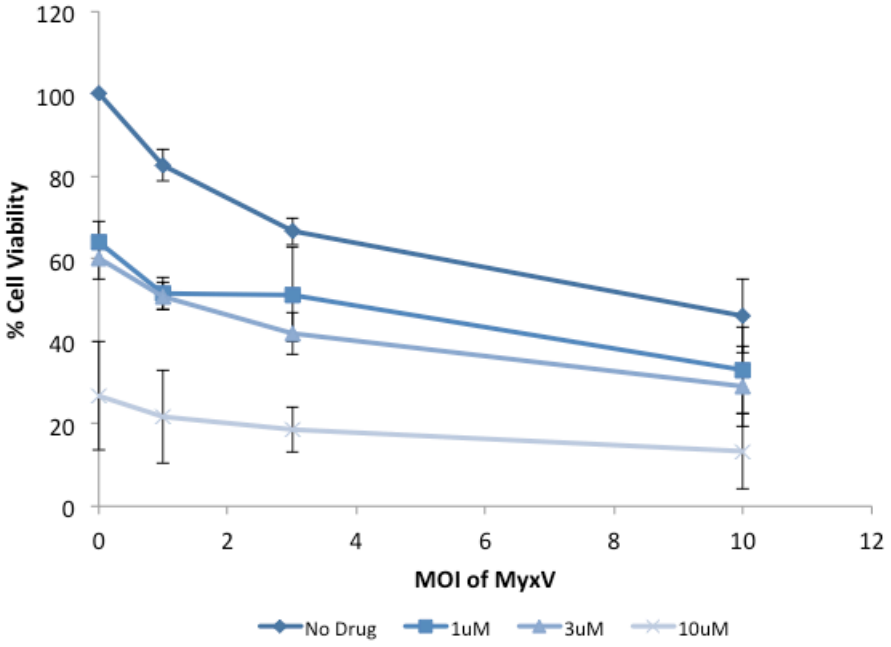
120
100
80
60
40
20
0
% Cell Viability
0
2
4
6
8
10
12
MOI of MyxV
No Drug
1uM
3uM
10uM

(E.)

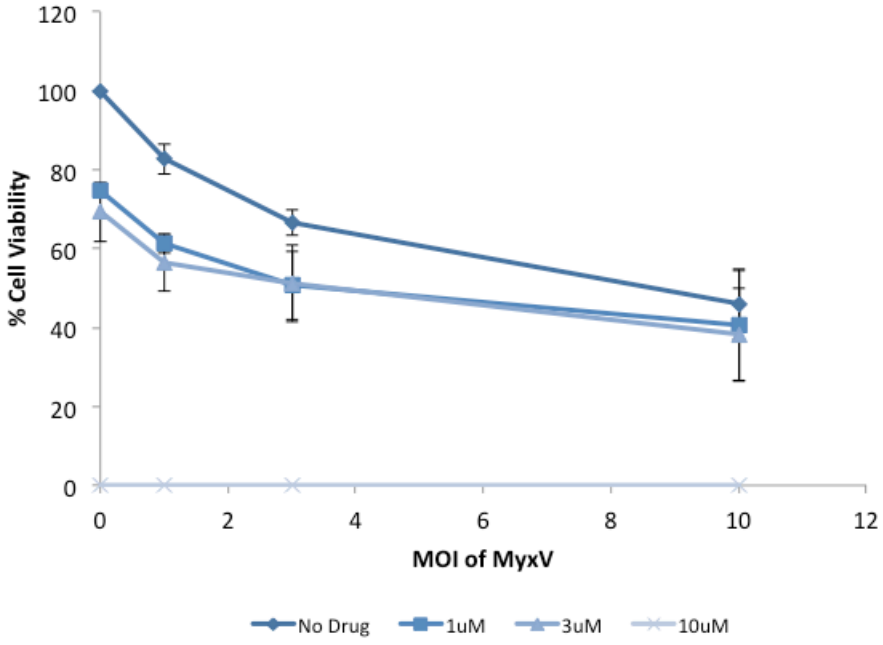
120
100
80
60
40
20
0
% Cell Viability
0
2
4
6
8
10
12
MOI of MyxV
No Drug
1uM
3uM
10uM

(F.)

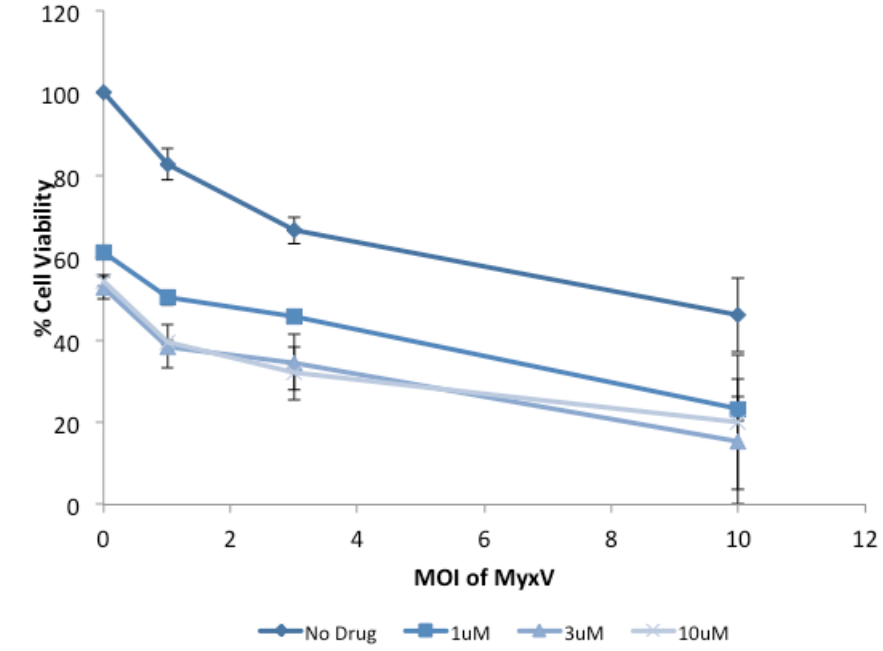
120
100
80
60
40
20
0
% Cell Viability
0
2
4
6
8
10
12
MOI of MyxV
No Drug
1uM
3uM
10uM

(G.)

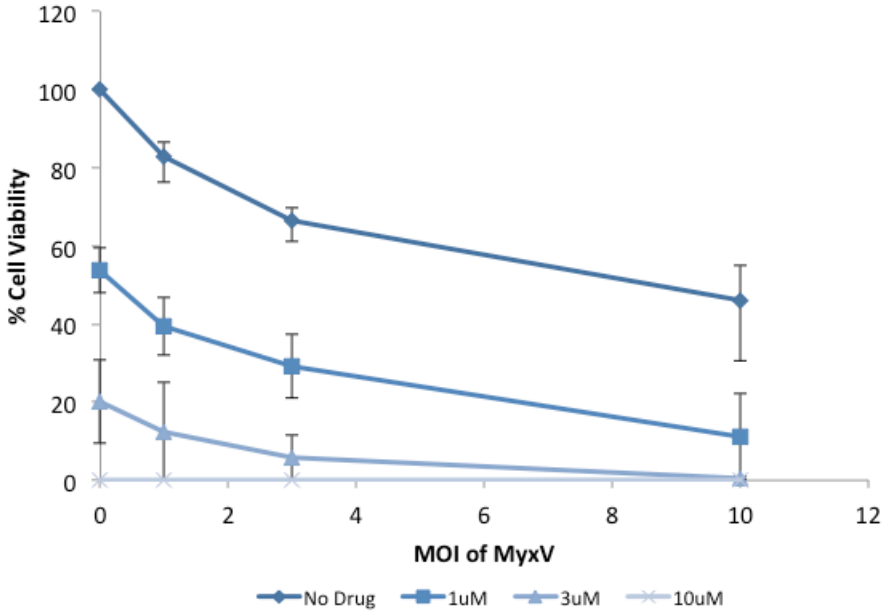
120
100
80
60
40
20
0
% Cell Viability
0
2
4
6
8
10
12
MOI of MyxV
No Drug
1uM
3uM
10uM

(H.)

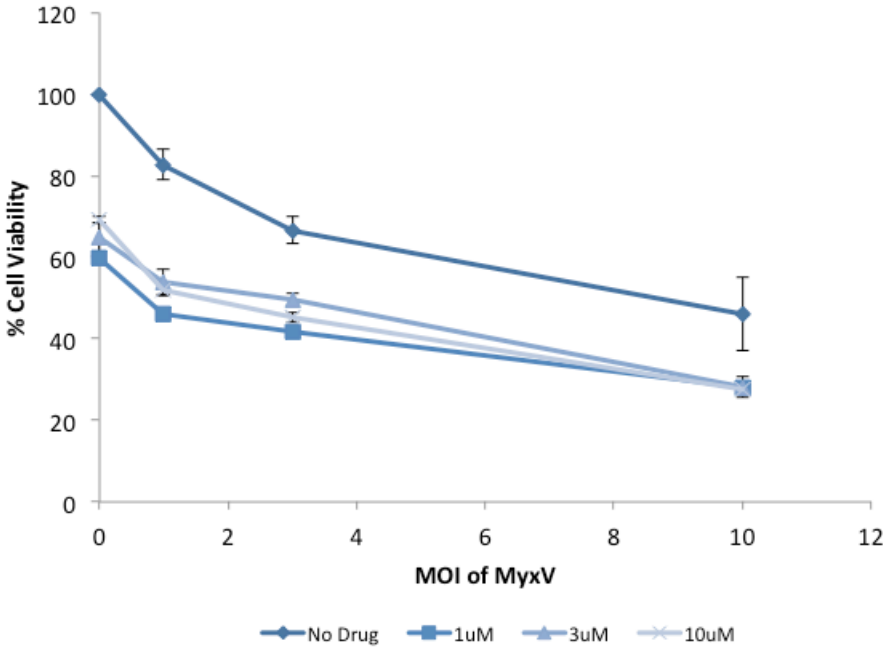
120
100
80
60
40
20
0
% Cell Viability
0
2
4
6
8
10
12
MOI of MyxV
No Drug
1uM
3uM
10uM

(I.)

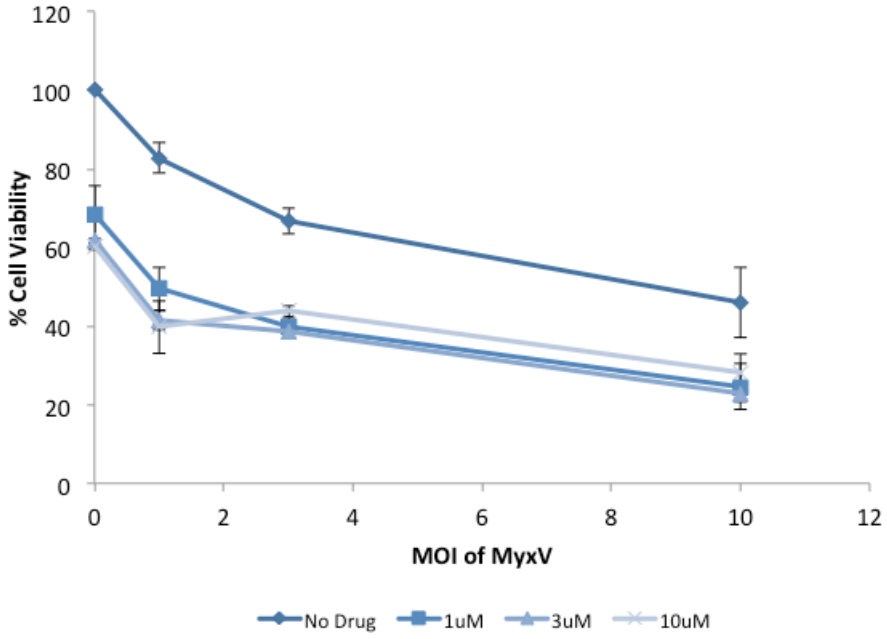
120
100
80
60
40
20
0
% Cell Viability
0
2
4
6
8
10
12
MOI of MyxV
No Drug
1uM
3uM
10uM

(J.)

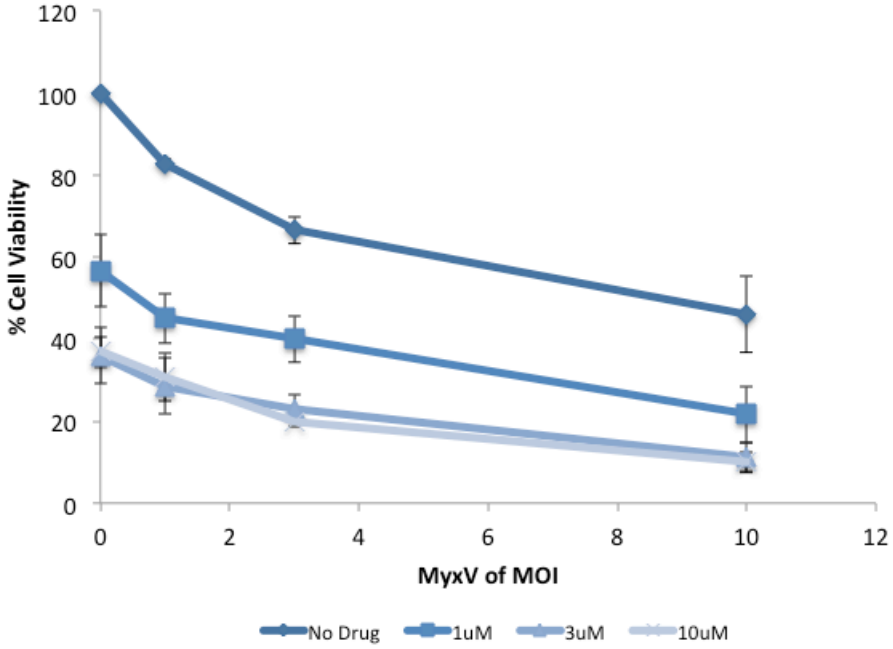
120
100
80
60
40
20
0
% Cell Viability
0
2
4
6
8
10
12
MyxV of MOI
No Drug
1uM
3uM
10uM

(K.)

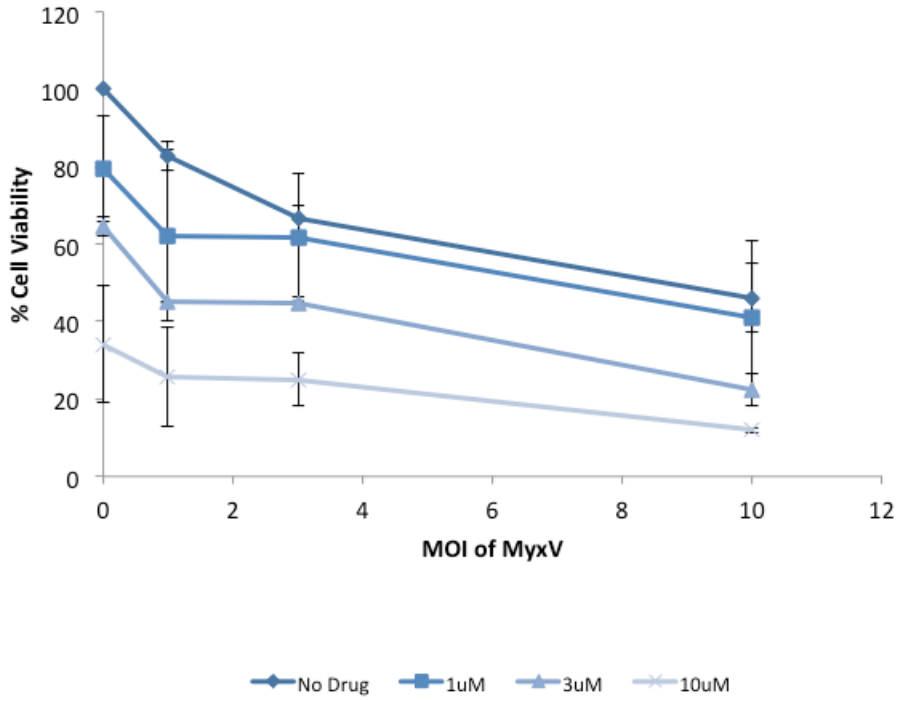
120
100
80
60
40
20
0
% Cell Viability
0
2
4
6
8
10
12
MOI of MyxV
No Drug
1uM
3uM
10uM